Universidade do Algarve

Faculdade de Engenharia de Recursos Naturais

Study of Genetic and Biochemical Interactions with Mouse *Cerberus-like* Genes

Ana Cristina Ribeiro Borges

Faro, 2004

Universidade do Algarve

Faculdade de Engenharia de Recursos Naturais

Study of Genetic and Biochemical Interactions with Mouse *Cerberus-like* Genes

Ana Cristina Ribeiro Borges

Faro, 2004

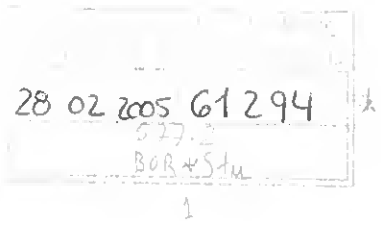
28 02 2005 61294
527.2
BOR+Stu
1

Dissertação de Candidatura ao Grau de Doutor em Biologia, Área de Biologia Molecular pela Universidade do Algarve.

Pd.D. Thesis proposal in Biology, Area of Molecular Biology by the Universidade do Algarve (Portugal).

As opiniões expressas nesta publicação são da exclusiva responsabilidade do seu Autor.

The contents of this dissertation are of the exclusive responsability of the Author.

(Ana Cristina Ribeiro Borges)

To my parents, Nuno and Inês.

Contents

Table of Figures

Acknowledgements

I would like to thank Prof. José António Belo for having accepted me in his lab at the Instituto Gulbenkian de Ciência when I was still an undergraduate student. Since then, my journey through science has been a challenge and an adventure. I feel I have learned a lot during the past five years and that this experience enriched me both scientifically and personally. Thank you for believing I could carry out this project, for all the support, scientific discussions, continuous commitment, and for help and encouragement to publish our results.

I thank Sara Marques for her precious collaboration in a major part of my work, for her friendship and help during all of these years, and also for the critical reading of this manuscript.

I also thank G. Liguori for her collaboration, scientific discussions and critical reading of this manuscript.

I want to acknowledge Dr. E. De Robertis, Dr. A. McMahon, Dr. M. Kuehn. Dr. D. Henrique and Dr. M. G. Persico for the gift of mutant mice, indispensable for the accomplishment of this work.

I wish to thank V. Teixeira for her patience, and for comments on this manuscript.

I also would like to thank everyone in the lab for suggestions, advices, exchanging experiences, discussions of results, friendship and support. Thanks M. Filipe, A. Tavares, A. Silva, S. Andrade, M. Carvalho, M. Bento, E. Morgado and J. Dias.

I am grateful to Prof. A. Coutinho for accepting me in the IGC, as a Ph.D. student.

I acknowledge Dr. S. Gulbenkian for all the effort in creating the PhDIGC, it greatly contributed to create better conditions to carry out my Ph.D project.

I also want to acknowledge the members of my Thesis Committee, A. Jacinto and A. Vicente, for advices, suggestions and evaluation.

I acknowledge Fundação para a Ciência e Tecnologia for the Ph.D. fellowship (SFRH/BD3214/2000) and the Scientific Council of the Faculdade de Engenharia de Recursos Naturais da Universidade do Algarve for accepting me as a Ph.D. student.

I would like to thank everyone in the IGC, in particular in the Developmental Biology wing for help, support and for making the IGC such a good place to work

To Nuno and Inês, thank you for all of your love, support, comprehension and patience.

To my parents, thank you for the inspiration and the continuous encouragement.

At last but not least, I would like to thank my friends and family, in particular to Inês´ grandparents for helping me to take care of her when I fully dedicated myself to the writing of this thesis. Thank you.

Resumo

O organismo dos vertebrados está organizado ao longo de 3 eixos principais, antero-posterior (A-P), dorso-ventral (D-V) e direito-esquerdo (D-E), que são especificados durante estádios precoces da vida embrionária. A base genética e molecular necessária para estabelecer os eixos principais tem sido descrita e as moléculas da superfamília "transforming growth factor-β" (TGF-β), como por exemplo, proteinas morfogenéticas do osso (BMPs) e Nodal, desempenham funções essenciais na padronização do embrião. A regulação da actividade destas moléculas é fundamental, de modo produzir a resposta biológica adequada. Cerberus-like (Cer-l) é um membro da família Cerberus/Dan, e da superfamília TGF-β, e um inibidor potente de BMPs e Nodal. Cer-l é expresso em estádios precoces do desenvolvimento embrionário de ratinho. Este gene foi inactivado por mutagénese dirigida em células estaminais embrionárias, mas não possibilitou uma caracterização funcional, uma vez que os mutantes se apresentam viáveis e sem fenótipo. Na tentativa de determinar a função biológica de *Cer-l,* foram gerados vários duplos mutantes. A partir destes estudos foi possível concluir que Cer-l não é epistático com Noggin, outro inibidor de BMPs, nem com o factor de transcrição Goosecoid. O estudo da dupla mutação de Cer-l e de Cripto, um co-receptor de Nodal, permitiu reconhecer a importância de Cer-l como importante regulador da actividade de Nodal. Esta análise revelou a existência de uma via de sinalização de Nodal, independente de Cripto, que pode ser inibida por Cer-l e está envolvida na especificação dos eixos A-P e D-V.

Foi recentemente isolado outro membro da família Cerberus/Dan em ratinho, ao qual foi atribuido o nome Cerberus-like 2 (Cerl-2). A análise funcional de Cerl-2 mostrou que este gene desempenha um papel importante na inibição de Nodal no nó do embrião de ratinho, e consequentemente, é necessário para o correcto estabelecimento do eixo E-D.

Globalmente, os resultados apresentados nesta tese, evidenciam a importância da inibição de Nodal, por membros da família Cerberus/Dan, de forma a especificar correctamente os principais eixos do embrião de ratinho.

Abstract

The vertebrate body plan is organized along three main axes, anterior-posterior (A-P), dorso-ventral (D-V) and left-right (L-R), that are specified during early stages of embryonic development. The genetic and molecular basis required to set-up the primary body axes is being unravelled/discovered/described and secreted molecules of the transforming growth factor-β (TGF-β) superfamily, like bone morphogenetic proteins (BMPs) and Nodal, were shown to play key roles in embryonic patterning. The tight regulation of the activity of these molecules is of primordial importance, in order to generate the appropriate biological responses. The Cerberus-Dan family member, mouse Cerberus-like (Cer-l) of the TGF-β superfamily, was shown to be a potent BMP and Nodal inhibitor, expressed during early stages of embryonic development. Its functional characterization by targeted inactivation in embryonic stem cells (ES) cells was not possible, due to the lack of phenotype of *Cer-l* null mutants. In an attempt to determine *Cer-l* biological function, several double mutants were generated. From these studies it was possible to conclude that Cer-l is not epistatic with the BMP antagonist Noggin, neither with the transcription factor Goosecoid. Interestingly, Cer-l is implicated in Nodal signalling regulation during early mouse development, as revealed by the analysis of the genetic interaction between Cer-l and the Nodal co-receptor, Cripto. This analysis unveiled the existence of a Cripto-independent Nodal pathway, antagonized by Cer-l that is involved in the specification of A-P and D-V axes of the mouse embryo.

Another member of the Cerberus/Dan family was recently isolated, and named mouse Cerberus-like 2 (Cerl-2). Functional analysis of Cerl-2 was carried out and showed that Cerl-2 plays an essential role in inhibiting Nodal activity in the mouse node, and therefore, in specifying the L-R body axis.

Together, the results presented in this thesis provide evidence for the importance of Nodal antagonism, performed by members of the Cerberus/Dan family, in order to pattern the mouse primary body axes.

Résumé

L'organisme des vertébrés est organisé autour de trois axes principaux : antérieur-posterieur (A-P), dorso-ventrale (D-V) et droite-gauche (D-G) dont le développement s'initie durant les stades précoces de la vie embryonnaire. La base génétique et moléculaire nécessaire pour établir ces principaux axes a été préalablement décrite de plus, les molécules de la super famille "transforming growth factor - β" (TGF-β), comme par exemple les protéines morphogénétiques de l'os (BMPs) et Nodal semblent jouer un rôle clé dans le modèle embryonnaire murin. La régulation de l'activité de ces molécules est cruciale dans le but d'induire la réponse biologique adéquate. Le gène *Cerberus-like* (*Cer-l*), membre de la famille des gènes *Cerberus/Dan* et de la super famille des TGF-β, est exprimé au cours des stades précoces du développement embryonnaire chez la souris et serait d'autre part, un inhibiteur potentiel de BMPs et Nodal. Ainsi, le gène *Cer-l* a été inactivé par mutagénèse dirigée par le biais de cellules souches embryonnaires cependant aucuns caractères fonctionnels n'a pu être observés chez les mutants viables dû à l'absence de phenotype. C'est pourquoi, plusieurs doubles mutants ont été générés dans le but de déterminer la fonction biologique du gène *Cer-l*. Ces analyses ont permis de conclure que le gène *Cer-l* n'interagit pas génétiquement avec le gène Noggin (autre inhibiteur de BMPs), ni avec le facteur de transcription Goosecoid. De plus, l'étude de la double mutation de Cer-l et de Cripto, un co-recepteur du factteur Nodal, a mis en évidence l'importance du gène *Cer-l* qui s'avére un régulateur essentiel de l'activité de *Nodal*. Ceci a révélé l'existance d'une voie de signalisation de Nodal indépendante de Cripto, qui peut être inhibée par Cer-l d'une part et d'autre part, être impliquée dans l'induction des axes A-P et D-V.

Il a été récemment isolé un autre membre de la famille Cerberus/Dan, nommé Cerberus like 2 (Cerl-2). L'étude fonctionnelle de *Cerl-2* a montré l'importance du rôle de ce gène dans l'inhibition de l'activité de Nodal au niveau du noeud de l'embryon et par conséquent dans la formation de l'axe G-D.

L'ensemble des résultats présentés au cours de cette thèse, met en évidence l'importance de l'inhibition de Nodal par des membres de la famille Cerberus/Dan dans le but d'induire correctement la formation des principaux axes de l'embryon murin.

Abbreviations

3′	- 3 prime
5′	- 5 prime
µg	– Microgram
µl	– Microliter
Ab	– Antibody
ActR	– Activin receptor
ADE	– Anterior definitive endoderm
ALK	– Activin like receptor
A-P	– Anterior-posterior
ASE	– Asymmetric enhancer element
AVE	– Anterior visceral endoderm
BMP	– Bone morphogenetic protein
Bp	– Base pair
CDNA	– Complemetar dehoxyribonucleic acid
Cer-l	– Cerberus-like
Cerl-2	– Cerberus like-2
Chd	– Chordin
CNS	- Central nervous system
CRD	– Cysteine rich domain
Dkk	– Dickkopf
DNA	– Dehoxyribonucleic acid
D-V	– Dorso-ventral
E	– Embryonic day
EGF-CFC	– Epidermal growth factor-cripto, frl-1, cryptic
EGO	– Early gastrula organizer
ES cells	– Embryonic stem cells
Fgf	– Fibroblast growth factor
Frzb	– Frizbie
Fz	- Frizzled
GDF1	– Growth and differentiation factor 1
GPI	– Glycosylphosphayidylinositol
Gsc	– Goosecoid

H – Hour
ICM – Inner cell mass
Iv – Inversus viscerum
Kb – Kilo base
KO .-Knock-out
KV – Kupfer´s vesicle
LDL – Low density lipoprotein
LPM – Lateral plate mesoderm
L-R – Left-right
Lrd – Left-right dynein
LRP – LDL-related protein
M – Molar
Mg – Milligram
Min - Minute
Ml – Mililiter
MRNA - Messenger ribonucleic acid
Nog – Noggin
Oep – One eye pinhead
PBS – Phosphate buffer saline
PCR – Polymerase chain reaction
P-D – Proximo-distal
PPE – Posterior epiblast enhancer
PS – Primitive streak
RT-PCR – Reverse transcriptase polymerase chain reaction
Sec – Second
Shh – Sonic hedgehog
TCF/LEF - T cell factor/lymphoid enhancer factor
TGF-β - Transforming growth factor β
U – Unit
UTR – Untranslated region
VE – Visceral endoderm
VYS – Visceral yolk sac
WISH – Whole mount *in situ* hybridisation
Wt – Wild-type

Chapter1 - Introduction

Chapter 1 - Introduction

Developmental biology has experienced great advances in the last decades. The attempt to understand the development of highly specialised organisms from a single fertilized cell, has prompted many scientists in the search for explanations about the mechanisms underlying embryonic development. Since the early 1930s, developmental processes are envisaged in terms of their underlying molecular and genetic components, a concept that has been more and more deepened. Current knowledge about the molecules that govern embryonic development has largely contributed to the detailed description of, for example, axis specification, neural tube development, organogenesis, etc. The data available today comes from the integration of studies carried in several model organisms that allow the complementation of different experimental approaches. The mouse is the primary model system for studying mammalian development and diseases, as the early embryo provides the developmental context to address many fundamental questions, including establishment of cell polarity, lineage differentiation and specification of embryonic axes.

This thesis will focus on the molecular mechanisms responsible for axis specification in the mouse embryo. Here, the molecular basis of the anterior-posterior (A-P), dorso-ventral (D-V) and left-right (L-R) axes will be presented and discussed.

1.1. Early steps in mouse development : pre-implantation

The complete mouse gestation takes approximately three weeks. The initial post-fertilization events are controlled by maternal molecules, since the zygotic genome is activated 24 hours post-fertilization, at 2-cell stage (Piko and Clegg, 1982). The first cell divisions occur relatively slow, taking between 12 and 24 hours each, consequently, the 16 cell-stage is apparent only at embryonic day 3 (E3.0) (reviewed in Beddington and Robertson, 1999). The first cleavages occur during the journey along the oviduct and not all cleavages occur at the same time, being frequent the existence of an odd number of cells. Until the 8-cell stage the blastomeres are indistinguishable in their biochemistry, morphology and potency. However, at 16-cell stage (morula stage) the cells undergo a dramatic change in their behaviour, through a mechanism called

compaction. The outside cells of the morula increase their contacts with one another by tight junctions and sealing off the inside of the sphere. Compaction creates the conditions to bring about the separation of the trophoblast or trophoectoderm -the external cells of the morula -from the internal cells -the inner cell mass (ICM; Pedersen et al, 1986). This is the first differentiation event in mammalian development. At 64-cell stage the two groups of cells are separated and neither contributes with cells to the other group (reviewed in Zernicka-Goetz, 2002 and Beddington and Robertson, 1999). Trophoblast cells secrete fluid into the morula to create a blastocoel and the ICM becomes localised on one side of the ring of trophoblast cells, thus creating a structure called the blastocyst. Part of the first layer of the blastocyst differentiates into epithelium and gives rise to the trophoectoderm that surrounds the blastocoelic cavity, the remainder serves as the site of attachment for the compact inner population of ICM cells. Hence, a polarized axis, usually referred as embryonic-abembryonic appears (Figure 1.1; reviewed in Zernicka-Goetz, 2002). At E4.5, the blastocyst is composed of three different tissues: two of them referred as extraembyonic – trophoectoderm and primitive endoderm- because they do not contribute with any descendants to the future embryo; and the third one is the ICM –also termed embryonic. In relation to the trophoectoderm, there are two types: the mural trophoectoderm, that surrounds the blastocyst cavity, and the polar trophoectoderm, which covers the entire ICM. The primitive endoderm differentiates on the surface of the ICM and encompasses one cell layer that is in contact with the blastocoel cavity (Figure 1.1). The primitive endoderm is destined to contribute to parietal and visceral endoderm. Finally, the core of the ICM will develop into the epiblast, the progenitor tissue for the whole animal (reviewed in Zernicka-Goetz, 2002, Bedington and Robertson, 1999, Tam and Behringer, 1997).

The mouse embryo has often been considered highly regulative, since it has the ability to recover from several types of experimental manipulations during the first stages of development. This view contrasts with the findings that in many other vertebrate and invertebrate embryos, some degree of patterning is imposed on the egg or on the early zygote, namely, by deposition of maternal determinants or cytoplasmic rearrangements upon fertilization by the sperm cell.

In the past few years this notion has changed (reviewed in Zernicka-Goetz, 2002), and the very first events in the life of the mouse embryo were shown to be required for the establishment of asymmetries and cell fates in the blastocyst.

It was shown that the site of sperm entry in the oocyte (Piotrowska and Zernicka-Goetz, 2001) and the protrusion site of the second polar body (Plusa et al, 2002), determine the plane of the first cleavage in the zygote. In addition, the 2-cell blastomere that inherits the sperm entry point divides first, giving rise to the 3-cell stage blastula. The descendants of the cell that divides first contribute preferentially to the embryonic part of the blastocyst –the ICM (Piotrowska et al, 2001; Piotrowska and Zernicka-Goetz, 2002; Gardner et al, 2001). These findings have assigned an important role to the sperm in the early patterning of the unperturbed embryo. Hence, contributing to the notion that the mouse embryonic plasticity co-exists with some degree of patterning and cell fate determination since the beginning of mouse embryogenesis. This may bring the mouse embryo, and probably other mammalian embryos as well, into the same league of embryos of other species where a pre-pattern of body plan has been identified.

1.2. Uterine implantation

The blastocyst must implant in the uterine wall of the mother in order to proceed with development. For that, the blastocyst hatches from the zona pellucida envolving it, so that it can adhere to the uterus and make direct contact between the mural trophoectoderm and the extracellular matrix of the uterine wall. The trophoectoderm cells contain integrins that promote the binding to the uterine extracellular matrix. Once attached, the blastocyst secretes protein-digesting enzymes that digest the extracellular matrix of the uterus, enabling the blastocyst to bury itself within the uterine wall (Perona and Wasserman, 1986; Carson et al, 1993)

When the mouse embryo implants, at E4.5, it changes dramatically in its form and shape. During the immediate post-implantation period (E5-E6), the embryonic tissue volume increases by about 40-fold. Proliferating polar trophoectoderm yields the extraembryonic ectoderm that seems to "push" the proliferating ICM complex and the enveloping visceral endoderm into the blastocyst cavity. In addition, a mixture of apoptotic and survival signals from the visceral endoderm, and the epiblast contribute to the formation of a cavity in the center of the epiblast- the proaminiotic cavity (Coucouvanis and Martin, 1995). This inward movement, and the epithelialiazition of the ICM, transform the embryo into an elongated cylindrical structure, so called, egg cylinder. The egg cylinder acquires the shape of a cup made up of two cell layers, the

inner epiblast and the outer visceral endoderm (VE) and has well delineated extraembryonic and embryonic regions that define a polarized proximo-distal (P-D) axis (Figure 1.1). At this stage the prospective dorso-ventral (D-V) axis of the embryo becomes apparent with the surface of the epiblast facing the proamniotic cavity corresponding to the dorsal side and the outer surface of the VE corresponding to the ventral side of the embryo (reviewed in Beddington and Roberson, 1999, Tam and Behringer, 1997).

Despite the embryo being derived from the epiblast cells, the extraembryonic tissues have important functions is supporting vital processes for the embryo, by assuring nutrient supply and gas exchanges. But they can also provide important cues for the patterning of the adjacent germ layers. For example, the VE plays an important role in the determination of the A-P axis in the mouse embryo before gastrulation, a subject that will be addressed in section 1.3.2.

1.3. Gastrulation: emergence of the embryonic body axes

Gastrulation is a morphogenetic process that results in the formation of mesoderm and the generation of the three germ layered embryo composed of ectoderm, mesoderm and endoderm. In the mouse, gastrulation also leads to the formation of a transient specialized structure called the node that generates new tissues with axis patterning activities (Fig. 1.1). When gastrulation begins, at E6.5, the antero-posterior axis can be unequivocally identified. At one point of the epiblast, in the proximal region, cells undergo an epithelial-mesenchymal transition to generate mesoderm and form a transient embryonic structure called the primitive streak. During the next 12-24 hours, the streak elongates from the proximal region to the distal tip of the embryo. During this process, the epiblast derived cells migrate between the epiblast and visceral endoderm and move laterally in both directions as well as proximally and distally to form the mesodermal wings. As the primitive streak elongates, the mesodermal wings continue to move until they meet at the anterior midline. During this process, epiblast cells are recruited from the epiblast to ingress into the primitive streak and then migrate and become incorporated into one of the three germ layers (reviewed in Tam and Behringer, 1997).

Fate map studies of the mouse gastrula, indicate that as the primitive streak lengthens, the mesodermal precursors that emerge have different embryonic fates,

according to the specific position along the A-P axis of the primitive streak (Lawson et al, 1991; Parameswaran and Tam, 1995; Tam et al, 1997; Kinder et al, 1999). The first cells that ingress through the primitive streak, at the posterior end of the primitive streak give rise to extraembryonic mesoderm. The middle region of the primitive streak produces cells fated to become lateral plate mesoderm, cardiac, cranial and paraxial mesoderm. The anterior primitive streak gives rise to cells of the axial mesendoderm. At the anterior end of the primitive streak, at late streak stage (E7.5), a specialized structure called the node is formed. The node becomes morphologically as an indentation of the distal tip of the embryo and has a bilaminar organization with a dorsal and a ventral cell layer. This transient structure has important organizing activities during development (see below).

As the streak elongates, cells that migrate through the node form the axial mesendoderm and will differentiate into the anterior definitive endoderm, prechordal mesendoderm and notochord (Tam et al, 1997). At the end of gastrulation, the prechordal plate -a patch of mesendodermal cells that underlies the anterior neural plate- is followed posteriorly by the notochord and anteriorly by the definitive endoderm. The extension of this midline tissues anterior to the node of the late primitive streak stage embryo, requires convergent extension, a concerted movement of the mesoderm and definitive endoderm layers in a direction opposite to that of epiblast expansion. The new population of definitive endoderm expands in an anterior-proximal direction and displaces most of the pre-existing visceral endoderm in direction to the extraembryonic tissues (Fig. 1.1; Tam and Behringer, 1997; Tam et al, 2001).

1.3.1. Node: the trunk organizer

In 1924, Spemann and Mangold reported the existence of an embryonic structure with axis forming and patterning activity in amphibians. They grafted the dorsal blastopore lip from a newt gastrula stage embryo into another embryo and found that it induced the formation of a secondary embryo with a normal body pattern. The transplanted tissue not only instructed cells in surrounding tissues to acquire new fates, but also provided global patterning signals regulating the dimension, orientation and position of the induced tissues along the A-P axis, hence, its name of organizer. Similar grafting experiments have more recently been used to identify homologous structures with axis inducing ability in other vertebrate species (Storey et al, 1992, 1995;

Beddington, 1994; Shih and Fraser, 1996; Tam et al, 1997). The axis-inducing organizer is called Hensen's node in chick, the shield in zebrafish and the node in the mouse (reviewed in Lemaire and Kodjabachian, 1996). In the mouse, the activity of the anterior primitive streak cells in early streak embryos show ability to induce a secondary axis in host embryos (Tam and Steiner, 1999), and have thus been given the name of early gastrula organizer (EGO). Therefore, the mouse organizer corresponds to the anterior primitive streak at the early streak stage and the node at the late streak stage.

Organizer cells in different species also have an overlapping set of genes encoding transcription factors (e.g. *Goosecoid, HNF3β/Foxa2*) and secreted molecules (e.g. *Noggin, Chordin, Nodal*), indicating that the mechanisms of organizer activity are conserved among different vertebrate species. In addition, the cells of the organizer of different vertebrate species have similar fates including prechordal mesoderm, notochord and gut endoderm and can induce secondary axes when transplanted (Beddington, 1994; Tam et al, 1997). These attributes make the mouse node equivalent to Spemann's organizer in frogs. Therefore, it would be reasonable to suppose that, like the frog organizer, it produces tissue that neuralizes ectoderm and provide it with A-P pattern. However, the mouse node has different capabilities from the Spemann's organizer, in the sense that it is unable to duplicate a complete axis; secondary axes invariably have anterior truncations and lack, for example, forebrain.

While the node does not initiate anterior pattern in the mouse embryo, it is undoubtedly important in maintaining and extending it. Recombination experiments in which the axial mesendoderm was cultured together with ectoderm show that the node derivatives are necessary for induction of the mid-hindbrain marker, Engrailed-1, in neuroectoderm (Rhinn et al, 1998). Therefore, axial mesendoderm from the node probably initiates A-P pattern in the trunk, including the hindbrain, but serves only to maintain and refine pre-existing A-P patterning further rostrally.

Several mouse mutants were generated in which the organizer function is affected. The winged-helix transcription factor, *Hnf-3β/Foxa2* is expressed in the

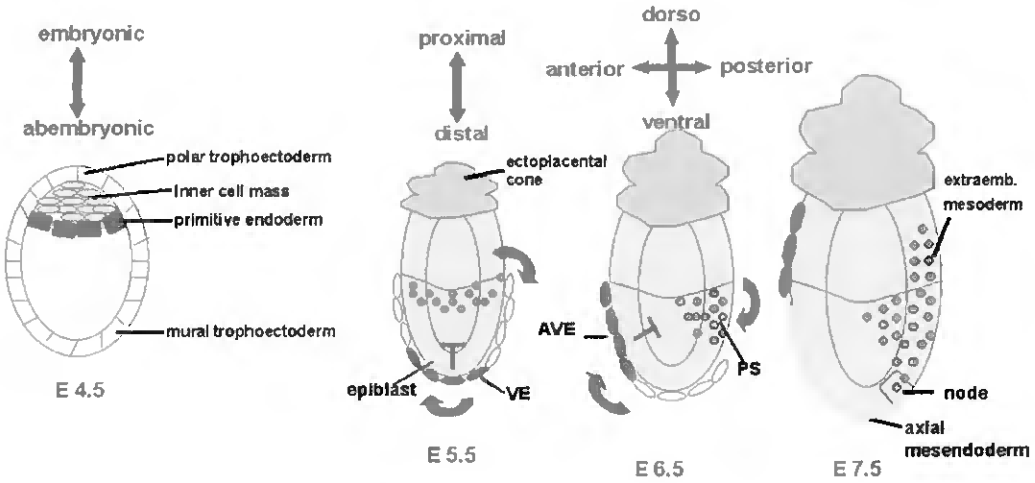

Figure 1.1. Cell movements and molecular signals controlling axis formation in the mouse embryo. The implanting blastocyst, at **E4.5**, is composed of three distinct tissue lineages: trophoectoderm, primitive endoderm and inner cell mass (or epiblast). At the egg cylinder stage, **E5.5**, the epiblast becomes organized into an epithelium surrounding the proamniotic cavity and is underlied by the visceral endoderm (VE). At this stage the region that expresses distal VE markers (*Hex, Lefty-1, Cer-l*) is represented in dark blue, and the proximal epiblast markers (*Brachyury, Fgf8, Nodal*) are depicted in red. Arrows point the direction of cell movements. At the early streak stage, **E6.5,** the proximal markers of the epiblast become restricted to the posterior region, demarcating the site where the primitive streak (PS) starts to be formed (red). The VE cells migrate anteriorwards (dark blue), and the initial P-D axis rotates and originates the A-P axis. The anterior visceral endoderm (AVE) inhibits Nodal signals emanating from the proximal and posterior regions of the epiblast. The primitive streak extends laterally, forming the mesodermal wings (red), and proximally giving rise to the extraembryonic mesoderm (green). At late primitive streak stage, **E7.5**, a morphological node is visible (yellow square) at the anterior end of the PS, and the node-derived axial mesendoderm (yellow line), extends from the node to the anterior midline of the embryo. The axial mesendoderm underlies the prospective neuroectoderm and differentiates into notochordal and prechordal plates, and anterior (or gut) endoderm. (Adapted from Beddington and Robertson, 1999).

anterior visceral endoderm (AVE), the node and its derivatives, the notochord and floorplate. *Hnf-3β/Foxa2* null mutants undergo gastrulation, display somites and lateral mesoderm, but do not have node and its derivatives (Ang and Rossant, 1994). The null mutant embryos show a rudimentary axis in which the neural tube is patterned along the A-P axis, but not D-V axis. Analysis of chimeras revealed that *Hnf-3β/Foxa2* function is required autonomously in the node and notochord for the formation of these structures. Thus, the node is not required for neural tube formation, neither for its A-P

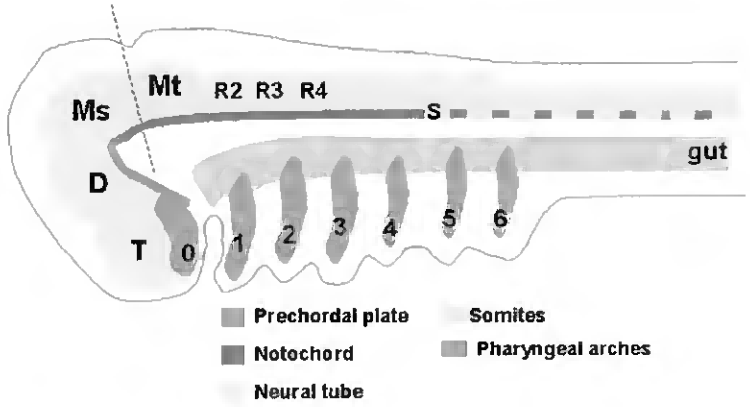

Figure 1.2. Schematic representation of the vertebrate neural tube and its relation with the underlying axial mesoderm. The vertebrate neural tube can be subdived into two broad domains along the A-P axis. The rostral domain comprises the Telencephalon (T), Diencephalon (D) and Mesencephalon (Ms). The Telencephalon and Diencephalon together form the forebrain, and the Mesencephalon is often called midbrain. The caudal domain of the neural tube is constituted by the Metencephalon (Mt) and Rhombencephalon (R), that together form the hindbrain. These domains are separated by the Mes-Metencephalic boundary (depicted as an interrupted line). Numbers one to six indicate the six pharyngeal arch elements. Zero (0) represents the premandibular visceral arch element or the trabecula that develops in close association with the telencephalon and prechordal plate. The notochord underlies the caudal domain of the neural tube, while the prechordal plate underlies the forebrain. The ventral localisation of these tissues is important in the determination of D-V polarity of the neural tube. (Adapted from Kuratani et al, 1997).

patterning, but is required for mesendoderm development. Interestingly, the EGO markers *Chordin* and *Goosecoid* are transiently expressed, meaning that EGO activity may be sufficient to induce neural tube formation and providing it with A-P pattern, but a mature node is required for mesendoderm formation that will later play an important role in the refinement of this pattern and D-V patterning of the neural tube.

At the molecular level, the anterior midline tissue can be subdived into two domains. The rostral segment, the prechordal plate that underlies the prospective forebrain (Figure 1.2), expresses *Gsc, Shh* and *Hnf-3β/Foxa2*. The rest of the anterior axial midline, which underlies the prospective midbrain and hindbrain, expresses genes such as *Lim1*, *Otx2, HNF3β, Shh* and *Bmp7*. Experiments in which the rostral anterior midline was ablated, the forebrain is severely affected, lacking expression of forebrain markers like *HesX1/Rpx, Six 3 and Fgf8*. The removal of the caudal segment of the anterior midline leads to loss of *Gsc* and *Nkx2.1* expression. Threfore, it seems that the

rostral segment, or prechordal plate, is required for the maintenance of the forebrain, while the caudal segment is required for the maintenance and the specification of the anterior midline comprising the prechordal plate and ventral diencephalon (Camus et al, 2000; reviewed in Kiecker and Niehrs, 2001).

Taken together, the current data from mouse fit well with a role of the anterior mesendoderm tissue in the maintenance of the segmental characteristics of the neural axis and subsequent regionalization of the developing forebrain along the A-P and D-V axes.

Interestingly, the axial mesendoderm emerging from the node corresponds to what is called dorsal mesoderm in other vertebrates, and the extraembryonic and lateral mesoderm that are derived from more posterior regions of the primitive streak, correspond to the ventral mesoderm. Thus, the prospective D-V axis is aligned with the A-P axis of the primitive streak. Hence, the origin of the primitive streak is critical in defining not only the A-P axis but also the D-V axis.

1.3.2. First molecular asymmetries in the embryo: the AVE

Although the first morphological sign of A-P asymmetry appears only with the appearance of the primitive streak at E6.5, evidence of a pre-existing molecular asymmetry in the visceral endoderm (VE), is already present at E5.5. The first sign of the existence of molecular asymmetry in the visceral endoderm came from the expression of the VE-1 antigen, that is expressed in the anterior region of the visceral endoderm (Rosenquist and Martin, 1995). Later on, more genes were shown to be expressed in the anterior visceral endoderm (AVE), namely, genes encoding secreted factors of the TGF-β superfamily *Cerberus-like* (Belo et al, 1997, Biben et al, 1998; Shawlot et al, 1998) and *Lefty-1* (Oulad-Abdelghani et al, 1998) and several encoding for transcriptioin factors such as *Lim-1* (LIM domain transcription factor), and the homeobox containing genes *Goosecoid, Otx2*, *Hex* and *Hesx1/Rpx* (Belo et al, 1997; Ang and Rossant, 1994; Acampora et al, 1995; Thomas et al, 1998; Thomas and Beddington, 1996). The expression of these genes is restricted to a medial strip of the AVE underlying approximately the anterior third of the epiblast, at least 12 hours before the streak had formed. Thus, as gastrulation starts in the epiblast, the visceral endoderm is already patterned in relation to its A-P axis. The homeobox gene, *Hex* was found to be expressed in the distal visceral endoderm (VE) prior to gastrulation, and at later

stages is restricted to the AVE, suggesting that the VE cells are the precursors of the AVE. Tracing the fate of distal VE by DiI injection confirmed that these cells are indeed the precursors of the AVE (Thomas et al, 1998). Thus, at E5.5 the egg cylinder is patterned along the P-D axis. The proximal ring of the epiblast already expresses typical primitive streak marker genes, such as *Brachyury, Nodal* and *Fgf8* and the distal VE expresses *Cer-l, Hex, Lefty-1*. Then, it seems that an anteriorwards movement of the VE cells occurs prior to gastrulation in the mouse embryo. Shortly, after this anterior movement has started, it is mirrored by a posteriorward movement of epiblast cells at the embryonic-extraembryonic junction (Lawson et al, 1991). In this way, the ring of gene expression in the proximal epiblast of primitive streak markers, becomes confined to the posterior epiblast where gastrulation begins, while the distal VE genes are displaced to the prospective anterior region of the embryo (Figure 1.1). This rotation, reflects cellular movements and is brought about by anterior movement of the AVE and posterior movement of posterior epiblast. This axis rotation is essential for the proper positioning of the A-P axis of the developing mouse embryo, before the gastrulation starts (reviewed in Beddington and Robertson, 1998).

Interestingly, some genes expressed in the AVE are also expressed in the node and its derivatives, like *Gsc, Hnf-3β/Foxa2* and *Lim-1*. This molecular characterization led to the proposal that the AVE might have some organizing activity (Belo et al, 1997).

1.3.3. Functional analysis of the AVE

To assess the function of the AVE, several experiments were done in which AVE was physically removed in early gastrulating embryos that were subsequently cultured in vitro. The AVE extirpation resulted in a loss or reduction of the developing forebrain, after 1 day of development in culture and to the depletion or reduction of the rostral neural marker *Hesx1/Rpx* (Thomas and Beddington, 1996). These results suggested that the AVE plays a key role in anterior induction in the mouse embryo.

Moreover, genetic analysis has greatly contributed to understand the role of the AVE in head induction in the mouse. For example, targeted inactivation factors expressed in the AVE, like *Otx2* (bicoid-like homeodomain protein), *Lim-1* (Lim-class homeobox), and the signaling molecule *Nodal* (TGF-β member), resulted in animals with severe anterior truncations of the fore- and midbrain (Acampora et al, 1995; Ang et al, 1996; Shawlot and Behringer, 1995; Conlon et al, 1994; Varlet et al, 1997).

However, since these genes have additional domains of expression in the embryo, the abnormal anterior development could not be directly attributed to the AVE. The generation of chimeras allowed a technical solution to answer this question. When embryonic stem (ES) cells are injected into host blastocysts they preferentially colonize epiblast and its derivatives, and therefore, it is possible to make chimeras in which the extraembryonic tissues can be of one genotype and the epiblast and its derivatives of another (Beddington and Robertson, 1989). By performing chimera studies, a number of genes have been shown to be required in the extraembryonic tissues. For example, chimeras containing wild-type embryonic tissues and *Otx2* mutant extraembryonic tissues phenocopy the *Otx2* mutants. The converse chimeras composed of mutant embryonic tissues and wild-type extraembryonic tissues show an initial rescue of anterior neuroectoderm (Rhinn et al, 1998). Similar results were obtained with chimeric embryos for *Nodal* (Varlet et al, 1997) and *Lim-1* (Shawlot et al, 1999). Thus, *Otx2, Nodal* and *Lim-1* all have essential roles in extraembryonic tissues, presumably in the AVE, for rostral brain development.

Taken together, the genetic analysis of mouse mutants, chimera studies and surgical manipulations, strongly contributed to the notion that contrarily to the Spemann´s organizer, the mouse organizer is split in two organizer centers: while the node functions as a trunk organizer, the anterior visceral endoderm has head organizing activities.

1.3.4. Mechanism underlying AVE inductive activity

Hesx1/Rpx gene is first expressed in the AVE and later in the rostral domain of the neural tissue that underlies the AVE (Hermesz et al, 1996). The AVE ablation experiment resulted in a reduction of the expression domain of *Hesx1/Rpx* in the underlying neuroectoderm, suggesting that an inductive signal from the AVE is required in order to the proper development of anterior neural tissue (Thomas and Beddington, 1996).

Surprisingly, the AVE alone cannot induce anterior neural tissue when grafted into an ectopic location (Tam and Steiner, 1999), neither in explant/culture assays (Kimura et al, 2000). It was shown that the AVE explant cannot induce neither maintain the expression of the rostral neural marker *Otx2*. Contrarily, it was found that AVE explants could suppress posterior epiblast markers such as *Brachyury* and *Cripto*

(Kimura et al, 2000). This data supports a model in which the AVE provide signals that repress posterior fate in the anterior epiblast of the mouse gastrula, in order to allow anterior neural development in a region free of posterior signals (Figure 1.1). However, the nature of the anti-posteriorizing agents had not been established, although several lines of evidence implicated the role of secreted antagonists in the AVE. Indeed, the AVE was shown to be a source of secreted molecules that act as antagonists of signaling molecules (reviewed in Perea-Gomez et al, 2001). Mouse *Cerberus-like* (*Cer-l*) is a member TGF-β superfamily, and was shown to effectively inhibit BMP-4 and Nodal signaling (Belo et al, 2000). *Lefty-1* is also a TGF-β member that inhibits Nodal signals (Meno et al, 1997). Mouse *Dickhopf-1* (*Dkk1*) is a secreted protein that acts as a Wnt inhibitor (Glinka et al, 1998). The function of these AVE secreted proteins was proposed to mediate the neural inducing activity of the AVE, however gene targeting experiments failed to assign such a role to these genes (Belo et al, 2000, Stanley et al, 2000; Shawlot et al, 2000; Meno et al, 1999; Mukhopadhyay et al, 2001), despite functional redundancy might account for those results. Nevertheless, this model has been reinforced and experimental results are consistent with a protective role of the AVE, mediated by Nodal antagonists (see below).

1.4. Nodal signaling pathway

Nodal is a TGF-β related factor that has essential roles in vertebrate development. In the mouse, *Nodal* is required for mesoderm formation, as revealed by the retroviral insertion mutation in the mouse *Nodal* gene. Mouse *Nodal* mutants lack a primitive streak and most mesoderm, displaying only sporadic formation of some posterior mesoderm (Conlon et al, 1994). The lack of mesoderm in *Nodal* mouse mutants is consistent with a conserved role for *Nodal* in vertebrates. In zebrafish, there are two Nodal ligands: Cyclops and Squint. Double mutants *Cyclops;Squint* failed to induce mesoderm and endoderm (Feldman et al, 1998). In *Xenopus*, there are six *Nodal*-related genes (*Xnr1* to *Xnr6*) and their functional analysis also revealed a role in mesendoderm induction (reviewed in Schier, 2003).

Second, *Nodal* genes are also important for generating left-right (L-R) asymmetric development. Some *Nodal* genes and several components of the Nodal pathway are asymmetrically expressed in the left lateral plate mesoderm (LPM) and

were implicated in L-R development (reviewed in Capdevila et al, 2000; Mercola and Levin, 2001; Hamada et al, 2002)

Recent studies have revealed a complex regulation of Nodal signaling pathway, as shown by the identification of EGF-CFC co-receptors and extracellular antagonists like Cer-l and Leftys. It is now apparent that cells can become competent to respond to Nodal by expressing EGF-CFC proteins, and can attenuate Nodal activity by expressing inhibitors of the Lefty and Cerberus families.

1.4.1. EGF-CFC factors

Members of the EGF-CFC family such as zebrafish *One eye pinhead* (*Oep*) and mouse *Cripto* and *Cryptic* encode for extracellular proteins that share amino-terminal signal sequence, a divergent epidermal growth factor (EGF)-like motif, a second conserved cysteine-rich domain (CFC motif) and a carboxy-terminal hydrophobic region (reviewed in Adamson et al, 2002). EGF-CFC factors are linked to the cell membrane by a glycosylphosphatidylinositol (GPI) anchor (Minchiotti et al, 2000). Genetic studies in zebrafish have shown that these extracellular proteins are essential for Nodal signaling (Gritsman et al, 1999). Thus, embryos that lack both maternal and zygotic *Oep* activity display the same phenotype as double mutants for the Nodal factors *Cyclops* and *Squint*. Similar to *Nodal* embryos, *Cripto* mutant mice do not form a primitive streak and embryonic mesoderm (Ding et al, 1998). Recent data indicate that EGF-CFC proteins are components of Nodal receptor complexes and facilitate the response to Nodal signals (Yeo and Whitman, 2001; Reissman et al, 2001).

1.4.2. Leftys

Members of the Lefty subfamily of TGF-β molecules appear to act as antagonists of Nodal signaling. Lefty proteins are predicted to be structurally distinct from other TGF-β molecules, lacking a long α-helix and a critical cysteine residue involved in stabilizing TGF-β homodimers and heterodimers (Meno et al, 1996; Meno et al, 1997; Thisse and Thisse, 1999). It is possible that Lefty act as monomers. These factors act as antagonists of Nodal, and in three different assays Leftys were shown to directly interact with Nodal, EGF-CFC factors and Activin receptor type IIB (Chen and Shen, 2004; Cheng et al, 2004; Sakuma et al, 2002). Therefore, Leftys may exhibit its inhibitory

activities by binding either to the Nodal ligand, receptor and/or co-receptor. In the mouse there are two Lefty genes and both were shown to be essential for proper embryonic development. For example, *Lefty-2* mutant mice have an enlarged primitive steak with more mesoderm progenitors; a phenotype that can be suppressed by decreasing Nodal activity, indicating that excess mesoderm formation may result from prolonged or hyperactivated Nodal signaling (Meno et al, 1999). Interestingly, *Lefty-2* expression closely follows that of *Nodal* in mice, and studies in zebrafish indicate that Nodal signaling leads to the induction and maintenance of *Lefty* expression (Meno et al, 1999; Bisgrove et al, 1999; Norris et al, 2002). *Lefty-1* mutants display L-R defects (Meno et al, 1998; see section 1.7.).

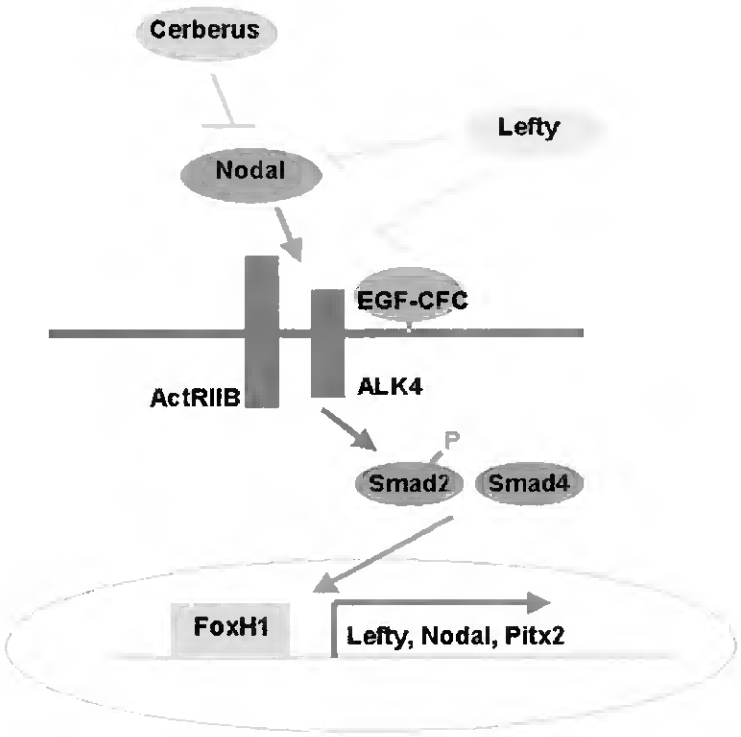

Figure 1.3. Schematic representation of the Nodal signaling pathway. Nodal interacts with type I and type II receptors (ActRIIB and ALK4, respectively) and EGF-CFC factors to transduce intracellular signals. The receptor complex activates Smad-2 proteins that in association with Smad-4 translocate to the nucleus and associate with FAST/FoxH1 transcription factor to activate gene expression. The extracellular inhibitors Cerberus and Lefty may prevent Nodal binding to the receptor complex, either by direct binding to Nodal, or via receptor or co-receptor interaction. (Adapted from Schier, 2003).

The negative feedback loop mediated by Lefty proteins effectively attenuates Nodal activity and renders it transient, allowing cells to respond to other signals after initial exposure to Nodal. This mechanism also blocks the positive autoregulation of *Nodal* expression, possibly restricting the spatial and temporal range of Nodal activity (Solnicka-Krezel, 2003; reviewed in Schier et al, 2003).

1.4.3. Cerberus

Cerberus is a member of the Cerberus/Dan family (TGF-β superfamily) and was identified in *Xenopus* as a head inducing molecule (Bouwmeester et al, 1996) that has multi-inhibitory activities (Piccolo et al, 1999). *Xenopus* Cerberus can block Nodal, BMP and Wnt ligands in the extracellular space. However, in *Xenopus* a truncated form of Cerberus (Cer-short) specifically blocks Nodal. In the mouse Cerberus-like (Cer-l) can inhibit Nodal and BMP, but not Wnt signals (Belo et al, 2000). Although *Cer-l* null mutants failed to show any type of defect (Belo et al, 2000, Stanley et al, 2000; Shawlot et al, 2000), *Cer-l* was shown to be required, together with *Lefty-1*, for A-P axis patterning (Perea-Gomez et al, 2002; Yamamoto et al, 2004; see section 1.5.1.).

1.4.4. Transduction of Nodal signals

Nodal was shown to bind the serine/threonine kinase Activin receptors type I and II (ActRI and ActRII). Upon Nodal binding to the ActRIIB, the type I receptor ActRI (ALK4) is activated and phophorylates the intracellular protein Smad2 (Yeo and Whitman 2001). This activation is dependent on EGF-CFC co-receptors, as shown by receptor reconstitution assays (Yeo and Whitman, 2001). In turn, Smad2 forms a nuclear complex with Smad4 and members of the FAST family of forkhead domain transcription factors (e.g FoxH1) to regulate the expression of downstream target genes (Fig. 1.3). Another type I receptor (ALK7) was proposed to be involved in Nodal transduction pathway. ALK7 can also bind Nodal and Activin receptors of type II to trigger Nodal signaling in a EGF-CFC independent fashion (Reissman et al, 2001).

Mouse *Smad2* and *ActRIB* mutants as well as *ActRIIA;ActRIIB* double mutants display gastrulation defective phenotypes, resembling those of mouse *Nodal* mutants (Waldrip et al, 1998; Weinstein et al, 1998; Nomura et al, 1998; Gu et al, 1998; Song et al, 1999).

Taken together, current genetic and biochemical data are consistent with a pathway in which Nodal, in conjunction with EGF-CFC proteins, activates Activin receptors or Activin-like receptors and Smad2 or related Smad proteins, resulting in the transcription of downstream targets, like its inhibitors *Lefty* and *Cerberus,* and other potential targets such as the transcription factors *Gsc*, *Hex* and *Pitx2* that mediate *Nodal* biological roles in both gastrulation and L-R development (reviewed in Shier et al, 2003).

1.5. Early roles of Nodal signaling

In the mouse embryo *Nodal* expression can be detected at E5.5 in the visceral endoderm and epiblast (Varlet et al, 1997). At E6.0 high levels are broadly detected in the proximal ring of the epiblast, and low levels in the visceral endoderm. When the primitive streak forms, at E6.5, the *Nodal* expression domain is restricted to the posterior side of the epiblast (Varlet et al, 1997); when the primitive streak is fully extended (E7.5), *Nodal* appears around the node and later it becomes apparent in the lateral plate mesoderm between 3-8 somite stage (E8.0-E8.5; Zhou et al, 1993; Lowe et al, 1996, Collignon et al, 1996).

The initial expression domain of *Nodal* in the posterior proximal epiblast is controlled by a cis-regulatory element within the 5´region (PPE; Brennan et al, 2001), however, the transcription factor responsible for its activation is not yet known. After this initial expression, *Nodal* is activated (E6.0) throughout the posterior epiblast (Brennan et al, 2001). This expression is dependent on a *Nodal* positive feedback loop, exclusively dependent on FoxH1 activity (Hoodless et al, 2001; Yamamoto et al, 2001; Norris et al, 2002), that allows a rapid expansion of *Nodal* expression domain throughout the posterior epiblast in a Smad-2 dependent process (Brennan et al, 2001). Strikingly, the expression of *Nodal* in the epiblast, besides being essential for the formation of the primitive streak and mesoderm, is also fundamental for the specification of the distal VE and the consequent patterning of the P-D axis (Brennan et al, 2001). In *Nodal* and *Smad-2* mutants, distal VE markers are not expressed, leading to the disruption of the P-D axis and subsequently, A-P patterning.

Quimeric embryos composed of *Nodal* mutant cells in the extraembryonic tissues and WT epiblast give rise to embryos that undergo gastrulation, but lack anterior head structures, meaning that *Nodal* plays an essential role in the extraembryonic tissues

responsible for head induction (Varlet et al, 1997). *Smad-2* is ubiquitously expressed in the mouse embryo at pregastrula, and gastrula stages. Mutant embryos for *Smad-2* also display a severe gastrulation phenotype, similar to the one of *Nodal* (Weinstein et al, 1998; Nomura et al, 1998). Quimera studies also revealed an essential role in the extraembryonic tissues for *Smad2* in A-P patterning (Waldrip et al, 1998). Taken together, these results suggest that Nodal signals mediated by Smad-2 in the epiblast are required for AVE specification. The activation of *Nodal* targets in the distal VE is required for the specification of the VE, that will subsequently play a role in anterior neural induction. These results clearly implicate Nodal signals in the generation of the A-P axis of the mouse embryo.

1.5.1. Anti-Nodal signals in the AVE

Nodal signals and anti-signals were recently implicated in the mechanism of AVE displacement, consolidating the previous proposed model in which the AVE is required as a source of antagonists to prevent posteriorization of the anterior epiblast. The insight came from the double mutant analysis of the *Nodal* antagonists *Cer-l* and *Lefty-1* (Perea-Gomez et al, 2002). In *Cer-l;Lefty-1* null mutants, the VE fails to migrate anteriorly and remains distally. During gastrulation, double mutants develop enlarged or duplicated primitive streaks. Curiously, this phenotype is opposite to the one of *Nodal* mutants and has not been observed in none of the *Cer-l* or *Lefty-1* single mutants. In addition, in the *Cer-l,Lefty-1* double mutant, targets of Nodal signaling (*Gsc* and *Hex*; Jones et al, 1995) are expressed in a broader domain suggesting increased Nodal activity. The removal of one copy of the *Nodal* gene in the double mutants, partially rescued the phenotype. These results indicate that the inhibition of Nodal signals emanating from the posterior epiblast by AVE secreted antagonists is required to restrict the primitive streak site. Moreover, it was shown that more than one Nodal antagonist is required to perform this function.

This mechanism was further dissected by Yamamoto et al, 2004, using *Cer-l;Lefty-1* double mutants. In this work, the authors reported that differential cell proliferation in the VE may be the driving force for AVE displacement. In fact, the AVE region where *Cer-l* and *Lefty-1* are expressed shows reduced levels of cell proliferation when compared to the rest of the embryo. Moreover, several mutants for the Nodal signaling cascade have deficient levels of cell proliferation in both the

epiblast and VE, revealing that Nodal signaling is implicated in this mechanism. In the presence of both Nodal antagonists Cer-l and Lefty-1, the cellular proliferation in the AVE is inhibited, causing a differential between the anterior and posterior regions that will lead to AVE migration anteriorwards. Contrarily, in the *Cer-l;Lefty-1* double mutants, the AVE has increased proliferative activity, leading to a failure of AVE displacement. This work provided clear insight into the mechanism of AVE migration, implicating Nodal signals and anti-signals in the process. Importantly, it showed that the driving force for AVE migration relies on cell proliferation, a process that is mediated by Nodal signaling.

1.5.2. The role of *Nodal* in the node and its derivatives

As described above, Nodal signals have sequential roles during early mouse development. Before gastrulation, *Nodal* is essential for the establishment of a P-D axis and for its subsequent rotation into an A-P axis. But Nodal signaling is also important for the patterning of the anterior primitive streak and the derivatives of the node. Genetic analysis of components of the *Nodal* pathway, and *Nodal* hypomorphic mutants shed light in the importance of graded Nodal signals during mouse development. In an attempt to study *Nodal* functions beyond gastrulation, Lowe et al. (2001) generated a *Nodal* hypomorphic allele. Mouse embryos heterozygous for the hypomorphic and a null allele ($nodal^{neo/-}$) undergo gastrulation but then display abnormalities that fall into three distinct mutant phenotypic classes, which may result from expression levels falling below critical thresholds in one or more domains of *Nodal* expression. At late streak stage, these mutants show an abnormal positioning of the A-P axis. Primitive streak markers (e.g. *Brachyury, Nodal*) are foreshortened and do not extend distally and the anterior markers (e.g. *Otx2, Hesx1/Rpx*) are not completely displaced anteriorly, they stay half way between the distal tip and the anterior extraembryonic region. This result indicates that early Nodal signaling has a role in the axial rotation that establishes the normal position of cells along the A-P axis. At E8.5 the defects are more pronounced and the mutant embryos can be divided in three classes. Type I embryos (less affected), lack prechordal plate and the most anterior foregut, and later show forebrain truncations and holoprosencephaly. Type I mutants have a morphologically normal node and, of three classes show the highest *Nodal* expression levels at the node. All type II embryos lack prechordal plate and have a deficiency of notochord in the

head, with some lacking notochord in the trunk. These embryos lack foregut, have a smaller and precocious closed hindgut, and a morphologically abnormal node. Expression levels of *Nodal* vary but are always below normal. Type III embryos have *Nodal*-positive cells in what might represent a disorganized node, and consistently develop a notochord while lacking a prechordal plate. Type III embryos completely lack gut endoderm. These results are consistent with a requirement for high *Nodal* levels in the node for correct development of the prechordal plate and foregut, and lower levels required for notochord, node and hindgut formation.

With a different approach Norris et al (2002), reached similar conclusions to the ones described above. In this study the authors generated a targeted inactivation of the *Nodal* intronic enhancer (ASE) that is dependent on the activation by the forkhead transcription factor FoxH1. Developmental abnormalities were seen in trans-heterozygous embryos carrying the ASE deletion and a null allele ($Nodal^{\Delta 600/-}$) and homozygous mutant embryos for $Nodal^{\Delta 600/\Delta 600}$. In $Nodal^{\Delta 600/\Delta 600}$ embryos, *Nodal* is efficiently expressed in the epiblast but absent from the VE. Unexpectedly, these embryos develop normal A-P axis. Later, at early somite stage, *Nodal* expression in the left LPM is significantly reduced. Leading to failure to activate *Lefty-2*, delayed activation of *Pitx2* and defective L-R patterning (for L-R axis development see section 1.7). In $Nodal^{\Delta 600/-}$ embryos, *Nodal* is expressed at low levels in the early epiblast, being confined to the proximal epiblast cells and is undetectable in the VE. Reduced *Nodal* expression levels in the epiblast are sufficient for VE induction and mesoderm induction. Many of these embryos, however, incorrectly position the A-P axis, leading to abnormal gastrulation and cell movements. Moreover, $Nodal^{\Delta 600/-}$ embryos lack anterior definitive endoderm (ADE) and display rostral neuroectoderm defects.

Taken together, these results pinpoint the requirement of highest Nodal levels in the epiblast for prechordal plate and anterior definitive endoderm formation, intermediate levels for node, notochord and foregut formation, and lower levels for the correct position of the A-P axis (Figure 1.4.). In conclusion, these studies indicate that graded levels of Nodal signaling activity in a cell can induce different cell fates, raising the importance of Nodal signaling modulation *in vivo*.

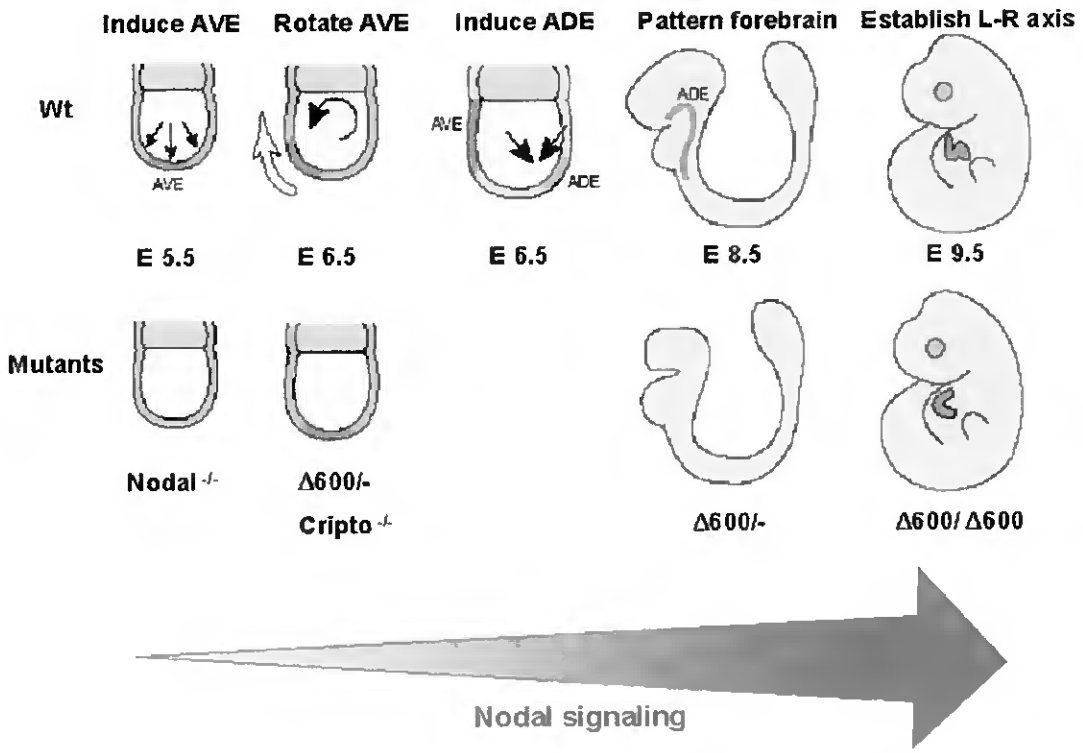

Figure 1.4. Nodal dosage-dependent signals are responsible for embryonic patterning. Nodal null embryos fail to induce an AVE at E5.5. *Cripto* null mutants, and some $Nodal^{\Delta 600/-}$ embryos induce but fail to rotate the AVE at E6.0. Other $Nodal^{\Delta 600/-}$ rotate the AVE but fail to induce the ADE at E6.5, resulting in reduction of the forebrain at E8.5. $Nodal^{\Delta 600 \Delta 600}$ embryos have higher level of Nodal signalling and correctly induce the ADE at E6.5, yet they fail to establish the L-R axis correctly at E8.5, resulting in defects in heart looping visible at E9.5. (from Norris et al, 2002).

1.6. The role of secreted signals by the organizer

In the *Xenopus* embryo, some secreted molecules expressed in the organizer induce a secondary axis when ectopically expressed (reviewed in Harland and Gerhart, 1997), suggesting that they play an important role in the activity of the organizer. Among these factors are the BMP4 antagonists Noggin, Chordin, Follistatin and Cerberus; and the Wnt inhibitors Frzb and Dickkopf (reviewed in De Robertis et al, 2001). Most of these signaling molecules have mouse homologs that are expressed in domains compatible with organizer activity, like the node and its derivatives. Given their potential to induce a secondary axis in *Xenopus*. It is surprising that mutations in *Cer-l* (Belo et al, 2000; Stanley et al, 2000; Shawlot et al, 2000), N*oggin* (McMahon et al, 1998; Brunet et al,

1998), *Chordin* (Bachiller et al, 2003), and *Follistatin* (Matzuk et al, 1996) do not cause defects in neural induction or A-P axis formation. The results of these mutant mice suggest the existent of redundant functions among these molecules, leading many labs to generate double mutants in order to uncover such compensation mechanisms. The results of some of these experiments will be presented below, on section 1.6.3.

1.6.1. BMP signaling pathway

Bone morphogenetic proteins (BMPs) represent the major group of the transforming growth factorβ (TGF-β) superfamily. These proteins have diverse and remarkable roles during early embryogenesis by regulating cell proliferation, differentiation, survival and even cell fate (reviewed in Zhao, 2003).

Similar to other members of the TGF-β superfamily, BMPs are synthesized and folded as large dimeric proteins in the cytoplasm and cleaved by proteases during secretion. The homo- or heteromeric BMP proteins bind to heteromeric receptor complexes that contain type I and type II serine/threonine kinase receptor subunits. The BMP transduction pathway bears remarkable similarities to the one described for Nodal signaling, since both Nodals and BMPs are members of the TGF-β superfamily (Fig. 1.5). Type II receptor activates type I receptor that in turn activates intracellular Smad proteins. The type I receptors involved may be ALK 1, ALK2, ALK3 and ALK6. Type II receptors may be BMPRII, ActRIIA, ActRIIB. The receptor complex phosphorylates effector Smad1, 5 or 8 proteins that oligomerize with Smad4 in the cytoplasm and translocate into the nucleus to serve as transcriptional regulators (reviewed in Zhao, 2003).

Like Nodal regulation, BMP activities are tightly regulated by secreted antagonists. This antagonism leads to a graded inhibition of ventralizing BMP signaling that is essential for neural induction and dorso-ventral patterning of the vertebrate embryo (De Robertis and Sasai, 1996).

In the mouse several BMPs are expressed during gastrulation, like *Bmp2, Bmp4, Bmp5* and *Bmp7* (reviewed in Zhao et al, 2003). *Bmp4* is the most widely expressed BMP gene throughout development. From E3.5 to E6.5 is expressed in the extraembryonic ectoderm. At E6.75 is also detected in the extraembryonic mesoderm. *Bmp4* null mutant embryos have a reduction in extraembryonic mesoderm typified by a lack or a very thin allantois, and a complete lack of primordial germ cells (Winnier et al,

1995). *Bmp2* and *Bmp4* share over 90% identity at the aminoacid level and are functionally interchangeable. *Bmp2* is expressed in the visceral endoderm from E6.0, with higher levels in the boundary region between the epiblast in the posterior area covering the future primitive streak. When *Bmp2* is inactivated, null embryos reveal a reduced extraembryonic mesoderm, a slender allantois and defective amnion, and a reduced number of primordial germ cells (Zhang et al, 1996). Other BMPs were inactivated and produced essentially defects in bone morphogenesis, spermatogenesis and organogenesis. *ALK3* encodes for a type I receptor, a putative BMP receptor, ubiquitously expressed throughout development. Its inactivation results in early embryonic lethality (before E7.0), due to impaired growth of the epiblast and a lack of

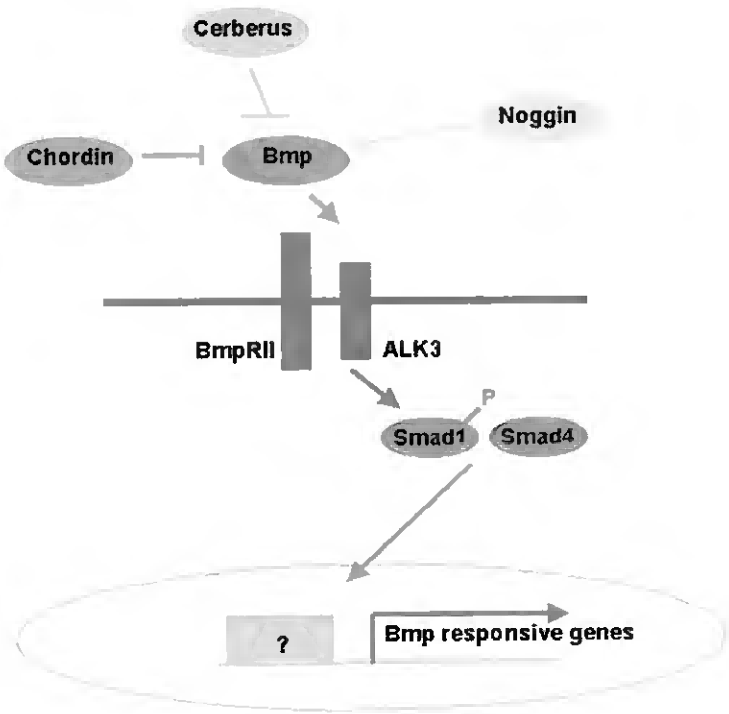

Figure 1.5. Schematic representation of BMP signaling pathway. BMP ligands bind to type II receptors to form complexes that interact with type I receptors. The receptors then form hetrotetrameres, which result in the phodphorylation and activation of Smads that subsequently form complexes with the common Smad4 . This complex translocates to the nucleus, where it regulates gene transcription. (Adapted from Waite and Eng, 2003).

mesoderm (Mishina et al, 1995). The inactivation of *ALK3* represents the most severe phenotype among all genes in BMP signaling pathways so far examined, indicating an absolute requirement of BMP signaling during gastrulation.
BMP antagonism is essential to the proper development of the mouse embryo, an issue that will be addressed on section 1.6.3.

1.6.2 Wnt signaling pathway

Wnt proteins are signaling molecules that regulate many stages of development, from patterning of the embryo and generation of tissues and cell types, to regulation of cell movements and polarity. The interaction of Wnt proteins with their receptors on the cell surface is the first step in transducing the extracellular signal into intracellular responses. The first identified Wnt receptors were members of the Frizzled (Fz) family of seven-pass transmembrane receptors (Wodarz and Nusse, 1998). In addition to Fz proteins, the canonical Wnt/β-catenin signaling pathway requires single-span transmembrane proteins that belong to a subfamily of low-density-lipoprotein (LDL) receptor related proteins (LRPs) and include vertebrate Lrp5 and Lrp6 and their Drosophila ortholog Arrow (reviewed in He et al, 2004).

The most intensively studied Wnt pathway is the canonical Wnt/β-catenin signaling pathway. The biological activity mediated by this pathway relies on the regulation of the stability/abundance of the β-catenin protein. β-catenin associates with, and acts as an obligatory nuclear activator for the TCF/LEF (T cell factor/lymphoid enhancer factor) family of transcription factors. In the absence of a Wnt ligand, the level of cytosolic β-catenin is kept low as a result of its amino-terminal phosphorylation-dependent ubiquitination/proteosome degradation. When β-catenin is low, TCF/LEF is associated with transcriptional co-repressors and suppresses Wnt-responsive gene expression. Upon Wnt stimulation, β-catenin phosphorylation and degradation is inhibited, and the accumulation of β-catenin promotes its association with TCF/LEF, leading to the activation of Wnt-responsive transcription. β-catenin phosphorylation is thus a crucial regulatory step in this Wnt pathway (Figure 1.6).

Wnt signaling is required for normal gastrulation in mouse. For example the *Wnt3* is expressed in the proximal epiblast before gastrulation; then is restricted to the posterior proximal epiblast and its associated visceral endoderm; subsequently localises in the primitive streak and mesoderm. Mouse mutants for *Wnt3* do not form a primitive

streak, mesoderm or node. The embryos lack A-P patterning, although AVE markers are expressed and correctly positioned (Liu et al, 1999). *β-catenin* deficient mice also have defects in the A-P axis formation: AVE markers remain distal and mesoderm and head structures are not formed (Huelsken et al, 2000). Taken together, these data indicate that signaling by members of the Wnt pathway plays a role in 1) establishment of anterior-posterior polarity; and 2) in the formation of posterior structures such as the primitive streak.

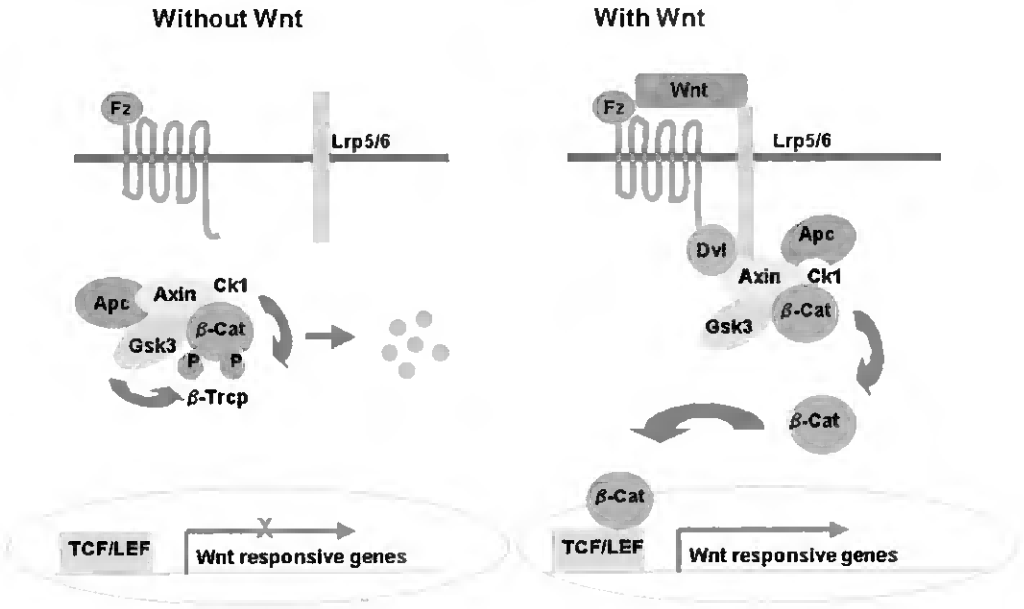

Figure 1.6. Schematic representation of Wnt signalling pathway. Without Wnt, the scaffolding protein Axin assembles a protein complex that contains Apc, Gsk3, Ck1, and β-catenin (β-cat). In this complex β-catenin is targeted to ubiquination and subsequently is degrated by the proteosome. Some proteins that mediate the process are omitted for simplicity. In the presence of Wnt, β-catenin phosphorylation and degradation is inhibited. Accumulated β-catenin forms a nuclear complex with the TCF/LEF transcription factor and together they activate Wnt-responsive genes. This signalling cascade is initiated by a Wnt-induced Fz-Lrp5/ co-receptor complex, which recruits Axin to the plasma membrane. Fz-associated Dihevelled (Dvl) protein may also promote Axin degradation. (Adapted from He et al, 2004).

In addition, Wnt signaling is subject to modulation by secretd antagonistic ligands in vertebrates. One family of such antagonists is Dickkopf (Dkk), which antagonize Wnt/β-catenin signaling through interactions with Lrp5/Lrp6. Wnt antagonism performed by Dkk causes the disruption of the Fz-Lrp5/Lrp6 complex formation. Dkk1 can bind directly to Lrp6, preventing the binding of Wnt molecules to the receptor complex, thereby leading to the inhibition of Wnt/β-catenin intracellular signaling (Figure 1.6; reviewed in He et al, 2004). The biological function of Wnt antagonism by Dkk, during mouse gastrulation is presented below, in section 1.6.3.

1.6.3. Genetic interactions between secreted antagonists

Mouse *Chordin*, encodes for a BMP4 antagonist, that is first expressed in the anterior primitive streak and then in the node and axial mesendoderm (Bachiller at al, 2000). Targeted inactivation of this gene results in postnatal defects in the inner and outer ear, abnormalities in pharyngeal and cardiovascular organization (Bachiller et al, 2003). *Noggin*, another BMP4 inhibitor, is co-expressed with *Chordin* in the node and axial mesendoderm (McMahon et al, 1998; Bachiller et al, 2000). *Noggin* null mutants undergo normal gastrulation and anterior central nervous system patterning, although at later stages a number of abnormalities are observed in the posterior spinal cord and somites (McMahon et al, 1998; Brunet et al, 1998). *Chordin;Noggin* (*Chd;Nog*) double mutants revealed severe defects in the development of the forebrain, displaying holoprosencephaly (Bachiller et al, 2000). At E12.5 the double mutants show head truncations corresponding to the lack of forebrain. In these mutants, the AVE markers (*Cer-l, Lim-1* and *Hesx1/Rpx*) are present at the onset of gastrulation, but *Cer-l* and *Hesx1/Rpx* are not detected at the early headfold stage. In addition, rostral mesendoderm of the forebrain and the foregut pocket is not formed, as well as notochord. These results indicate that the anti-BMP molecules secreted by the node have a head inducing activity, namely, by the maintenance of anterior patterning initiated by the AVE. Interestingly, *Chd,Nog* double mutants present defects in the main body axis: incomplete A-P patterning (forebrain defects) and abnormal dorso-ventral (lack of notochord and holoprosencephaly) This suggests a key role for BMP antagonism, in the node and its derivatives, for the generation of the vertebrate body axes.

Mouse Dickkopf-1 (Dkk1) is a secreted protein that acts as a Wnt inhibitor. *Dkk1* is expressed in the AVE, in the node and axial mesendoderm (Glinka et al, 1998).

Dkk1 mutants lack anterior head structures anterior to the midbrain (Mukhopadhyay et al, 2001). Analysis at late streak stage shows absence of the anterior neuroectoderm marker *Hesx1/Rpx*. In order to distinguish between a role in AVE or in the derivatives of the epiblast, chimeras were produced in which WT cells were injected in a $Dkk1^{-/-}$ blastocyst. The resulting chimeras showed a complete rescue of the forebrain structures, suggesting that the head truncation is due to a requirement of Dkk1 function in the embryonic rather than in the extraembryonic tissues. Therefore, *Dkk1* was proposed to be involved in induction of rostral neuroectoderm, from the adjacent axial mesendoderm. Together, the results of the *Chd;Nog* double mutant and *Dkk1* null mutant reinforce the role of the anterior mesendoderm in maintaining initial anterior neural induction by the AVE. In particular, the importance of BMP and Wnt antagonists secreted from the node and its derivatives, to accomplish this function.

Dual inhibition of Wnt and BMP signals has been proposed to confer head organizer activity. In *Xenopus*, simultaneous reduction of the BMP antagonists Chordin and Noggin, and the Wnt antagonist Dickkopf leads to anterior truncations. In mice, compound mutants for *Noggin* and *Dkk1* display severe head defects, with deletion of all head structures anterior to the mid-hindbrain boundary (Barrantes et al, 2003). These defects are apparent in the double heterozygous $Dkk1^{+/-};Nog^{+/-}$ embryos and are due to a defective anterior mesendoderm that fails to pattern the rostral epiblast (Barrantes et al, 2003). Taken together, these results clearly show the importance of the synergy of the node-secreted Wnt and BMP antagonists in the generation of the body plan, in particular for the head induction in vertebrates.

1.7. Left-right patterning in the mouse

As described above, gastrulation brings about the emergence of two main body axis: first the antero-posterior (A-P), and second, the dorso-ventral (D-V) axis. The third body axis, the left-right (L-R), appears probably as default, upon the formation of the previous two. Despite an apparent external bilateral symmetry, vertebrates display multiple asymmetries in the internal organs. Asymmetric morphology is required in order to fit all organs inside the limited space of the body cavitiy. Even bilateral organs (e.g. kidneys or testis) can present asymmetric insertion in the abdomen. During embryogenesis the heart loop is the first event that shows clear morphological asymmetry, which takes place at the early somite stage (6-8 somites in the mouse). In

addition to the heart, all other organs develop asymmetrical shape and/or position (reviewed in Fujinaga et al, 1997).

The production of L-R asymmetry is known to have a molecular basis and many genes involved are conserved among vertebrates. Conceptually, when a gene that functions upstream of a central L-R pathway is impaired, it would result in randomisation or complete inversion of the situs. On the other hand, when a gene that functions in a branched pathway is defective, it would result in abnormal positions of some organs but not others (partial inversion). This is what has been observed in various mouse mutants; the position of visceral organs may be co-ordinately reversed or independently affected, depending on the type of mutation. The terminology of L-.R situs includes specific terms that worth definition here. *Situs solitus* refers to normal situs (*totalis*); *situs inversus totalis* means a complete reversion; *heterotaxia* is used when partial *situs inversus* occurs, in this case some organs are reversed while others are normal; *isomerism* is a situation in which asymmetry is lost, two types are possible: *left isomerism* in which both sides become left, and *right isomerism*, when both sides become right (Fujinaga et al, 1997).

The whole process of L-R determination can be divided into four steps: (1) break in L-R symmetry, (2) transfer of L-R biased signals from the node to the lateral plate mesoderm, (3) L-R asymmetric expression of signaling molecules in lateral plate mesoderm, and (4) L-R asymmetric morphogenesis of visceral organs (reviewed in Capdevila et al, 2000). I will begin by step 3, where several aspects of laterality development appear to be conserved. Namely, members of the Nodal and Lefty families of TGF-β molecules and the transcription factor Pitx2 are expressed specifically on the left side in all vertebrates studied so far.

1.7.1. Asymmetric gene expression

The expression and function of the *Nodal* gene family suggest a central conserved role for Nodal signaling in vertebrate L-R patterning. *Nodal* genes are expressed asymmetrically in the left lateral plate mesoderm (LPM) during somitogenesis in zebrafish (*Cyclops* and *Southpaw*), frog (*Xnr1*), chick and mouse (*Nodal*).

In the mouse, the first gene expressed asymmetrically is *Nodal*, that shows an asymmetric pattern around the node at pre-somite stage (Lowe et al, 1996; Collignon et

al, 1996). The initial expression of *Nodal* is symmetric and assumes a horse-shoe shape around the perinodal region. A few hours later, the expression domain becomes asymmetric, becoming stronger on the left side of the node. The expression of *Nodal* in the mouse node precedes its expression in the left LPM. It is in the left LPM, that a cascade of genes asymmetrically expressed lead to the organ specific morphogenesis (Fig. 1.7).

Due to the early embryonic lethality of the *Nodal* null mutants it was not possible to determine the role of *Nodal* in the node. However, in recent studies (Brennan et al 2002; Saijoh et al, 2003) a link between the *Nodal* expression in the node and in the left LPM was established, by inactivating *Nodal* activity specifically in the mouse node. In both reports, the *Nodal* expression in the perinodal region was shown to be required for the subsequent expression of *Nodal* in the left LPM. In the absence of *Nodal* expression in the node, the genetic cascade expressed in the left LPM is not activated, leading to laterality defects in older embryos and newborn pups. In rescue experiments using transgenic mice, the *Nodal* expression in the node, restored normal *Nodal* expression pattern in the left LPM.

Once activated in the left LPM, *Nodal* induces the expression of downstream targets that will ultimately lead to the asymmetric organ morphogenesis. *Lefty-2* is one of the *Nodal* target genes and starts to be expressed in the left LPM shortly after *Nodal*. *Lefty-2* is essential to restrict the temporal and spatial expression of *Nodal*. In *Lefty-2* conditional mutants, *Lefty-2* expression was abolished in the left LPM, and *Nodal* expression in the LPM is prolonged in time (Meno et al, 2001). Based on this result and on the analysis of the *Lefty-2* null mutant (Meno et al, 1999), *Lefty-2* was proposed to act in a negative feedback loop to regulate the extent of *Nodal* activity (reviewed in Hamada et al, 2002 and Solnika-Krezel, 2003).

Shortly after asymmetric *Nodal* expression disappears from the left LPM, situs-specific morphogenesis begins (step 4). The cardiac tube loop towards the right side and the embryo turns along the A-P axis in a clockwise direction, followed by asymmetric lobe formation in the lungs, rotation and coiling of the digestive tract, and regression of parts of the vascular system on one side. This asymmetric morphogenesis occurs in response to Nodal signalling and organ primordia will adopt left-side morphology in the presence of Nodal signals, but in the absence of Nodal activity they will adopt right-side morphology.

Pitx2 is a bicoid-type homeobox transcription factor whose expression is initiated in the left LPM in response to Nodal signals (Ryan et al. 1998; Logan et al, 1998; Yoshioka et al, 1998; Piedra et al, 1998; Campione et al, 1999). *Pitx2* is also expressed asymmetrically in organ primordia of most asymmetric organs. Consistent with its expression domain and presumptive function, *Pitx2* null mutants show a vast range of defects that include right isomerism of the lungs and abnormalities in the heart formation (Kitamura et al. 1999; Gage et al. 1999; Lu et al. 1999; Lin et al. 1999).

The midline structures, such as the floorplate and the notochord, are also important for L-R patterning. For example, surgical removal of the midline structures, including the notochord, from *Xenopus* embryos randomises heart looping and gut coiling, and leads to bilateral expression of *Xnr1*, a Nodal-related gene in *Xenopus* (Danos et al, 1996; Lohr et al, 1997). Analysis of *Lefty-1* mutant mice indicates that *Lefty-1* functions as a specific midline barrier (Meno et al, 1998). Midline structures, including the floor plate and the notochord, develop normally even in the absence of *Lefty-1*, but a lack of *Lefty-1* leads to typical midline barrier defects, such as bilateral expression of left-specific genes *Nodal, Lefty-2* and *Pitx2*, and pulmonary left-isomerism. This phenotype indicates that *Lefty-1* induces or functions as the midline barrier that prevents an unknown left-side specific signaling molecule from crossing the midline. A recent study, revealed that *Lefty-1* expression in the midline structures is dependent on the Nodal signaling in the left LPM. Thus suggesting that Nodal activity travels from the node to the left LPM, and from the left LPM to the midline (Yamamoto et al, 2003). These observations underscore the central role of Nodal activity in coordinating several components required for the establishment of the L-R axis.

Nodal, Leftys and *Pitx2* genes form the central part of the L-R pathway that is conserved among vertebrates. Similar patterns of expression and activities were described in fish, frog, chick and mouse. In addition, *Nodal* and *Pitx2* are also involved in L-R development in other chordates such as the urochordates (e.g. Ascidians) and cephalochordates (e.g. Amphioxous), revealing a conserved developmental pathway that evolved before the separation of the lineages leading to living chordates (Boorman and Shimeld, 2002).

In addition, there are other genes, such as *Shh* and *Fgf8*, that have different roles in chick and mouse (Meyers and Martin, 1999). In the chick, *Shh* is expressed on the left side of the node and can induce a left-side program, but in the mouse, *Shh* is

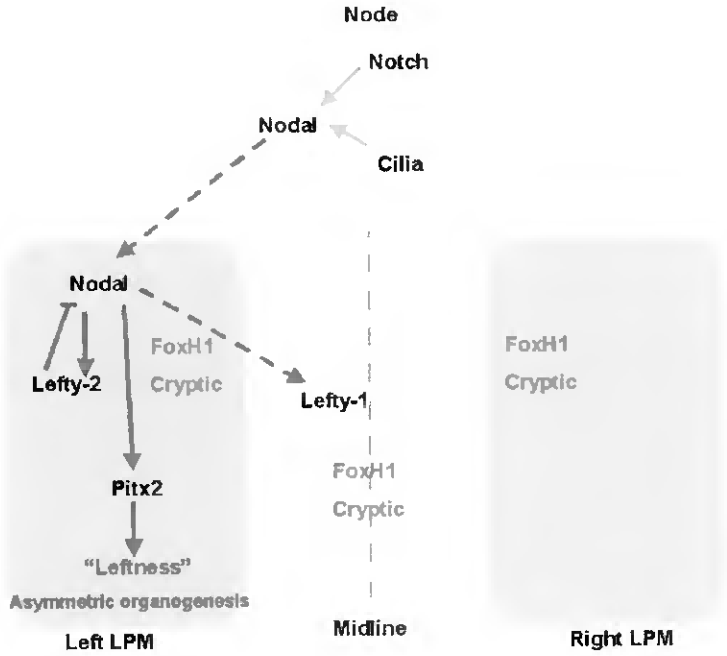

Figure 1.7. Schematic representation of Left-Right genetic cascade. *Nodal* expression in the node is under the regulation of node cilia and Notch activity and induces its own expression in the left lateral plate mesoderm (LPM), via an unknown mechanism (depicted an interrupted arrow). In the left LPM, *Nodal* induces the expression of its negative regulator, *Lefty-2* and of *Pitx2*. This activation is mediated by FoxH1 and Cryptic, that are expressed bilaterally in the LPM and in the midline. *Lefty-1* expression in the midline is restricted to the left side. The asymmetric activation of Nodal cascade in the left LPM determines asymmetric organogenesis, required for the correct development of the vertebrate organism. (Adapted from Schier, 2003).

required for the formation of the midline, including the floorplate (Echelard et al, 1993). *Shh* null mutants lose *Lefty-1* expression and have midline defects and bilateral *Nodal* expression in the LPM, which is associated with left isomerism in the lung. In addition, fibroblast growth factor 8 (*Fgf8*) is also involved; it seems to function upstream of *Nodal* both in the chick and mouse, but in the chick it acts as one of the right-side determinants (Boettger et al, 1999), whereas in the mouse it is required for left-side signaling. Therefore, vertebrates seem to have adopted diverse strategies for setting up asymmetric *Nodal* expression.

1.7.2. Regulation of gene expression

As mentioned before, *Nodal* and *Lefty* genes are regulated by negative and positive feedback loops. Both *Nodal* and *Lefty-2* have an asymmetric enhancer (ASE), which is necessary and sufficient for left-side expression and contains FoxH1 binding sites (Adachi et al, 1999; Norris et al, 1999). Interestingly, FoxH1 is expressed on both sides of the LPM, at the time of *Nodal*, *Leftys* and *Pitx2* asymmetric expression. As described for the Nodal signals transduction in A-P patterning, FoxH1 is activated by intracellular Smads that are downstream of the Activin-like receptors (Fig. 1.3). *Nodal* induction of *Lefty-2* and its own expression is mediated by FoxH1 that in turn, interacts with ASEs (Saijoh, et al, 1999; 2000). This indicates that *Nodal* is able to amplify its own and *Lefty-2* expressions throughout the LPM by acting on the ASEs (Hoodless et al, 2001; Yamamoto et al, 2001).

Pitx2 asymmetric expression is conferred by an enhancer that contains FoxH1 and Nkx2.binding sites. Therefore, the left-sided expression of *Pitx2* is initiated by Nodal signaling and is maintained by Nkx2 (Shiratori et al, 2001).

Components of the Nodal signaling pathway, including the EGF-CFC co-factor, Cryptic, FoxH1, Smad2/Smad4 regulatory complex, and Activin receptors, are all required for the maintenance of *Nodal* expression and for the induction of *Lefty-2* and *Pitx2* expressions. It is possible that the following sequence of events establishes the asymmetric expression of *Nodal, Lefty-2* and *Pitx2* in the left LPM. First, the left-sided expression of *Nodal* in the LPM is initiated by Nodal signals coming from the perinodal region. *Nodal* regulates its own expression in the left LPM in a positive feedback loop dependent of FoxH1 and activates *Lefty-2* and *Pitx2* expression on the left side of the LPM. Lefty-2 activity in the left LPM counteracts Nodal activity, leading to the abolition of *Nodal* expression in the LPM. *Pitx2* on the left LPM triggers situs-specific morphogenesis of organ primordia.

1.7.3. Breaking of symmetry

As mentioned above, the first overt morphological L-R asymmetry is the heart loop, and is followed by embryonic turning and situs-specific morphogenesis of many organs. This way, breaking of symmetry and L-R polarity must occur before these

events (step 1). Several lines of evidence suggest that the symmetry is first broken, in the mouse, at the neural fold stage (pre-somite stage) in or near the node. The use of several chemical compounds were shown to cause *situs inversus* in the mouse embryo, at E8.0 (reviewed in Fujinaga, 1997). In particular, the use of agonists of α1 adrenoreceptors and KN-62, a Ca 2+/calmodulin dependent kinase II antagonist caused situs inversus in a narrow time window at pre-somite stage. Second, L-R asymmetry in gene expression first becomes apparent in small domains adjacent to the node (in the mouse: *Nodal, Lefty-1* and *Cerl-2* genes).

In the mouse two classical mutations show defects correlated with the initial L-R determination step: *iv/iv* and *inv*. The *iv/iv* mutation is a recessive mutation in which L-R specification is randomised (randomisation of gene expression means that the genes that are normally asymmetric, can be found in the left, right or in both sides). The *iv/iv* encodes for left-right dynein (Lrd), a protein related to axonemal dynein (Supp et al, 1997, 1999). The *iv/iv* mutation generates immotile cilia in the node. Lrd may be a component of a motor that carries certain molecules essential for cilial motility. The *inv* mutation is a recessive insertional mutation in which L-R specification is reversed (Yokoyama et al, 1993). All *inv/inv* mice show *situs inversus* along with kidney defects. The *inv* gene encodes for a protein (called inversin) that contains ankyrin repeats (Mochizuki et al, 1998; Morgan et al, 1998). Other mutants have been described in which randomisation of L-R axis was observed e.g. *Kif3A* (Marszalek et al, 1999; Takeda et al, 1999) and *Kif3B* (Nonaka et al, 1998). The L-R defects observed in these mutants are due to the lack of node monocilia. *Kif3A* and *Kif3B* encode for kinesin superfamily proteins (KIFs) that function in intraciliary transportation of materials for ciliogenesis of motile primary cilia.

1.7.4. Nodal flow

A link between cilia and L-R axis specification was recently established. Cells on the ventral side of the node (node pit cells) are known to possess a monocilium (Sulik et al, 1994). These cilia project into the extraembryonic space. These cilia are called primary cilia due to its 9+0 structure. (There is also another type of cilia 9+2 containing a ring of 9 peripheral doublets of microtubles plus 2 central microtubles; 9+0 lack the central microtubles. 9+2 cilia can be found in the respiratory epithelium whereas 9+0 are present in the embryo node). *In vivo* observations (Nonaka et al, 1998)

revealed that the node monocilia are indeed motile and move rapidly in a clockwise direction. This rotation generates a leftward flow (nodal flow) of the extraembryonic fluid around the node that may transport an unknown factor that acts as a left determinant.

In an elegant experiment, the nodal flow was unequivocally shown to be essential in L-R axis specification. By culturing embryos in an artificial chamber, embryos were subject to an artificial rightwards flow that caused the inversion of the L-R polarity of the embryos. In addition, when *iv/iv* mutant mice were subject to the artificial flow in the normal leftward direction, the correct L-R development was rescued (Nonaka et al, 2002).

The nodal flow was proposed to be required to transport a morphogen that becomes accumulated on the left side of the node (reviewed in Hamada, 2002). Although the molecule that might be carried by the nodal flow is unknown, growth differentiation factor 1 (Gdf1) may be a good candidate. *Gdf1* encodes for a TGF-β molecule that is expressed in the node and bilaterally in the LPM (Rankin et al, 2000). *Gdf1* null mutants lack left-sided expression of *Nodal*, *Lefty-2* and *Pitx2*, which is consistent with an initial role in L-R patterning. Another candidate for the L-R determinant is *Nodal* itself.

Nodal flow may be impaired in several mouse mutants. As mentioned above, the *iv/iv* mutants have immotile cilia and therefore lack the leftward flow. *Kif3A* and *Kif3B* mutants show randomised situs due to the lack of primary cilia in the node. The *inv* mutation remains largely unexplained. In the *inv* mutants, the node is deformed, but cilia are present and are motile. Unexpectly, despite the majority of null mutant display *situs inversus*, the nodal flow is leftward and not rightwards as may have been predicted. Nevertheless, the flow is affected, since it is turbulent (Okada et al, 1999).

In a recent study of fluid dynamics, Cartwright at al (2004) explained the mechanism of nodal flow in physical terms. Using quantitative measures the authors were able to characterize the fluid flow and calculate the time in which a given morphogen can be displaced across the node. The conclusions drawn by the authors state that only a tilt in the monocilia towards the posterior side can explain the global leftward observed in the node by Nonaka et al (1998). The calculations predict that in *inv* mutants, the cilia tilting is diminished, generating a less efficient fluid flow to the left side. This leads to an increase in the time needed for a molecule to be displaced by the cilia and therefore, the diffusing morphogen arrives at the node floor on the right

side of the node and activates right side receptors instead of the left. The authors favour a hypothesis in which the nodal flow function is the left-side displacement of a morphogen and rule out the possibility that the cilia may act as mechanosensors, as has been proposed by McGrath et al, 2003 (see below).

1.7.5. Upstream of Nodal expression

In a recent report (McGrath et al, 2003) the intracellular calcium in the node cells was shown to be the first molecular L-R asymmetric distribution in the mouse embryo. According to the authors in the node there are two types of cilia: motile and immotile. The motile cilia are confined to the central region and the immotile cilia are distributed in the periphery of the node. Motile cilia create the leftward flow that is sensed by the immotile cilia that trigger an increase of intracellular calcium. By this mechanism, the immotile cilia cells located on the left side become different from the ones on the right side of the node, with respect to calcium that can trigger the cellular responses that will lead to differential gene expression. This model attributes a novel role to the monocilia: mechanosensing; and for the first time implicates intracellular calcium in the specification of the L-R axis.

Extracellular calcium has also been implicated in L-R patterning in the chick (Raya et al, 2004). Asymmetric distribution of calcium precedes asymmetric gene expression of *Notch* in Hensen´s node. The authors uncovered a mechanism in which *Notch* is activated by the transient accumulation of extracellular calcium, which in turn depends on left-right differences in H^+/K^+-ATPase activity. The involvement of H^+/K^+-ATPase transporter had previously been implicated in L-R development in chick and Xenopus (Levin et al, 2002).

In mouse, zebrafish, and chick, *Notch* signaling activity in the node region (although symmetric) is responsible for the activation of *Nodal* expression (Raya et al, 2003; Krebs et al, 2003). It was noticed that in *Delta-1* mutant mice, *Nodal* expression in the node is absent, leading to L-R abnormalities. Whether *Notch* activation in the mouse node is also dependent on local extracellular calcium, as in chick, awaits further research.

Although, the mechanism responsible for *Nodal* activation in the node, by the *Notch* pathway seems conserved among vertebrates, the molecular events that determine the asymmetric activity of this cascade were only traced in the chick embryo. This

subject is of primordial interest, since it can harbour the answer to the central question: how is symmetry broken in vertebrates, particularly, in mammalian embryos.

Nevertheless, the breaking of symmetry in the embryo may occur at previous stages. For example, it was proposed to occur between cleavage and gastrula in the frog, and at early-streak stage in chick embryo. Pharmacological or genetic perturbation of endogenous gap junctional communication at these early stages disrupts expression of normally unilaterally expressed genes and alter organ situs (Levin and Mercola, 1998; Levin and Mercola, 1999). This implies that the breaking of symmetry in these species occurs prior to the node formation. Whether the same happens in the mouse embryo is not known since the first asymmetries reported so far occur after gastrulation and are correlated with the nodal flow generated by node monocilia.

The existence of ciliated cells in structures analogous to the mouse node in chick, *Xenopus* and zebrafish (Essner et al, 2002), suggests a possible conserved role for monocilia in the establishment of L-R asymmetries. Interestingly, the presence of ciliated cells in these specialised structures occurs prior to asymmetric *Nodal* expression in all species analised. Whether the node monocilia play important roles, in symmetry breaking, in other vertebrates, as in the mouse is not known But al least in the chick and *Xenopus*, the breaking of symmetry occurs at earlier stages.

Moreover, in zebrafish, the importance of specific gene expression in ciliated cells of the node equivalent, the kupfer's vesicle (KV) revealed to be essential for correct L-R development. The specific knock-down of *Notail* (the *Brachyury* fish homolog), generates L-R defects in the zebrafish embryo (Amack and Yost, 2004). These defects include randomisation of *Lefty1* and *Lefty-2* expression and inverted cardiac looping. The targeted cells still have cilia, however, the shape and organization of the KV is highly affected. In another report (Hashimoto et al, 2004) the Cerberus/Dan family protein Charon was shown to be a negative regulator of Nodal signaling during left-right patterning in zebrafish. *Charon* is expressed around the KV in a horse-shoe shape domain. This protein functions as a Nodal inhibitor and *Charon* specific knock down by morpholino injection yielded embryos with L-R abnormalities evidenced by randomisation of gene expression in the lateral plate mesoderm and diencephalon, and defects in heart formation. Morpholino-mediated inhibition of *Charon* and *Southpaw* (one of the *Nodal* homologs in the zebrafish) led to a reduction or loss of expression of the left side-specific genes, suggesting that *Southpaw* is epistatic with *Charon* in left-side formation. This data indicate that antagonistic

interactions between Cerberus/Dan and Nodal proteins in the adjacent region of the KV, play an important role in L-R patterning in zebrafish. This process, may be mediated by *Notail,* since it is one possible *Nodal* target gene, though this hypothesis needs further investigation.

1.7.6.Transfer of molecular asymmetries

After the initial symmetry breaking, the left-biased information needs to be transfered to the left LPM (step 2). How is this goal achieved? In the mouse this mechanism is largely unknown. However in the chick embryo, one molecule that mediates this process was identified. It was named Caronte, is a member of the Cerberus/Dan family (Rodriguez-Esteban et al, 1999; Yokouchi et al, 1999) and functions as a BMP inhibitor. It is expressed in the paraxial mesoderm, in the vicinity of the node, simetrically, and spreads to the left LPM where it can induce *Nodal* expression. *Nodal* induction was proposed to be via BMP inhibition, since the activation of *Nodal* ectopically in the right LPM can be mimicked by Noggin and the excess of BMP protein in the left side blocks *Nodal* endogenous induction in the left LPM- According to the data, the transfer of left-biased signals from the node to the left LPM, may be performed by Caronte. *Caronte* starts to be expressed in the node vicinity, downstream of *Shh*, spreads to the left LPM, where it inhibits BMP, therefore, allowing the expression of *Nodal*. On the right LPM, *Caronte* is not present, and *Nodal* expression is repressed by the presence of BMP signaling (reviewed in Capdevilla et al, 2000).

In the mouse, a molecule with similar function to *Caronte* was not described and therefore two possibilities arise to explain the transfer of left side information from the node to the left LPM. The first hypothesis is the existence of a diffusible molecule that can travel from the node to the LPM. The second mechanism could be via intercellular signaling across the cells in between the node and the LPM (reviewed in Hamada et al, 2002). So far, there are no evidences favouring any of the hypothesis presented.

1.8 - Objectives

1.8.1. – Functional characterization of *Cerberus-like*

As mentioned above (section 1.6.3), secreted antagonists of Nodal, BMP and Wnt play key roles in mouse development, by modulating signaling activities in the embryo. In this context, when Cerberus was first identified in Xenopus raised great interest since it has multi-antagonist activities (Bouwmeester et al, 1996; Piccolo et al, 1999). However, its inactivation by morpholino injection in the early *Xenopus* embryo (Silva et al, 2003) failed to show a defective phenotype. Moreover, the mouse homolog, Cerberus-like is simultaneously an anti-BMP and anti-Nodal molecule, expressed in the mouse AVE, definitive endoderm emerging from the node and later, in somites (Belo et al, 1997; 2000). The early domains of expression and functional activities of *Cer-l* are consistent with a role in rostral neuroectoderm induction (AVE) and later, in the refinement of neural patterning imposed by the node derivatives (prechordal plate). However, *Cer-l* null mutants failed to yield phenotypic defects. Nevertheless, the importance of the regulation of the Nodal and BMP signaling pathways was clearly established, and it may involve functional redundancy between its players. Thus, it is possible that in the mouse, *Cerberus-like* loss-of-function may be compensated by other molecules, namely, BMP and/or Nodal antagonists. With the purpose to test this hypothesis we generated several double mutants.

The first candidate gene tested for a genetic interaction with *Cer-l* was *Noggin*. Both genes are BMP4 inhibitors and share domains of expression in the node derivatives. Therefore we assessed for a genetic compensation during the forebrain induction. The results of this study are presented in chapter 3.

The second candidate gene studied was the homeobox transcription factor *Goosecoid (Gsc)*. *Xenopus Goosecoid*, when overexpressed in *Xenopus* embryos may lead to the formation of a double body axis, revealing essential roles in embryonic organizing activity. In the mouse, *Gsc* is co-expressed with *Cer-l* in gastrulation, in the prechordal plate and was shown to be involved in the ventral patterning of the skull. In addition, *Gsc* mutant mice do not display gastrulation defects, as predicted by its expression domain in the anterior primitive streak and node derivatives, therefore, *Gsc* may be redundant with another gene that acts in a commom pathway. In order to test if

Cer-l and *Gsc* play redundant roles during embryogenesis we generated double *cer-l;gsc* null mutants. The results of this study are presented in chapter 4.

As described in section 1.5, *Nodal* has multiple essential functions during mouse development. Hence, the regulation of its activity is absolutely required. *Cer-l* was shown to be an important antagonist that shares redundant functions with *Lefty-1*. Here, we tried to modulate Nodal activity by genetic manipulation in order to better understand the biological roles of this signaling pathway. Our approach was to inactivate *Cer-l* in the context of the *Cripto* null mutant. *cripto* $^{-/-}$ mutants display severe defects at early stages of development, since they are not able to correctly position the A-P axis. Our approach was to generate *cer-l;cripto* double mutants. Cer-l inhibits Nodal by direct protein-protein interaction, so, in the absence of Cer-l we predict that the Nodal protein levels may be increased. By disrupting *cripto* function, we prevent Cripto-dependent Nodal signaling. In this context, Nodal may exert some of its functions by an alternative pathway apparent by the rescue of *cripto* null mutant phenotype. The results of this study are presented in chapter 5.

1.8.2 – Functional study of *Cerberus-like 2*

A novel Cerberus/Dan family member, mouse Cerberus-like 2 (Cerl2), was identified. At the protein level, it shares some similarities with mouse Cerberus-like. At the biochemical level it is also an inhibitor of Nodal and Bmp signaling. Moreover it was shown to be involved in L-R axis specification. The study of the *Cerl-2* function as well as its position within the L-R genetic cascade is one of the goals of this thesis. The results of the functional analysis of *Cerl-2* point to divergent roles of the Cerberus/Dan family members in the establishment of the vertebrate L-R asymmetry. These results will be presented and discussed in chapter 6.

Chapter 2 –Materials and Methods

Chapter 2 – Materials and Methods

2.1. Generation of double mutant mice

cer-l$^{+/-}$ animals in the C57b/6 genetic background (Belo et al, 2000) were intercrossed with *noggin*$^{+/-}$ (McMahon et al, 1998) in the 129Sv background, *gsc*$^{+/-}$ (Yamada et al, 1995) and *cripto*$^{+/-}$ (Xu et al, 1999), both of the C57b/6 background to generate double heterozygous animals that were intercrossed to obtain double null mutants. *cerl-2* $^{+/-}$ animals in the C57b/6 genetic background were intercrossed to obtain homozygous null mutants that were intrecrossed with *nodal*$^{+/-}$ (Lowe et al, 1996) animals in the C57b/6 genetic background to generate compound *cerl-2*$^{-/-}$;*nodal*$^{+/-}$ mutants.

Animals were maintained under a controlled 12h day/12h night cycle. Males and females bred overnight and females were checked for vaginal plug during the following morning. Noon of the day in which the plug was found was considered to be embryonic day 0.5 (E0.5). Embryos were collected from pregnant mothers according to the desired developmental stage. The deciduas were dissected in cold PBS, embryos were fixed overnight in 4% paraformaldehyde, and dehydrated in methanol:PBSw (PBS, 1% Tween-20) series until 100% methanol and stored at –20°C.

2.2. Genotyping

For genotyping purposes, DNA was extracted from tail biopsies of adult and newborn mice and from the extraembryonic membranes of E8.5 and older embryos. Biopsies were incubated overnight in 50 mM Tris-hCl pH8.0, 100 mM EDTA, 100 mM NaCl, 1% SDS, 0,5mg/ml proteinase K, at 55°C. After adding NaCl to a final concentration of 1M the mix was centrifuged for 15 min, the supernatant recovered, and DNA precipitated with an equal volume of isopropanol. DNA pellet was washed in 70% ethanol and ressuspended in T.E. (tris EDTA). Embryos collected earlier than E8.5 were genotyped after in situ hybridisation and taken photographies. For that, the embryos were digested in 15µl (E6.5) or 30µl (E7.5) of Tris-HCl 0,01M pH7.5, KCl 0,05M, $MgCl_2$ 2mM) with proteinase K (final concentration of 0,5mg/ml) at 55°C, overnight. pK was inactivated at 95°C for 10 min. and cooled on ice. Then, 2µl of this solution

were used for genotyping. The genotypes were determined by polymerase chain reaction according to the conditions described below:

Cerberus-like EcoF1 (5′-GAC GAA TTC ACC CAC CTG CTG ACC ACC TGC TTC C-3′) and L4 (5′- CTC TTT CTA TTT TGC CGT TTG TC-3`) yield a band of 700bp corresponding to the WT allele; and IRES2 (5`-CGT TGT GAG TTG GAT AGT TGT GG-3`) and Lacz2 (5′-GAT AGG TTA CGT TGG TGT AGA TGG-3`) yield a band of 525 bp of the mutated allele. The amplification conditions are:96°C for 1 minute, 57°C for 1 minute, 72 °C for 1min. and 15 sec., 32 cycles.

Noggin Nog1 (5′- GCA TGG AGC GCT GCC CCA GC -3′), Nog 2 (5′- GAG CAG CGA GCG CAG CAG CG –3′) and βGal (5′- AAG GGC GAT CGG TGC GGG CC –3′).Nog 1 plus Nog 2 yield a band of 211 bp, of the WT allele and Nog 1 plus βGal yield a band of 160 bp of the mutated allele. The amplification conditions are: 94°C for 1 min., 70°C for 30 sec. and 72°C for 45 sec., 35 cycles.

Goosecoid GF1 (5′- CAG ATG CTG CCC TAC ATG AAC GTG G -3′), GR1 (5′- GGC GTT TTC TGA CTC CTC CGA GG -3′)and NF2 (5′- GAG GAT CTC GTC GTG ACC CAT GG –3′). GF1 plus GR1 amplify a band of 600 bp and GF1 plus NF2 yield a band of 900 bp corresponding to the mutated allele. The amplification conditions are: 94°C for 1 min., 60°C for 1 min. and 72°C for 1 min, 33 cycles.

Cripto CRAE3G (5′- GCC AAG AGC CAT GAC AGA GAT GG –3′), CRAIS2 (5′- GGG GAC AGG GCT GCT CAG TGT CGC –3′) and KOTPNEO (5′- AGC GCA TGC TCC AGA CTG CCT T –3′). CRAE3G and CRAI2S yield a band of 308 bp of the WT allele and CRAI2S and KOTPNEO yield a band of 125 bp corresponding to the mutated allele. The amplification conditions are: 94°C for 1 min, 57°C for 1 min. and 72°C for 30 sec., 35 cycles.

Cerberus-like 2 GenCer2Fwd (5′- GGA AGA TTT TAT GCA AGC AAG AGT GTG G –3′), P3 (5′- CAC ACA GCT GTT GCA GAA GAC –3′), and Lower2 (5′- GGT GAC TTC TTT TTT GCT TTA GCA GG –3′). GenCer2FWD and Lower2 yield a band of 300 bp corresponding to the WT allele, and Lower 2 and P3 yield a band of 500 bp corresponding to the mutated allele. The amplification conditions are: 94°C for 1 min., 60°C for 1 min. and 72°C for 45 sec., 32 cycles.

Nodal F1 (5′- AAG AGA GGA AAG TAG GCT TGC –3′), R4 (5′- GCG AAC AGA AGC GAG AAG C –3′) AND 3F3 (5′- GCA CAT AAG AAC TGA TGG TGG TGC CTG –3′). F1 and 3F3 yield a band of 240 bp corresponding to the wt allele, F1 and R4

yield a band of 560 bp corresponding to mutated allele. The amplification conditions are: 94°C for 1 min., 60°C for 1 min. and 72°C for 1 min., 30 cycles.
All PCRs were done using #10 PCR buffer (10X; Promega), 0,2mM dNTP mix (Roche), 2U Taq polymerase (MBI Fermentas), 0,8 μM of each primer, in a final volume of 25μl, diluted in Nuclease-free water (Promega).

2.3. Skeletal analysis

For the skeletal analysis of the neonates, Alcian blue/ Alizarin red staining was performed as in Belo et al. (1998). Briefly, skin and viscera were removed from the newborn mice, tissue fixed in ethanol 95% overnight and stained with 0,045% Alcian blue, 80% ethanol and 20% acetic acid for 3 days. Placed in 95% ethanol for 12 hours, digested in 2% KOH for 12 hours and stained with 0,03% Alizarin red S (Sigma) in 1% KOH for 12 hours. Specimen were cleared with 1% KOH, 20% glycerol and passed through glycerol/ethanol solution series: 50%, 80%, 100% glycerol.

2.4. mRNA antisense probe preparation and labelling

Plasmids containing probes for molecular markers were linearized using restriction enzymes that cut at the 5´end. DNA inserts were transcribed using 10 U of RNA polymerase (T3, T7 or SP6) that produces an antisense transcript. Transcription reaction was performed using 1μg of template DNA, 10X transcription buffer (Boheringer Manheim), RNA guard (Roche) and 10X labelling mix in RNAse free water. Probes were labelled either with Digoxigenin labelling mix (Boheringer Manheim) or Fluorescein labelling mix (Boheringer Manheim; for double in situ experiments). Transcription reaction occurred at 37°C for 2 h. The RNA probes were spun through Quick Spin Columns (Boehringer Mannheim) to remove unincorporated nucleotides and stored at -70°C.

2.5. mRNA *in situ* hybridisation

Whole mount in situ hybridisation and anti-sense probe preparation was carried out as described in Belo et al. (1997). All solutions were treated with DEPC and filtered. The hybridization vials and caps were treated with RNAZap (Ambion). All

steps before pre-hybridization were performed on ice except the proteinase K treatment. Embryos were fixed in 4% paraformaldehyde/PBSw (PBS + 0.1% Tween-20) at 4°C overnight. The embryos were treated with proteinase K/PBSw (4.5 mg/ml) at room temperature (3 min for day 6 embryos, 5 min for day 7.5 embryos, 7 min for day 9.5 embryos, 9 min for day 10.5 embryos or 11 min for day 11.5 embryos). Digestion was stopped by washing in freshly prepared 2 mg/ml glycine/PBSw. The embryos were re-fixed in 4% paraformaldehyde –0.2% glutaraldehyde/PBSw for 15 min, prehybridized (in 50% formamide, 5´ SSC (pH 7.0), 1% Boehringer Mannheim blocking reagent, 100 mg/ml heparin, 0.1% Tween-20, 1 mg/ml Torula tRNA, 0.1% CHAPS and 5 mM EDTA) at 65°C for 3 h. The embryos were hybridized at 70°C overnight in probe solution (pre-hybridization solution containing 200 ng/ml of heat denatured probes). For double in situ experiments, both probes were hubridized at the same time. The embryos were washed in pre-hybridization solution, then in a 1:1 dilution of pre-hybridization buffer and 2X SSC (pH 4.5) at 70°C, then in 2X SSC (pH 7.0)/0.1% CHAPS at 70°C and finally in maleic acid buffer (MAB;100 mM maleic acid, 150 mM NaCl (pH 7.5)) at 70°C (30 min each) and washed in PBSw at room temperature. The embryos were then incubated in blocking solution (10% heat inactivated goat serum, 1% Boehringer Mannheim blocking reagent/PBSw) for 2 h at 4°C. The antibody conjugate was pre-adsorbed in blocking solution at a dilution of 1:10 000 for 2 h at 4°C. Embryos were washed five times in 0.1% BSA/PBSw (45 min each) and in PBSw (2 ´ 30 min), changed to alkaline phosphatase buffer twice for 10 min at room temperature and stained in BM purple substrate (Boehringer Mannheim) or NBT-BCIP (Roche) at 4°C in the dark (a few hours to several days). For double in situ experiments, after stopping the development the first reaction with NBT-BCIP in PBSw, alkaline phosphatase was inactivated in methanol series 25%, 50%, 75%, 100%, 75%, 50%, 25% in PBSw, 5 min each step and embryos undergone blocking, anti-fluorescein Ab incubation, washes and development with INT-BCIP (Roche) to develop the second probe, in the same conditions as described for the first antibody.

2.6. Histology

Embryos used for histology after mRNA in situ hybridization were embedd in 7,5% gelatin (SIGMA) in 15% sucrose (SIGMA), frozen on cool isopentan. Blocks were cut at 12µm using a cryostate and mounted onto glass slides with Aquatex

(Merck). Newborn hearts of *cerl-2* mutants were fixed in 4% paraformaldehyde, dehydrated in ethanol and embedded in paraffin. Blocks were cut at 8μm in a microtome, mounted onto glass slides, dewaxed and eosin/hematoxylin stained.

2.7. Cloning of the full length *Cerl-2* cDNA

A cDNA clone (GenBank AA289245) containing the second exon and the 3'UTR of *cerl-2* was obtained by database search for proteins similar to mCer-l. A hypothetical human protein (FLJ38607) was found by searching NCBI database for proteins homologous to *cerl-2* and its' corresponding cDNA blasted against the mouse genome. A primer designed to align in the predicted 5'UTR
(5'-CGGAATTCCGCCAGAAAACAACTCTCAAGCTGCTCTCC-3')
and a reverse primer complementary to the second exon of *cerl-2*
(5'-CCACACCACAGCGTCACCGATGTCCAGC-3') were used in a RT-PCR with E7.5 mouse total RNA. The resulting 5' cDNA portion was subcloned into pGEM-Teasy vector, and the full-length cDNA was assembled into pCS2+ plasmid and sequenced. The GenBank accession number for mouse *cerberus-like2* is AY387409.

2.8. Targeted disruption of the *Cerl-2* gene

A mouse 129/Ola genomic library was screened for *cerl-2* using a partial cDNA clone (GenBank AA289245), and 2 positive clones were obtained.
In our targeting vector a 0.6 Kb SmaI/NcoI DNA fragment containing the second exon was replaced with a neomycin and a lacz cassette. The linearized vector was electroporated into 129/Ola embryonic stem cells. One heterozygous embryonic stem cell clone was used to generate chimeric mice by blastocyst injection, and mutant animals were bred in both 129/Ola and 129/Ola X C57BL/6J mixed background. Genotyping was done by Southern blotting and PCR assays. For Southern blot analysis, genomic DNA was digested with PstI and hybridized with a 3' probe. The 3' probe was a 1.0Kb (PstI / XbaI) genomic DNA fragment downstream of the 3' recombination arm. Primers for PCR analysis were
P1 (5'-GGAACCACCTTTGTAGTCAAGACTGG-3'),
P2 (5'-GGTGACTTCTTTTTTGCTTTAGCAGG-3'),
P3 (5'-CACACAGCTGTTGCAGAAGAC-3').

2.9. mRNA Synthesis, Microinjection and RT-PCR analysis

Capped sense mRNAs were synthesized using Ambion mMessage mMachine kit. In vitro fertilization, microinjection of *X. laevis* embryos and RT-PCR analysis were performed as described previously (Belo et al. 2000; Bouwmeester et al. 1996). The primer sets used are described in http://www.hhmi.ucla.edu/derobertis/protocol_page/oligos.PDF. For all RT-PCR reactions *ef1* was used as loading control. Detailed description of the expression constructs used are available from the authors on request.

2.10. Co-immunoprecipitation Analysis

A Flag-tagged version of *cerl2* was constructed by standard PCR methods and subcloned in pCS2+, using the above mentioned forward primer and the following reverse primer :
(5'-CCGCTCGAGTCACTTATCGTCGTCATCCTTGTAATCTCCTCCTCCCAGCTT CGGGCGGCACTGACACTTCTGG-3'). 1 ng and 5 ng of HA*Xnr1* and Flag*cerl-2* mRNA, respectively, were injected in the animal poles of *Xenopus* embryos and co-immunoprecipitation was performed as previously described (Yeo and Whitman, 2001). Anti-Flag mouse monoclonal antibody (Sigma) and anti-HA rabbit polyclonal antibody (Covance), were used for immunoprecipitation and Western blot analysis. Proteins were visualized using ECLWestern blotting detection reagents (Amersham Pharmacia Biotech,Piscataway, NJ).

Chapter 3 – Results I

Chapter 3 – Results I

The BMP antagonists Cerberus-like and Noggin do not interact during mouse forebrain development

Ana Cristina Borges [1,2] , Sara Marques [1] and José António Belo [1,2]

1. Instituto Gulbenkian de Ciência, Rua da Quinta Grande 6, Apartado 1781-901 Oeiras
2. Faculdade de Engenharia de Recursos Naturais, Universidade do Algarve, Campus de Gambelas, 8000-010 Faro, Portugal

Published in International Journal of Developmental Biology (2001) 45: 441-443.

The contribution of A. C. Borges for this paper was the elaboration of experimental work (with the exception of mRNA in situ hybridisation, performed by the second author S. Marques), analysis and interpretation of results and writing of the manuscript.

3.1. Abstract

Mouse *Cerberus-like* encodes for a secreted factor of the Cerberus/Dan family. This molecule has neural inducing capabilities and can bind to BMP-4 and Nodal molecules in the extracellular space. When *Cerberus-like* is inactivated, its function may be compensated for another molecule, since no abnormalities can be observed in the mouse mutant. Compensation mechanisms have been shown to occur between the BMP antagonists Chordin and Noggin. Here we report the generation of *Cerberus-like*$^{-/-}$;*Noggin*$^{-/-}$ double mutants to uncover a possible compensation by *Noggin* in *Cer-l*$^{-/-}$ mutant. Double mutants were obtained and failed to show any further detectable defects beside the ones presented by the *Noggin*$^{-/-}$ single mutant. Contrarily to *Chordin* and *Noggin*, mouse *Cerberus-like* and *Noggin* cannot compensate for each other during mouse embryogenesis.

3.2. Introduction

The secreted factors Chordin, Noggin, Follistatin and Cerberus (Reviewed in De Robertis *et al.*, 1997) share a common biochemical activity: BMP-4 (bone morphogenetic protein-4) inhibition by direct binding to it (Iemura *et al.*, 1995; Piccolo *et al.*, 1996; Zimmerman *et al.*, 1996; Piccolo *et al.*, 1999). This antagonism leads to a graded inhibition of ventral BMP signaling and is essential for neural induction and dorsoventral patterning of the vertebrate embryo (De Robertis and Sasai, 1996).

Xenopus Cerberus (*Xcer*) encodes for a secreted protein with neural inducing activity (Bouwmeester et al., 1996). Besides having anti-BMP-4 activity, XCer was shown to inhibit Xnr-1 (Xenopus nodal related-1) and Xwnt-8 by direct binding to them (Piccolo *et al.*, 1999). In the mouse embryo, a gene related to *Xenopus Cerberus*, mouse *Cerberus-like* (*Cer-l*) was isolated (Belo *et al.*, 1997; Biben *et al.*, 1998; Shawlot *et al.*, 1998). This gene starts to be expressed at E5.5 in the Anterior Visceral Endoderm (AVE). At neural plate stage, the expression is found in the endoderm underlying anterior neural plate. In histological sections, expression is found in all cells of the midline from the rostral end of the embryo to the proximity of the node, and includes anterior endoderm and mesoderm from the prechordal and notochordal plates (Belo *et al.*, 1997). Animal cap explants experiments led to the conclusion that both *Xcer* and *Cer-l* can induce the same molecular markers like *Otx2*, although *Cer-l* mRNA was not

able to induce ectopic head-like structures as in the case of *Xcer* mRNA injection. Later, it was demonstrated that Cer-*l* exhibits anti-BMP as well as anti-Nodal activities, but unlike *Xenopus* Cerberus cannot inhibit XWnt8 signaling. This activity together with its expression in the AVE, a tissue implicated in the induction of the forebrain, suggested that Cer-l could be an important factor for head development (Belo *et al.*, 1997). However, careful phenotypical analysis of induced *Cer-l*$^{-/-}$ loss of function animals failed to show any defect (Belo *et al.* 2000; Stanley *et al.*, 2000; Shawlot *et al.*, 2000).

This result suggests that some genes may be compensating for the lack of function of *Cer-l*. This phenomenon was shown to occur between the BMP inhibitors Chordin and Noggin, as described in Bachiller *et al.* (2000). Targeted inactivation of *Noggin* originates a recessive lethal phenotype during embryogenesis. The mutants display a vast number of defects in spinal cord and somites (McMahon *et al.*, 1998; Brunet *et al.*, 1998). *Chordin* null mutation results in stillborn animals which show abnormalities in ear development, pharyngeal and cardiovascular organization (Bachiller *et al.*, 2000). Both genes are expressed in the node of the mouse embryo, at late gastrula stage. Later they are co-expressed at the level of the notochordal and prechordal plates. The double homozygous *Chordin;Noggin* mutants present defects at the level of the forebrain development in addition to defects related to left-right patterning and mesoderm maintenance (Bachiller *et al.*, 2000). In that study the double mutant shows defects not exhibited by the single mutations alone, meaning that some compensation was occurring when only one BMP inhibitor was missing.

This fact led us to test whether *Cer-l* and *Noggin* could compensate for the lack of function of each other. Although *Cer-l* has other activities, they are both BMP-4 inhibitors sharing some domains of expression at the level of the prechordal and notochordal plates. In the present work, we used a similar approach as in Bachiller *et al.* (2000) for the generation of *Cer-l;Noggin* double mutants.

3.3. Results and Discussion

With the purpose of analysing *Cer-l;Noggin* double mutants, 160 neonates resultant from intercrosses of compound heterozygous mice (*Nog*$^{+/-}$;*Cer-l*$^{+/-}$) were recovered. Among them, 5 resembling *Noggin* mutants (McMahon et al. 1998) were

born dead, presented open neural tube, shortened body axis, truncated limbs, no tail and variability in cranial neural tube closure. After genotyping the neonates by PCR (Figure 3.1), it was found that all possible genotype combinations were observed (Table 3.1) but not in accordance with the expected Mendelian rate: the combinations $Nog^{-/-};Cer\text{-}l^{+/+}$, $Nog^{-/-};Cer\text{-}l^{+/-}$ and $Nog^{-/-};Cer\text{-}l^{-/-}$ accounted for only 5 newborns while a total of 40 were expected, a sign of embryonic lethality. Contrarily to all other genotypes, these combinations display the defects described above. The common feature of these three genotypes is the Noggin homozygous mutation. All $Nog^{-/-}$ neonates, independently of the

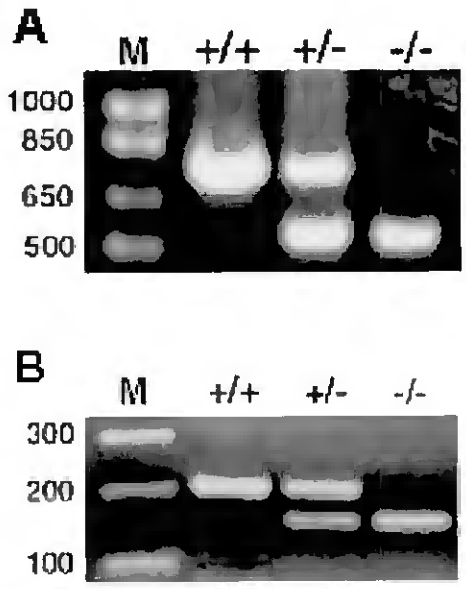

Figure 3.1. PCR analysis of intercrosses. **(A)** genotyping for *Cerberus-like* wild type and mutated alleles. **(B)** *Noggin* genotyping. The molecular marker (M) is on the left lane, the numbers indicated correspond to base pairs (bp).

Table 3.1- Genotyping results of the neonates recovered from *cer-l*$^{+/-}$;*nog*$^{+/-}$intercrosses

	$Nog^{+/+}Cer^{+/+}$	$Nog^{+/+}Cer^{+/-}$	$Nog^{+/+}Cer^{-/-}$	$Nog^{+/-}Cer^{+/+}$	$Nog^{+/-}Cer^{+/-}$	$Nog^{+/-}Cer^{-/-}$	$Nog^{-/-}Cer^{+/+}$	$Nog^{-/-}Cer^{+/-}$	$Nog^{-/-}Cer^{-/-}$	N
No. Observed	19,00	21,00	14,00	29,00	45,00	27,00	1,00	2,00	2,00	160,00
No. Expected	10,00	20,00	10,00	20,00	40,00	20,00	10,00	20,00	10,00	160,00
% Observed	11,88%	13,13%	8,75%	18,13%	28,13%	16,88%	0,63%	1,25%	1,25%	100,00%
% Expected	6,25%	12,50%	6,25%	12,50%	25,00%	12,50%	6,25%	12,50%	6,25%	100,00%

N=number of neonates recovered

Cer-l genotype display severe abnormalities, the same ones as described for *Noggin* null mutation (McMahon *et al.* 1998).

In contrast, *the Cer-l* null mutant neonates do not show any defects (as reported in Belo *et al.*, 2000; Stanley *et* al., 2000; Shawlot *et al.*, 2000). $Nog^{+/-};Cer\text{-}l^{-/-}$, a genotype that could lead to defects related to a dose dependent mechanism, are also normal, at least by observation of the external morphology. Curiously, the double mutants $Nog^{-/-};Cer\text{-}l^{-/-}$ show the same set of abnormalities as the $Noggin^{-/-}$ mutant alone.

We decided to assess for morphological defects at the base of the cranium by Alcian blue/ Alizarin red staining. The skulls were dissected to allow the careful observation of its base (Figure 3.2). Again, defects were observed only in *Noggin* mutants, independently of the *Cer-l* genotype (compare Figures 3.2A, 3.2B, 3.2C with 3.2D, 3.2E, 3.2F). Due to $Nog^{-/-}$ mutation, skeletal preparations are fragile and some bones may be broken during the procedure. In these preparations we can observe the fusion of presphenoid, basisphenoid and basioccipital bones (Figure 3.2D, 3.2E, 3.2F). This can readily be seen because frontal, parietal and interparietal bones are loose or absent. In the cases where these bones were absent, the neonates had the brain exposed at birth. In addition, occipital condyles are also loose, showing variability in the distance separating them. In cases of a large separation between the two occipital condyles, the occipital and basioccipital bones might not remain in place during bone/cartilage staining procedure, leading to differences in the preparations obtained (Figure 3.2F). Nevertheless, these differences are caused by an artifact rather than a defect in the occipital and basioccipital bones. These bones were always present and were not affected in abnormal animals. This abnormal phenotype at the base of the cranium was observed in $Nog^{-/-};Cer\text{-}l^{+/+}$, $Nog^{-/-};Cer\text{-}l^{+/-}$ and $Nog^{-/-};Cer\text{-}l^{-/-}$, meaning that the additional loss-of-function of *Cer-l* does not cause any abnormality besides the ones presented by *Noggin* single mutants.

We then, dissected pregnant mothers at E9.5 and E10.5 to assess for defects visible only at earlier stages of development. The yolk sac was used for genotyping these embryos. Embryo genotyping results are resumed in Table 3.2. By these results one can see that all genotype combinations are now present approximately at the expected Mendelian ratio. We found 8 empty deciduas meaning that some embryos are reabsorbed during development, due to embryonic lethality.

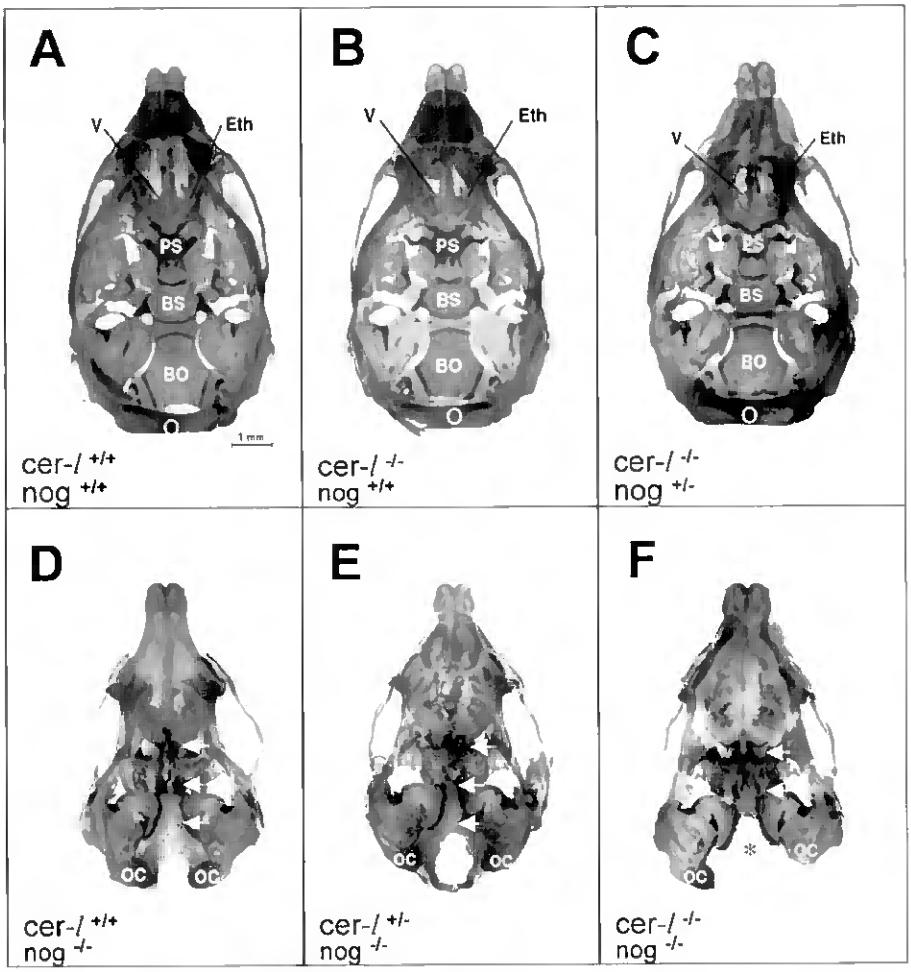

Figure 3.2. *Cer-l*$^{-/-}$;*Nog*$^{-/-}$ neonates show bone fusions in the base of the cranium, the same defect presented by *Nog*$^{-/-}$ single mutants. Dorsal views of the base of the cranium. (A) Wild type neonate. (B) *Cer-l*$^{-/-}$;*Nog*$^{+/+}$ and (C) *Cer-l*$^{-/-}$;*Nog*$^{+/-}$ littermates do not present defects. (D) *Cer-l*$^{+/+}$;*Nog*$^{-/-}$ shows fusion of the presphenoid (PS), basisphenoid (BS) and basioccipital (BO) forming a single unit (arrows) and absence of cartilage between these bones. (E) *Cer-l*$^{+/-}$;*Nog*$^{-/-}$ displays the same set of defects as the ones observed in *Cer-l*$^{+/+}$;*Nog*$^{-/-}$. (F) *Cer-l*$^{-/-}$;*Nog*$^{-/-}$ double mutant exhibits the same abnormalities as in (D) and (E). Absence of BO (*) is result of degradation of the tissue during preparation of the specimen. The removal of N*er-l* and *Noggin* does not alter the phenotype observed in the *Nog* single mutant (compare with panels D and E). The skeletons of neonate mice were stained with alcian blue and alizarin red for cartilage and bone, respectively. BO, basioccipital; BS, basisphenoid; Eth, ethmoid; O, occipital; OC, occipital condyles; PS, presphenoid; V, vomer;.

Once again, all *Noggin* mutants (regardless of *Cer-l* genotype) show abnormalities in neural tube closure, particularly in the brain vesicles between diencephalon and myelencephalon, but sometimes from the diencephalon to the caudal limit of the embryo.

In order to uncover the existence of dorsoventral patterning defects caused by excessive BMP-4 activity, we performed *Sonic hedgehog (Shh)* mRNA *in situ*

hybridization in embryos of E10.5 At this stage, in the Wt, *Sonic hedgehog* is expressed in the ventral diencephalon, floor plate and notochord (Figure 3.3). Expression is also detected in the zone of polarizing activity of the limb buds.

In the *Noggin* null mutant *Shh* expression pattern is unaltered at the level of the central nervous system (CNS) and forelimbs but is severely reduced at hindlimb level, where no *Shh* expression is detected at the ventral midline of the neural tube (McMahon et al., 1998). Interestingly, the same result was obtained for double mutants *Cer-l*$^{-/-}$;*Nog*$^{-/-}$. Also, expression at the level of the CNS seemed unaltered in *Cer-l*$^{-/-}$;*Nog*$^{-/-}$ mutants (Figure 3.3B, 3.3C). *In situ* hybridization using *En-1*, a mid-hindbrain and limb bud

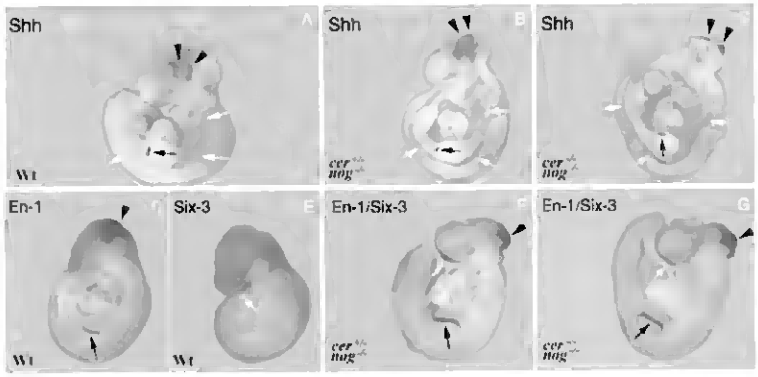

Figure 3.3. mRNA *in situ* hybridization in E10.5. **(A)** wild type embryo showing *Shh* expression in the ventral fore- midbrain (black arrowheads), ventral neural tube (white arrows) and forelimb ZPA (black arrow). **(B, C)** mutant embryos exhibits unaltered *Shh* expression pattern, in spite of having open neural tube in the brain (arrowheads) and anterior spinal cord. **(D)** Wild type embryo showing *En-1* expression in the mid-hinbrain boundary (black arrowhead) and in the limb bud (black arrow). **(E)** Expression of *Six-3* in the ventral forebrain (white arrow) in a wild type embryo. **(F,G)** Expression of *En-1* and *Six-3* shows that in the mutants the brain regionalization is not affected as judged by their expression in the forebrain (white arrows) and in the mid-hinbrain boundary (black arrowheads). *En-1* expression in the limb buds (black arrows) is also unaffected.

Table 3.2- Genotyping results of the embryos recovered from *cer-l*$^{+/-}$;*nog*$^{+/-}$ intercrosses

	Nog$^{+/+}$Cer$^{+/+}$	Nog$^{+/+}$Cer$^{+/-}$	Nog$^{+/+}$Cer$^{-/-}$	Nog$^{+/-}$Cer$^{+/+}$	Nog$^{+/-}$Cer$^{+/-}$	Nog$^{+/-}$Cer$^{-/-}$	Nog$^{-/-}$Cer$^{+/+}$	Nog$^{-/-}$Cer$^{+/-}$	Nog$^{-/-}$Cer$^{-/-}$	N
No. Observed	1,00	5,00	8,00	5,00	14,00	11,00	1,00	8,00	4,00	57,00
No. Expected	3,56	7,13	3,56	7,13	14,25	7,13	3,56	7,13	3,56	57,00
% Observed	1,75%	8,77%	14,04%	8,77%	24,56%	19,30%	1,75%	14,04%	7,02%	100,00%
% Expected	6,25%	12,50%	6,25%	12,50%	25,00%	12,50%	6,25%	12,50%	6,25%	100,00%

Number of empty deciduas: 8

N=number of embryos analysed

marker (Joyner *et al.*, 1987) and *Six-3*, an anterior forebrain marker (Oliver *et al.*, 1995) as probes, also showed no alteration in the double mutant (Figure 3.3D-G).

Defects in the midline of the cranium could also be observed in *Goosecoid-1* (G*sc*) null mutants as described by Belo *et al.* (1998). According to these authors, the midline defects of those mutants develop in close association with *Goosecoid* expressing cells at the prechordal plate. The region where the defects appear (vomer, ethmoid and presphenoid bones) is previously occupied by the prechordal plate. In *Nog*$^{-/-}$ the defective bones of the cranium are essentially the presphenoid, basisphenoid and basioccipital and the region where these bones are formed is previously occupied by notochord and prechordal plates, where *Cer-l* expression can also be observed. The fact that these midline defects are observed in *Nog*$^{-/-}$;*Cer-l*$^{+/+}$, *Nog*$^{-/-}$;*Cer-l*$^{+/-}$ and *Nog*$^{-/-}$; *Cer-l*$^{-/-}$ and not in animals with the rest of the genotypes, means that the loss of function of the *Cer-l* gene, when accumulated with the *Noggin* mutation do not cause additional abnormalities. *Noggin* transcripts can be seen at early stages of development in these structures and probably, the bone malformations observed here are related to misregulation of BMP activity in the notochordal and prechordal plates.

In addition, *Nog*$^{-/-}$ mutation causes bone malformations in the entire skeleton (Brunet et al., 1998). Misregulation of the factors that control this mechanism, like BMPs, results in lack of definition of shape of each skeletal element. This happens in the cranium of *Noggin* mutants, because some of the bones of the midline, did not acquire the correct shape becoming fused. However, the loss of function of *Cer-l* in addition to *Nog*$^{-/-}$ mutation was expected to increase BMP activity. Subsequently, this double mutation could have lead to a more severe phenotype than the ones observed in N*og*$^{-/-}$ single mutant, because the expression of both genes partially overlap in the regions where the base of the cranium will form (prechordal and notochordal plates). However, this did not occur and unless some subtle abnormalities could have been missed in this analysis, cumulative defects in *Cer-l*$^{-/-}$;*Nog*$^{-/-}$ double mutants were not found.

This is further confirmed by the *sonic hedgehog in situ* hybridization. We used this probe to assess for dorsoventral patterning defects as BMPs have been implicated in this process. Since *Noggin* and *Cer-l* are BMP antagonists, we adressed the relationship between the excessive BMP activity and the dorsoventral patterning of the CNS. *Shh* is responsible for inducing ventral cell fates and is expressed in the floor plate and dorsal

side of the notochord. Failure in CNS dorsoventral patterning would lead to displacement of expression of *Shh*. In *Nog*$^{-/-}$ single mutants *Shh* expression pattern is unaltered in the anterior region of the spinal cord and notochord. In accordance with our previous results the *Shh* expression pattern is identical in *Nog*$^{-/-}$ single mutant and in *Nog*$^{-/-}$;*Cer-l*$^{-/-}$ double mutant.

In conclusion, the interaction between *Cer-l* and *Noggin* could have led to defects at various levels. The first being defects in D-V patterning; the second being composed of mesodermal defects because BMP-4 is essential for mouse gastrulation, for mesoderm formation and neural induction (Winnier *et al.* ,1995). Excess of BMP-4 activity, in this case provided by lack of BMP inhibitors, could lead to mesoderm and more importantly to neural defects during embryogenesis. This fact was not observed in *Nog*$^{-/-}$;*Cer-l*$^{-/-}$ embryos. Defects in the head could also have been expected because *Cer-l* is expressed in the AVE and prechordal plate, tissues implicated in head induction and patterning respectively. As the single mutation of *Cer-l* did not cause any defects in head formation, we tested the genetic interaction between Noggin and *Cer-l*. Our results led to a different conclusion than the one obtained in the *Chordin;Noggin* double mutation. In that work it was found that the BMP inhibitors Noggin and Chordin could compensate for each other during development. From our results we can conclude that *Noggin* cannot compensate for the loss-of-function of *Cer-l,* since the removal of the two gene products shows only the defects visible in *Nog*$^{-/-}$ single mutants. The question that led us to test this interaction remains: which factors may be compensating for the *Cer-l* loss of function? We propose that other BMP antagonists might be performing this function. Another possibility is the existence of other members of the Cerberus family that may compensate for lack of *Cer-l* activity. Cerberus-like has also been shown to be a Nodal antagonist (Belo *et al.*, 2000). Thus, this issue should also be addressed when looking for other compensatory factors that might be rescuing *Cer-l* loss-of-function.

To clarify these questions it would be of interest to generate other double mutant combinations: *Chordin;Cer-l* to test for the compensation of the anti BMP activity; *Otx2;Cer-l* to test for the *Cer-l* function in the AVE ; *Gsc-1;Cer-l* to understand the function of *Cer-l* in the prechordal plate and in the formation of the cranium; and *Lefty-1;Cer-l* to test the compensation by other Nodal antagonist.

Chapter 4 – Results II

Chapter 4 – Results II

Goosecoid and *Cerberus-like* do not interact during mouse embryogenesis

Ana Cristina Borges [1,2,#], Sara Marques [1,#] and José António Belo [1,2]

1. Instituto Gulbenkian de Ciência, Rua da Quinta Grande 6, Apartado 1781-901 Oeiras
2. Faculdade de Engenharia de Recursos Naturais, Universidade do Algarve, Campus de Gambelas, 8000-010 Faro, Portugal

# These authors contributed equally to this work.

Published in International Journal of Developmental Biology (2002) 46: 259-262.

The contribution of A. C. Borges for this paper was the elaboration of experimental work (in collaboration with the second author S. Marques), analysis and interpretation of results and writing of the manuscript.

4.1. Abstract

Mouse Cerberus-like (Cer-l) is a neural inducer molecule, capable of inhibiting Nodal and BMP-4 signals in the extracelular space. *Cer-l* expression domain in the Anterior Visceral Endoderm (AVE) and prechordal plate, tissues involved in head induction and patterning, respectively, suggested a role for this gene in head formation. However, animals homozygous for *Cer-l* null allele failed to show any abnormality, leading us to propose the existence of other factor(s) that might compensate for *Cer-l* loss-of-function. Since *Goosecoid* (*Gsc*) shares some domains of expression with *Cer-l* and was shown to be essential for head morphogenesis, we tested its ability to interact genetically with *Cer-l*. With this aim we generated *Cer-l;Gsc* double mutants. These animals were analyzed at birth for skeletal defects and revealed the same phenotype as $Gsc^{-/-}$ single mutants. We also investigated the proper patterning of structures adjacent to the prechordal plate by performing *in situ* hybridization of HNF-3β/Foxa2, Six-3 and BF-1, genes whose expression domains remained unchanged. In conclusion, the analysis carried out suggested that *Gsc* does not compensate for *Cer-l* loss-of-function and that these genes do not interact genetically.

4.2. Introduction

Mouse *Cerberus-like* (*Cer-l*) encodes for a secreted protein that binds to BMP-4 and Nodal in the extracellular space, thus preventing the binding of these ligands to their corresponding receptors (Belo *et al.*, 2000). Its *Xenopus* counterpart, Cerberus (Xcer) was also found to be a XWnt-8 inhibitor (Piccolo *et al.*, 1999), which Cer-l was not (Belo *et al.*, 2000). *Cer-l* is expressed in the mouse embryo in tissues that are involved in head induction and patterning. At E 5.5. *Cer-l* is present in the Anterior Visceral Endoderm (AVE), the head organizing tissue; and at E7.5 *Cer*-l transcripts can be found in the anterior endoderm and mesoderm of the prechordal and notochordal plates (Belo *et al.*, 1997). Furthermore, in *Xenopus* animal cap experiments, *Cer-l* mRNA, like *Xcer*, was shown to be a neural inducer: both mRNAs induce the expression of the pan-neural marker NCAM and the anterior neural marker *Otx2* (Bouwmeester *et al.*, 1996; Belo *et al.*, 1997).

All of these results, together with the fact that the related *Xcer* mRNA is capable of inducing an ectopic head when injected in the most ventral vegetal blastomere of the *Xenopus* embryo (Bouwmeester *et al.*, 1996), suggested the involvement of *Cer-l* in the mechanism of head induction in the mouse.

Cer-l was inactivated by homologous recombination in ES cells and the resulting null mutants failed to show any defect (Belo *et al.*, 2000; Stanley *et al.*, 2000; Shawlot *et al.*, 2000). This fact led to the proposal that another factor may compensate for the loss of function of *Cer-l.* So far, no gene related to *Cer-l* has been described in the mouse, thus, the mechanism of redundancy may rely on a molecule with functional similarities. In order to test for the compensation of *Cer-l* by another BMP-4 inhibitor, we tested the interaction between *Noggin* and *Cer-l* by generating double mutants. These animals were analysed and did not display any further defects besides the *Noggin* phenotype, suggesting that Noggin is not the factor that compensates for the loss of *Cer-l* (Borges *et al.*, 2001).

Here we report a similar study with another candidate gene, *Goosecoid (Gsc).* This homeobox containing gene, in *Xenopus,* represses the expression of BMP-4 in the marginal zone (Fainsod *et al.*, 1994) and can induce the expression of *Chordin* (Sasai *et al.*, 1994), another BMP antagonist (Piccolo *et al.*, 1996). In the mouse, *Gsc* is expressed at various phases of embryogenesis (Blum *et al.*, 1992). Before gastrulation *Gsc* is expressed in the AVE (Belo *et al.*, 1998) whereas during gastrulation it is expressed in regions of the embryo with axial patterning activity – the anterior primitive streak, the node and the prechordal plate (Blum *et al.*, 1992; Belo *et al.*, 1998). At later stages of embryogenesis, at E10.5, *Gsc* is expressed in craniofacial regions, ventral body wall and limbs (Gaunt *et al.*, 1993; Belo *et al.*, 1998). Homozygous *Gsc* mutants generated by targeted inactivation in ES cells do not present any gastrulation defects, which would be related with its early phases of expression (Yamada *et al.*, 1995; Rivera-Perez *et al.*, 1995). However, the null mutants are lethal at birth due to craniofacial malformations, defects related with *Gsc* expression during later phases of embryogenesis. Later on, these mutants were the subject of a detailed analysis at the level of the base of the skull and malformations correlated with the site of expression between E7.5 and E8.5. were described (Belo *et al.*, 1998). These malformations are deletions and fusions in the midline of the prechordal chondrocranium, a region that develops in close association with the prechordal plate (where *Gsc* is expressed), thus suggesting a role for *Gsc* during gastrulation.

In addition, in the study of the genetic interaction between *Gsc* and HNF-3β/Foxa2, *Gsc* was shown to play a role in axial development. The generation of *Gsc*$^{-/-}$*;HNF3β*$^{+/-}$ mutants led to the proposal that these genes act synergistically to regulate neural tube patterning and head development (Filosa *et al.*, 1997). Double mutant studies have been very useful in the study of gene networks. For example, the *chordin;noggin* double mutant revealed the requirement of both BMP-4 antagonists emanating from the node in order to maintain the head inductive activity of the AVE (Bachiller *et al.*, 2000).

Since *Gsc* and *Cer-l* share some domains of expression in the AVE and prechordal plate, and seem to be involved in the process of head formation, we decided to investigate the existence of functional redundancy between them. With this purpose, we generated *Cer-l;Gsc* double mutants using the same approach as described in Borges *et al.* (2001).

4.3. Results and Discussion

Double heterozygous animals were intercrossed and a total of 84 neonates were recovered at birth and genotyped by PCR (Table 4.1). By analysing the results of this genotyping, we could observe that all classes of genotypes are present at approximately the expected Mendellian ratio. Within the litters recovered, 19 animals died at birth and, from the observation of the external morphology, we did not detect any differences between them. After genotyping, we could observe that these newborns belonged to three different classes: *Cer-l*$^{+/+}$*;Gsc*$^{-/-}$, *Cer-l*$^{+/-}$*;Gsc*$^{-/-}$ and *Cer-l*$^{-/-}$*;Gsc*$^{-/-}$, meaning that the lethality affects all *Gsc*$^{-/-}$ classes, independently of the *Cer-l* genotype.

In order to study the recovered animals in detail and detect possible skeletal defects in addition to the ones described for *Gsc*$^{-/-}$ single mutants, we performed Alcian Blue/Alizarin Red staining and carefully analyzed the base of the skull. Two classes of phenotypes were observed: the first corresponding to the wild type and the second composed of preparations that displayed the *Gsc*$^{-/-}$ phenotype described by previous reports (Yamada *et al.*, 1995; Rivera-Perez *et al.*, 1995; Belo *et al.*, 1998). These defects are visible in a dorsal view of the base of the cranium and consist in the loss of the tympanic rings, fusion of the ethmoid and the presphenoid into a single unit, and reduction of the vomer and the presphenoid (Figure 4.1). These malformations are due

to the proximity of the ancestral structure from which the prechordal cranium develops, the trabecula, and the prechordal plate, during skull morphogenesis (Belo *et al.*, 1998).

All the preparations that presented *Gsc* null mutant phenotype belonged to the following classes of genotypes: *Cer-l*$^{+/+}$;*Gsc*$^{-/-}$, *Cer-l*$^{+/-}$;*Gsc*$^{-/-}$ and *Cer-l*$^{-/-}$;*Gsc*$^{-/-}$. As we did not observe increased severity of the defects in the double mutant neonates when compared with *Gsc*$^{-/-}$ single mutants, we went on to study the existence of abnormalities during earlier stages of development. With this purpose, we dissected 44 embryos at E9.5 and genotyped them by PCR. The results of genotyping are resumed in Table 4.2. All the classes of genotypes are present, and, as in the case of the neonates, at approximately the expected Mendelian percentages. To study the role of these genes in the prechordal plate, we decided to investigate the existence of abnormalities in the structures that develop adjacent do it. For that purpose, we performed mRNA *in situ* hybridization for the forebrain markers *Six-3* and *BF-1* and for the axial marker *HNF-3β/Foxa2*. Six-3 is normally expressed in the telencephalon, the ventral diencephalon, the developing eye and the Rathke's pouch (Oliver *et al*, 1995). Since it has been suggested that the prechordal plate may be involved in the patterning of the forebrain, we could expect that the normal expression of this marker would be affected in the double mutants. By comparison between the wild type (Figure 4.2A) and the mutant embryos (Figure 4.2B, C), we can observe that Six-3 expression domain is unchanged in either the single *Gsc*$^{-/-}$ mutant or in the *Cer-l*$^{-/-}$*Gsc*$^{-/-}$ compound mutant. The results of BF-1 *in situ* hybridization confirm the lack of abnormalities in forebrain patterning of the studied mutants. As we can observe in the wild type E9.5 embryo (Figure 4.2D), BF-1 is expressed in the telencephalon (Tao and Lai, 1992). In the mutants (Figure 4.2E,F),

Table 4.1- Genotyping results of the neonates recovered from *cer-l*$^{+/-}$;*gsc*$^{+/-}$intercrosses

	Gsc$^{+/+}$Cer$^{+/+}$	Gsc$^{+/+}$Cer$^{+/-}$	Gsc$^{+/+}$Cer$^{-/-}$	Gsc$^{+/-}$Cer$^{+/+}$	Gsc$^{+/-}$Cer$^{+/-}$	Gsc$^{+/-}$Cer$^{-/-}$	Gsc$^{-/-}$Cer$^{+/+}$	Gsc$^{-/-}$Cer$^{+/-}$	Gsc$^{-/-}$Cer$^{-/-}$	N
No. Observed	4,00	14,00	11,00	6,00	17,00	13,00	5,00	11,00	3,00	84,00
No. Expected	5,25	10,50	5,25	10,50	21,00	10,50	5,25	10,50	5,25	84,00
% Observed	4,76%	16,67%	13,10%	7,14%	20,24%	15,48%	5,95%	13,10%	3,57%	100,00%
% Expected	6,25%	12,50%	6,25%	12,50%	25,00%	12,50%	6,25%	12,50%	6,25%	100,00%

N=number of neonates recovered

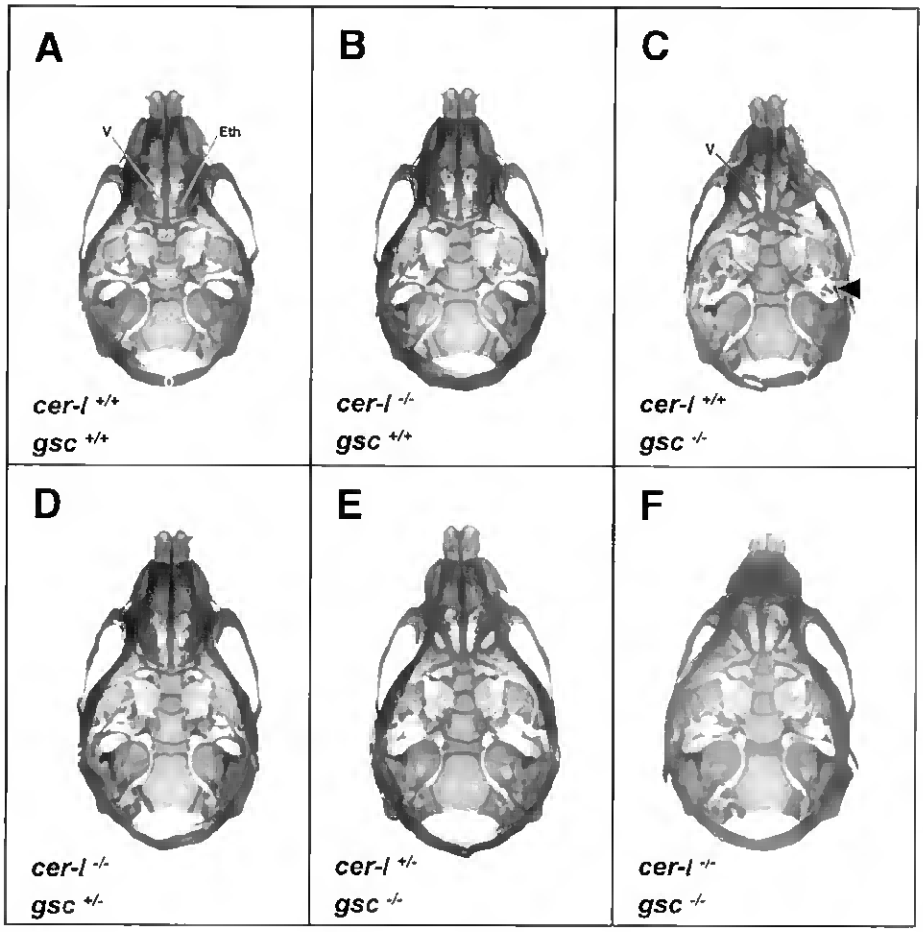

Figure 4. 1. *Cer-l*$^{-/-}$;*Gsc*$^{-/-}$ neonates display the same defects presented by *Gsc*$^{-/-}$ single mutants.
(A) Wild type neonate. **(B)** *Cer-l*$^{-/-}$;*Gsc*$^{+/+}$ littermate does not present defects. **(C)** *Cer-l*$^{+/+}$;*Gsc*$^{-/-}$ show reduction of the vomer (V), fusion of the ethmoid (Eth) with the presphenoid (PS; white arrow) and absence of the tympanic rings (black arrowhead). **(D)** *Cer-l*$^{-/-}$;*Gsc*$^{+/-}$ littermate presents the wild type phenotype. **(E)** *Cer-l*$^{+/-}$;*Gsc*$^{-/-}$ and **(F)** *Cer-l*$^{-/-}$;*Gsc*$^{-/-}$ present the same defects as *Cer-l*$^{+/+}$;*Gsc*$^{-/-}$ (compare with panel C). The skeletons of neonatal mice were stained with alcian blue (for cartilage) and alizarin red (for bone). BO, basioccipital; BS, basisphenoid; O, occipital.

Table 4.2- Genotyping results of the embryos recovered from *cer-l*$^{+/-}$; *gsc*$^{+/-}$ intercrosses

	Gsc$^{+/+}$Cer$^{+/+}$	Gsc$^{+/+}$Cer$^{+/-}$	Gsc$^{+/+}$Cer$^{-/-}$	Gsc$^{+/-}$Cer$^{+/+}$	Gsc$^{+/-}$Cer$^{+/-}$	Gsc$^{+/-}$Cer$^{-/-}$	Gsc$^{-/-}$Cer$^{+/+}$	Gsc$^{-/-}$Cer$^{+/-}$	Gsc$^{-/-}$Cer$^{-/-}$	N
No. Observed	1,00	12,00	4,00	4,00	12,00	2,00	3,00	3,00	3,00	44,00
No. Expected	2,75	5,50	2,75	5,50	11,00	5,50	2,75	5,50	2,75	44,00
% Observed	2,27%	27,27%	9,09%	9,09%	27,27%	4,55%	6,82%	6,82%	6,82%	100,00%
% Expected	6,25%	12,50%	6,25%	12,50%	25,00%	12,50%	6,25%	12,50%	6,25%	100,00%

N=number of embryos recovered

the expression of this marker is unaltered in both *Gsc*$^{-/-}$ mutants and *Cer-l*$^{-/-}$;*Gsc*$^{-/-}$ double mutants. We have also analized the expression of *HNF-3β/Foxa2* mRNA at E 9.5. At this stage, this gene is normally expressed along the anterior-posterior (A-P) axis in the notochord, the neural tube and floorplate, with its anterior limit at the level of the posterior diencephalon (Filosa *et al.*, 1997). The rostral limit of this expression domain is adjacent to the prechordal plate, so, we considered the hypothesis of an abnormal *HNF-3β/Foxa2* expression pattern in the region associated with the prechordal plate. However, by the observation of the results of the *in situ* hybridization (Figures 4.2G-I), we could see that the pattern of expression of *HNF-3β/Foxa2* is also unaffected in both classes of mutants (Figures 4.2 H, I). The expression in the notochord and floorplate is normal along the A-P axis of these embryos.

Taken together, our results indicate that the double mutants *Cer-l*$^{-/-}$;*Gsc*$^{-/-}$, do not display patterning defects neither at the level of the forebrain nor in the midline tissues along the body axis. At the level of the skull, the defects visible in the *Cer-l*$^{-/-}$;*Gsc*$^{-/-}$ mutant coincide with the ones present in the *Gsc*$^{-/-}$ single mutant. These results led us to conclude that *Cer-l* and *Gsc* do not interact genetically during mouse embryogenesis and that *Gsc* is not the factor that compensates for the loss of function of Cer-*l*.

In vertebrates, in addition to *Gsc*, two *Goosecoid* related genes were described, *Gsx*, in chick (Lemaire *et al.*, 1997) and *Gsc-like (Gscl)* in the mouse (Galili *et al.*, 1997). *Gsx* has not been cloned in the mouse, but sequence comparisons strongly indicate that *Gsx* and *Gscl* represent distinct genes in amniotes (Belo *et al.*, 1998), suggesting that *Gsc* may be redundant with these *Gsc*-related genes. Despite of these genes being expressed in the prechordal plate, their expression pattern has not been described in the AVE, nor in the topological equivalent tissue in the chick, the hypoblast; and they have not been implicated in head formation/morphogenesis, therefore, they are unlikely to compensate for *Cer-l* loss of function.

It has been proposed that trunk signals, like Nodal, Wnts and BMPs, must be inhibited in order to allow for the induction of the anterior head field. (Piccolo *et al.*, 1999). According to this model, the role of the AVE is to secrete molecules that inhibit the posteriorizing action of factors such as Nodal, Wnts and BMPs. Molecules secreted by the AVE that may play this role are the Nodal antagonist, Lefty-1, the Wnt inhibitor, Dickkopf-1 (Dkk1) and Cer-l. By inhibiting these signals, the AVE and the

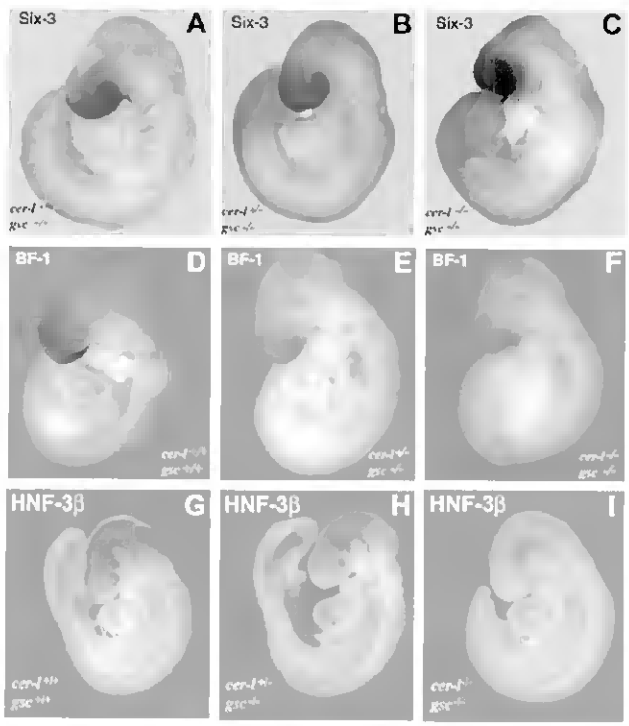

Figure 4.2. Six-3, BF-1 and HNF-3β/Foxa2 mRNA *in situ* hybridization in E9.5 embryos. **(A)** Wild type embryo showing Six-3 expression in the telencephalon, the ventral diencephalon and the developing eye. **(B)** *Cer-l*$^{+/-}$;*Gsc*$^{-/-}$ and **(C)** *Cer-l*$^{-/-}$;*Gsc*$^{-/-}$ mutant embryos exhibiting unaltered Six-3 expression pattern. **(D)** Wild type embryo presenting BF-1 expression in the telencephalon. **(E)** *Cer-l*$^{+/-}$;*Gsc*$^{-/-}$ and **(F)** *Cer-l*$^{-/-}$;*Gsc*$^{-/-}$ embryos do not present any alteration in BF-1 expression relative to the wild type littermate. **(G)** Wild type embryo showing *HNF-3β* expression along the notochord, neural tube and floorplate. **(H)** *Cer-l*$^{+/-}$;*Gsc*$^{-/-}$ and **(I)** *Cer-l*$^{-/-}$;*Gsc*$^{-/-}$ mutant embryos present the same HNF-3β expression pattern as shown in **(G)**. The tail of the embryo in **(I)** was removed for photographic purposes.

underlying anterior epiblast become regions free of posteriorizing agents, thus, allowing the formation of the anterior head (Piccolo *et al.*, 1999).

Since *Cer-l* is not compensated by *Gsc*, neither by *Noggin* (Borges *et al.*, 2001) nor *Chordin* (E. M. De Robertis, personal communication), we propose that it may interact with other genes expressed in the AVE. Data from several studies have suggested an interaction between *Cer-l* and *Otx-2*. In *Xenopus* animal cap assays, *Cer-l* induces *Otx-2* expression (Belo *et al.*, 1997) and experiments of tissue recombination in the mouse, also reveal the requirement of *Cer-l* for the maintenance of *Otx-2* expression (Shawlot *et al.*, 2000). Taken together, these observations point to the existence of some interaction between *Cer-l* and *Otx-2*. The generation of the *Cer-l;otx-2* double mutant may help to unravel this process. Other antagonists expressed in the AVE that may play key roles in the restriction of posteriorizing factors, like *Lefty-1* and *Mdkk-1*, may be

redundant with *Cer-l*. Therefore, the generation of further *Cer-l* double mutants may contribute to a better understanding of the mechanisms of early mouse patterning and head induction.

Chapter 5 – Results III

Chapter 5 – Results III

Regulation of Nodal signaling by Cerberus-like and Cripto

Ana Cristina Borges [1,2] , Giovanna Liguori [3] , M. Graziella Persico [3] and José António Belo [1,2]

1. Instituto Gulbenkian de Ciência, Rua da Quinta Grande 6, Apartado 1781-901 Oeiras
2. Faculdade de Engenharia de Recursos Naturais, Universidade do Algarve, Campus de Gambelas, 8000-010 Faro, Portugal
3. Institute of Genetics and Biophysics, "Adriano Buzatti-Traverso", Consiglio Nazionale delle Ricerche, 80131 Naples, Italy.

Manuscript in preparation (2004)

The contribution of A. C. Borges for this paper was the elaboration of the project, experimental work, analysis and discussion of results.

5.1. Abstract

Nodal signaling pathway is highly conserved among vertebrates and is essential for their embryogenesis. Nodal has multiple roles during embryonic development: it is required to define the anteroposterior (A-P) axis, to induce mesoderm and definitive endoderm and to determine the left-right (L-R) asymmetry. In the mouse, *Nodal* null mutants fail to gastrulate, to establish the A-P axis and to specify the anterior visceral endoderm (AVE). In addition, the targeting of several genes involved in the Nodal signaling causes severe phenotypes during gastrulation. Nodal extracellular antagonists have been shown to be crucial for the formation of the anteroposterior axis. In particular, in the *Cerberus-like;Lefty-1* double mutant, the excess of Nodal activity leads to the formation of multiple primitive streaks. Moreover, Cripto, an EGF-CFC factor that works as co-receptor of Nodal, is required for mesoderm formation and the proper positioning of the A-P axis. In spite of *Nodal* and *Cripto* mutant phenotypes being both very severe, they differ from each other. The *Cripto* mutants are capable of forming a proximo-distal (P-D) axis that fails to rotate, and to generate a proper A-P axis. In contrast, in *Nodal* mutants a P-D axis cannot be found, suggesting that Nodal might also act in a Cripto-independent manner during early mouse development.

In order to gain insight into Nodal signaling pathway and its dependence on Cripto co-receptor, we generated *Cerberus-like;Cripto* double mutants. In the *Cripto* null mutant, the loss of *Cer-l* may increase Nodal levels and redirect Nodal to a Cripto-independent receptor complex.

According to our results, Nodal can signal in the absence of Cripto, and this alternative pathway yields molecular responses that are capable of rescuing gastrulation in the *Cer-l;Cripto* double mutants in comparison to *Cripto*$^{-/-}$ embryos.

5.2. Introduction

Nodal proteins are ligands of the TGF-β superfamily that interact with the activin receptor complex, triggering a cascade of intracellular events that ultimately lead to transcriptional activation (Fig. 1.3). The receptor complex that transduces Nodal signal, consists in type I and type II activin serine/threonine kinase receptors. Upon binding to Nodal, the type II receptor (ActRIIA or ActRIIB) becomes activated and

phosphorylates the type I receptor (ActRIB or ActRIB), that in turn will activate Smad factors by phosphorylation (Yeo and Whitman, 2001; Reissman et al, 2001). Phosphorylated Smad proteins form complexes with FAST transcription factors that translocate to the nucleus and may activate or repress transcription of target genes.

The binding of Nodal to the activin receptors requires the presence of EGF-CFC co-receptors at the cell surface. In mouse, the EGF-CFC family members, Cripto and Cryptic were shown to be essential components of the Nodal signaling pathway and required for normal embryonic development (Ding et al, 1998; Xu et al, 1999; Yan et al, 1999). Cripto is bound to the cell membrane by a GPI anchor (Minchiotti et al, 2000), and is part of the receptor complex that includes Nodal, ActRI (ALK4) and ActRIIB (Reissman et al, 2001; Yeo and Whitman, 2001; Sakuma et al, 2002). Because Cripto appears to bind to ALK4 even in the absence of Nodal, it is thought that Nodal assemble a complex of ActRIIB and ALK4/Cripto to activate downstream signaling events. ALK7 can also act as a type I receptor for Nodal, and in the presence of Cripto increases Nodal responsiveness.

Cryptic was shown to be specifically required for the transduction of Nodal signals during the establishment of L-R polarity. *Cryptic* is specifically expressed in the lateral plate mesoderm (LPM) at somite stages. In its absence, *Nodal* and its downstream targets in the LPM are not expressed. Recently, Cryptic has also been implicated in GDF1 (another TGF-β superfamily member required for L-R development) signaling (Cheng et al, 2003). Therefore, *Cryptic* may play an essential role in integrating GDF1 and Nodal signals for the establishment of the L-R asymmetry.

Cripto is essential for mouse gastrulation (Ding et al, 1998). At pre-streak stages it is expressed in the entire epiblast (Dono et al, 1993; Ding et al, 1998; Xu et al, 1999), but with the onset of gastrulation, its expression is restricted to the posterior proximal epiblast, the region where the primitive streak will appear. During gastrulation *Cripto* expression is found in the primitive streak and in the wings of embryonic mesoderm. At neural plate stage *Cripto* expression decreases in the mesoderm and becomes confined to the primitive streak and head process. Between E8.0 and E10.0, it is specifically detected in the developing heart and *truncus arteriosus*.

Targeted inactivation experiments demonstrated that *Cripto* is required for proper positioning of the A-P axis, mesoderm formation and heart development (Ding et al, 1998; Xu et al, 1999; Parisi et al, 2003). *Cripto* null mutants are embryonic lethal; they show an arrest at gastrulation, and are reabsorbed around E9.5. At E6.5, in WT

embryos a primitive streak starts to form, but *Cripto* null mutants lack the primitive streak and the node. The primitive streak markers (e.g. *Brachyury, Nodal, Fgf8*) do not localise in the posterior epiblast region, instead, they remain in a proximal epiblast ring, close to the embryonic-extraembryonic boundary. AVE markers (e.g. *Cer-l, Hesx1, Hex*), that at this stage are expressed in the anterior region of the WT embryo, remain in a distal position in the *Cripto* mutants. This indicates in the *Cripto*$^{-/-}$ embryos, the P-D axis fails to rotate and elicit the proper positioning of the A-P axis

Cripto and *Nodal* null mutants share some similarities: both lack embryonic mesoderm and fail to induce an A-P axis. Despite such similarities they display important differences: *Cripto* mutants show a P-D axis even though it fails to rotate (Ding et al, 1998). In contrast, in *Nodal* mutants a P-D axis cannot be found (Brennan et al, 2001), suggesting that *Nodal* has *Cripto*-independent roles during early mouse development in the establishment of P-D molecular asymmetries.

The failure of gastrulation observed in the *Cripto* mutants leads to a remarkable phenotype at later stages. At E8.5, the mutant embryos consist essentially of anterior neuroectoderm, as assessed by the expression of *Otx2* and *Sox2* genes (Liguori et al, 2003). Interestingly, these mutants develop anterior neural patterning, displaying expression of fore- and midbrain markers, sequentially, in a distal-proximal disposition. Therefore, in *Cripto*$^{-/-}$ embryos, anterior neural induction occurs and is maintained in the absence of the node and its derivatives. These data suggest that the node and the axial mesendoderm are not absolutely required for the specification and maintenance of the anterior neural plate (Liguori et al, 2003). This characteristic is also disparate from the *Nodal* mutants, in which no anterior structures are formed (Conlon et al, 1994).

Nodal extracellular antagonists play important roles in restricting Nodal activity in time and space, thus, modulating Nodal signaling responses (Meno et al, 1999; Schier et al, 2003). In mouse and chick, the Nodal antagonists, *Cer-l* and *Lefty-1* are crucial for the formation of the A-P axis (Perea-Gomez et al, 2002; Yamamoto et al, 2004; Bertocchini and Stern, 2002). The mouse *Cerberus-like;Lefty-1* double mutant, shows an upregulation of Nodal target genes and form multiple primitive streaks (Perea-Gomez et al, 2002). These defects are partially suppressed when one *Nodal* allele is removed in the double mutant context, in agreement with the hypothesis that an axcess of Nodal signaling might be the cause of the abnormal phenotype. Moreover, chimeric embryos, in which the epiblast is predominantly composed of WT cells and the extraembryonic tissues are depleted of *Cer-l* and *Lefty-1*, phenocopy *Cer-l;Lefty-1*

double mutants. This suggests an important role of the Nodal antagonists in the AVE for the inhibition of Nodal activity, restricting the site of the primitive streak formation.

More recently it was shown that the Nodal signaling promotes cell proliferation in the epiblast and VE. The AVE region where *Lefty-1* and *Cerberus-like* are expressed at E5.7 does not show cell proliferative activity. The differential proliferative activity between the cells in the anterior and posterior sides of the embryo was proposed to be the driving force for visceral endoderm displacement towards the future anterior side of the embryo. The displacement of the VE to the anterior side mediates the proper formation of the A-P axis, and therefore, allows correct gastrulation. These studies reinforce that Nodal activity has to be tightly regulated, namely by its antagonists *Cer-l* and *Lefty-1,* in order to establish asymmetries and correct morphogenetic movements in the early mouse embryo.

In the present work we generated *Cerberus-like;Cripto* double mutants in order to uncover a genetic interaction between these two factors. According to our hypothesis, in the context of the *Cripto* null mutation, the loss of *Cer-l* would increase the level of free Nodal protein in the extracellular space. By increasing Nodal levels, in the absence of Cripto (and consequently, of the Nodal canonical pathway), we might redirect Nodal molecules to a Cripto-independent receptor complex and rescue the *Cripto* null mutant phenotype. This strategy may allow us to uncouple *Nodal* and *Cripto* functions during mouse embryonic development.

5.3. Results

In order to test our hypothesis we crossed *Cer-l* null mutants with *Cripto* heterozygous mice to obtain *Cer-l*$^{+/-}$;*Cripto*$^{+/-}$ double heterozygous mice. The latter ones were intercrossed and embryos were collected from pregnant females at several stages of development.

Since *Cripto* null mutants fail to position the A-P axis at E 6.5, we first assessed for the localisation of both posterior epiblast and AVE markers in the *Cer-l;cripto* double mutants. With this purpose, we performed double whole mount *in situ* hybridisation (WISH) using a cross reactive probe that detects both *Lefty-1* and *Lefty-2 genes*, and a probe for *Brachyury* (Fig. 5.1). In the WT embryo, at the beginning of gastrulation, *Lefty-1* is expressed in the AVE, and *Lefty-2* and *Brachyury* are expressed posteriorly in the nascent primitive streak (Fig. 5.1A). In the *Cripto* mutants, *Lefty*

genes are specifically downregulated, since its expression is absent (Figure 5.1B) contrarily to other AVE and primitive streak markers; and *Brachyury*, is confined to the proximal epiblast ring (not shown, Ding et al, 1998). Noteworthy, the analysis of Lefty genes expression allow us to test for the presence of Nodal signaling activity, being these genes direct *Nodal* downstream targets. After the WISH, we genotyped the embryos by PCR. We detected *Lefty* genes expression in most of the *Cer-l;Cripto* double mutants analised (considering both *Cer-l*$^{+/-}$; *Cripto*$^{-/-}$and *Cer-l*$^{-/-}$;*Cripto*$^{-/-}$ genotypes), even if with a patchy distribution (Figure 5.1C). However, a small percentage (approximately 15%, N=9) displayed a normal expression of the anterior (*Lefty-1*) and posterior (*Lefty-2* and *Brachyury*) markers (Figure 5.1D). The finding that the *Cer-l;Cripto* double mutants possess a different phenotype than that of *Cripto*$^{-/-}$ mutants clearly indicates that *Cer-l* and *Cripto* genetically interact.

To analyse the extent of rescue during late gastrulation, we collected embryos at E7.5. In the wt embryo at E7.5, the primitive streak is fully extended and the node is visible at its anterior region, as shown by the expression of *Brachyury*. (Fig. 5.2A) At this stage the expression of *Otx2* marks the prospective fore- and midbrain and is confined to the anterior third of the embryo (Fig. 5.2A). In the *Cripto* null mutant, *Brachyury* expression is restricted to the posterior proximal region of the epiblast, while *Otx2* is ectopically expressed in almost the entire epiblast (Fig. 5.2B).

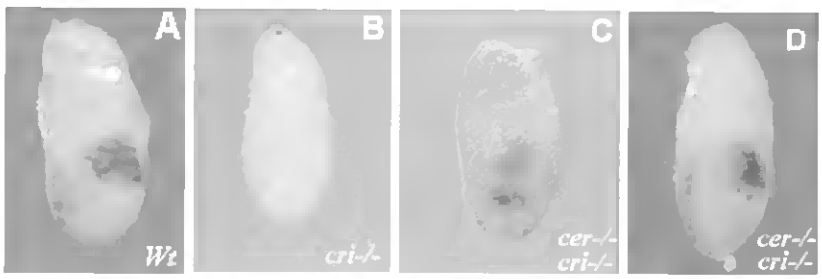

Figure 5.1. Analysis of A-P axis markers at E6.5 in *Cer-l*$^{-/-}$;*Cripto*$^{-/-}$ double mutants. **A**) Double *WISH* in WT embryo for *Lefty-1/2* genes (in blue) and *Brachyury* (in red); **B**) WISH for *Lefty1* and *Lefty2* in *Cripto* null mutant; **C)** *Cer-l*$^{-/-}$;*Cripto*$^{-/-}$ double mutant showing abnormal localisation of both *Lefty* genes (blue) and *Brachyury* (red) **D)** *Cer-l*$^{-/-}$;*Cripto*$^{-/-}$ double mutants with normal expression of *Lefty-1/2* (blue) and *Brachyury* (red).

A small percentage of *Cer-l;Cripto* double mutants (12,5%, N=8) showed a peculiar morphology (Fig. 5.2C), however, very different from the *Cripto*$^{-/-}$ embryos. *Brachyury* expression domain elongates towards the distal tip of the embryo, while *Otx2* expression is restricted to the extremity of the embryonic tube, suggesting that the embryo develops outside of the visceral yolk sac (VYS).

The morphological analysis of E8.5 embryos allowed us to divide the embryos into four classes, here in order of increasing abnormalities: 1) normal embryos; 2) embryos showing an incomplete embryonic axis with reduced headfolds; 3) abnormal embryos that develop partially or completely external to the VYS; 4) very abnormal embryos, almost corresponding to an empty VYS, with very amorphous embryonic structures. After genotyping them we could conclude that embryos grouped in the first group correspond to *Wt*, *Cer-l* $^{+/-}$, *Cripto* $^{+/-}$, *Cer-l*$^{-/-}$, *Cer-l*$^{+/-}$;*Cripto*$^{+/-}$ *and Cer-l*$^{-/-}$;*Cripto*$^{+/-}$. The second and third classes correspond to either *Cer-l*$^{+/-}$;*Cripto*$^{-/-}$ or *Cer-l*$^{-/-}$;*Cripto*$^{-/-}$ genotypes. Embryos grouped in the fourth class belong to the following genotypes: *Cer-l*$^{+/+}$;*Cripto*$^{-/-}$, *Cer-l*$^{+/-}$;*Cripto*$^{-/-}$ *and Cer-l* $^{-/-}$;*Cripto*$^{-/-}$ (Table 5.1).

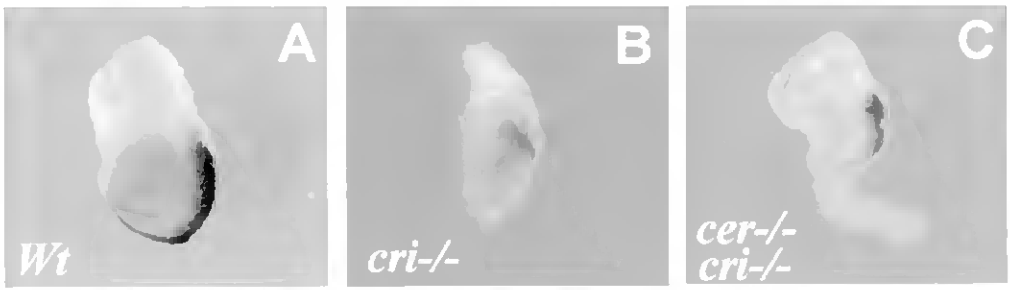

Figure 5.2. Molecular marker analysis of *Cer-l;Cripto* double mutants at E7.5. **A)** double *in situ* hybridization for *Brachyury* (blue) in the primitive streak and *Otx2* (red) in the anterior region of the WT embryo. **B)** *Cripto* null nutant showing proximal expression of *Brachyury* and expanded *Otx2* expression. **C)** *Cer-l;Cripto* double mutant displaying abnormal development outside the visceral yolk sac, reduced *Otx2* expression at the tip and *Brachyury* expression in a primitive streak-like structure.

	Genotypes	Phenotype
Class 1	*Wt* *cer-l* $^{+/-}$ *cripto* $^{+/-}$ *cer-l* $^{-/-}$ *cer-l* $^{+/-}$*;cripto* $^{+/-}$ *cer-l* $^{-/-}$*;cripto* $^{+/-}$	normal
Class 2	*cer-l* $^{+/-}$*;cripto* $^{-/-}$ *cer-l* $^{-/-}$*;cripto* $^{-/-}$	incomplete embryonic axis; reduced headfolds
Class 3	*cer-l* $^{+/-}$*;cripto* $^{-/-}$ *cer-l* $^{-/-}$*;cripto* $^{-/-}$	partially or completely outside the VYS
Class 4	*cer-l* $^{+/+}$*;cripto* $^{-/-}$ *cer-l* $^{+/-}$*;cripto* $^{-/-}$ *cer-l* $^{-/-}$*;cripto* $^{-/-}$	empty VYS; very abnormal embryos;

Table 5.1. E8.5 *Cer-l;Cripto* mutants are divided into 4 phenotypic classes.

From the analysis of the table 5.1 we could conclude that the genotypes *Cer-l* $^{-/-}$*;Cripto* $^{-/-}$ *and Cer-l* $^{+/-}$*;Cripto* $^{-/-}$ can be found in classes 2, 3 and 4. This means that the compound mutants can yield a range of phenotypes that vary from very abnormal embryos showing no rescue (class 4) to embryos with a rudimentary body axis (class 2) and that the removal of just one *Cer-l* allele is sufficient to rescue the *Cripto* null mutant phenotype.

To better define these phenotypic classes, we performed the molecular analysis of the E8.5 embryos by monitoring a panel of diagnostic markers. First of all, we examined the expression of the neural genes *Otx2, Gbx2* and *Krox-20*. In the Wt embryo at E 8.5, *Otx2* and *Gbx2* expression domains are adjacent, defining, the first, the fore- and midbrain, and the second, the anterior hindbrain (Fig. 5.3A). At the same developmental stage, *Cripto* $^{-/-}$ mutants present complementary domains of expression for *Otx2* and *Gbx2*. However, the former is localised in the distal region, and the later in the proximal region of the embryo (Fig. 5.3 B; Liguori et al, 2003). In Cer-*l;Cripto* double mutant embryos, *Otx2* and *Gbx2* expression domains are not oriented along a P-D axis, as in the *Cripto* $^{-/-}$ embryos, but show an A-P pattern (Fig. 5.3C). This data is in agreement with the results obtained at previous stages and indicate the rescue of the A-P axis rotation in the double mutants.

Moreover, *Cripto* $^{-/-}$ mutants completely lack the posterior hindbrain domain as shown by the absence of markers such as *Krox-20* (Ding et al, 1998). In order to test if the hindbrain is specified in the *Cer-l;Cripto* double mutants we performed double

WISH for *Krox-20* and used *Otx2* probe as reference marker for the rostral brain (Fig 5.3D-F). In the WT embryos the expression of *Krox-20* is localised in the rhombomeres 3 and 5, in a position more caudal to the fore- and midbrain marker *Otx2*. In the *Cripto* null mutant only *Otx2* is expressed, contrarily to the *Cer-l;Cripto* double mutants in which *Krox-20* is expressed in two separate domains, both caudal to *Otx2* (Fig. 5.3F). This result indicated that in the *Cer-l;Cripto* double mutants, the hindbrain is rescued, at least, until the level of rhombomere 5.

In order to assess for mesoderm development we performed double *WISH* using *Brachyury* as an axial mesodermal marker and *Otx2* as a brain reference marker (Fig. 5.3G-J). In the WT embryos, at E8.5, we can see the expression of *Brachyury* in the tail bud region and along the notochord of the developing embryo. In the *Cripto* null mutant, at this same stage, Brachyury is not detected and *Otx2* is ectopically expressed in almost all the embryonic region. In the *Cer-l;Cripto* double mutants a striking phenotype was found. Most of them display an abnormal morphology forming an embryonic tube outside the VYS, as already shown at E7.5. In these double mutants (Fig. 5.3I-J) the *Otx2* expression domain was detected only at the tip of the tube. Interestingly, B*rachyury* expression was found (Fig. 5.3J). A notochord-like structure is recognizable continuously to the primitive streak region. This result confirms the development of posterior mesoderm and primitive streak derivatives in the *Cer-l;Cripto* double mutants.

To test for the formation of derivatives of the anterior primitive streak in the double mutants, we performed double in situ hybridization using *Hnf3β/Foxa2* as an axial mesendoderm marker, and *krox-20,* as a hindbrain marker (fig. 5.3K). In the *Cripto* null mutant none of the genes is expressed (Fig. 5.3 L), but in the *Cer-l;Cripto* double mutant, a neural fold is apparent (Fig. 5.3M) in which *Krox-20* is expressed and a patchy expression of *Hnf3β/Foxa2* is also visible (Fig. 5.3N). By histological examination of sagittal sections (Fig. 5.1R) we could confirm the expression of *Hnf3β/Foxa2* in the anterior endoderm underlying the neuroepithelium where *Krox-20* is expressed. The expression of *Hnf3β/Foxa2* suggests the existence of an anterior primitive streak-derived organizer activity

Cripto null mutants are embryonic lethal at E9.5 and at this stage consist only in an empty VYS (Fig. 5.3P). In order to see if the *Cer-l;Cripto* double mutant develop further and display some degree of dorso-ventral patterning in the axial structures

(notochord and floorplate), we performed double WISH using *Shh* as a ventral midline marker (Fig. 5.3O-Q) and *Otx2* as a rostral brain marker. Normally, *Shh* is expressed in the ventral neural tube and notochord along the A-P axis of the WT embryo. (Fig. 5.3O). In the *Cer-l;Cripto* double mutant *Otx2* is expressed in one of the extremities of the rudimentary embryonic axis along which is possible to observe expression of *Shh*. This gene is not expressed in a continuous domain as in the WT, but is present in a dotted expression pattern forming a discontinuous line, indicating the rudimentary nature of the midline tissues. Nevertheless, the *Shh* expression pattern detected provides evidence for the existence of dorso-ventral patterning along the axial structures.

In order to calculate the percentage of rescue of the *Cer-l;Cripto* double mutants, the data obtained from the *in situ* hybridisation experiments was pooled and is summarized in table 5.2. The rescue occurs in about 33% of *Cer-l*$^{-/-}$;*Cripto*$^{-/-}$embryos and in 40% of *Cer-l*$^{+/-}$;*Cripto*$^{-/-}$ embryos. The fact that we could observe class 2 and 3 embryos in both *Cer-l*$^{+/-}$;*Cripto*$^{-/-}$ and *Cer-l*$^{-/-}$;*Cripto*$^{-/-}$ indicates that the removal of one copy of *Cer-l* allele, causes the same developmental effect as the removal of both alleles, despite it happens in a graded fashion, generating different degrees of severity.

	E 6.5	E 7.5	E 8.5	E 9.5	Total
cer-l$^{-/-}$;*cri*$^{-/-}$	1/3	0/3	3/7	1/2	5/15 (33%)
cer-l$^{+/-}$;*cri*$^{-/-}$	4/6	1/5	3/7	1/4	9/22 (40%)

Table 5.2. Number of double mutant embryos that display rescue (by age and genotype)

5.4. Discussion

From the double *WISH* analysis of Cer-*l;Cripto* double mutants, we can conclude that *Cerberus-like* and *Cripto* interact at the genetic level, in the positioning of the A-P axis. *Cripto*$^{-/-}$ embryos fail to gastrulate and to form an A-P axis, but the removal of *Cer-l* is able to partially rescue this phenotype and to correctly position the A-P axis. Cripto is a co-factor for Nodal signal, while Cer-l is an inhibitor able to directly bind Nodal and to block its activity. Cripto is important for Nodal activity and in its absence the expression of Nodal target genes, such as *Lefty* genes, are downregulated. However, the simultaneous removal of *Cer-l* and *Cripto* rescues the expression of Nodal target genes, thus, rescuing Nodal signaling pathway. These data

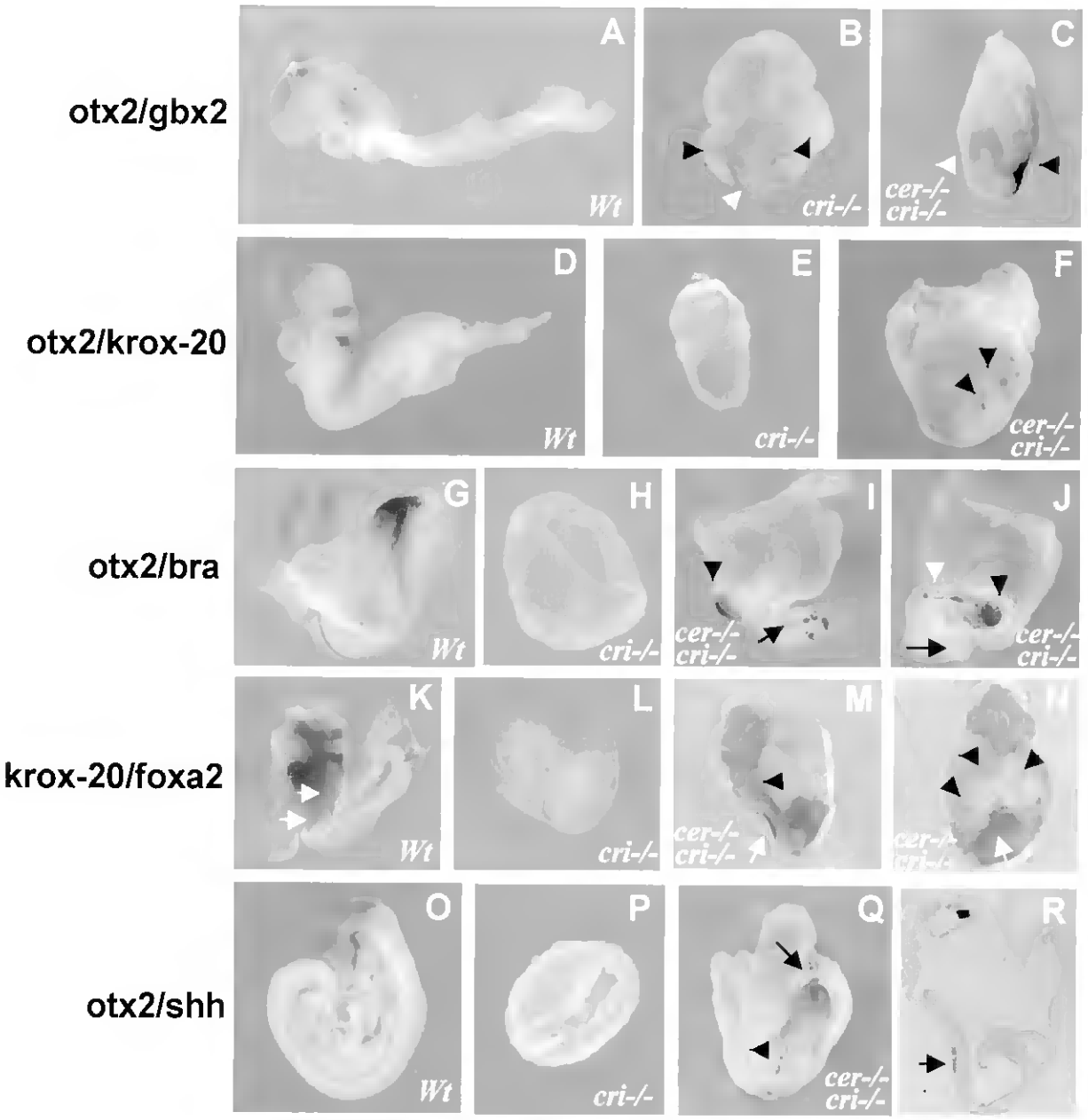

Figure 5.3. Molecular analysis of *Cerberus-like;Cripto* double mutants at E8.5 and E9.5. **A)** expression of *Otx2* (red) in the fore- and midbrain and *Gbx2* (blue) in the hindbrain and paraxial mesoderm in WT embryos at E8.5. **B)** *Cripto* null mutant showing *Otx2* expression distally (white arrowhead) and *Gbx2* proximally (black arrowheads). **C)** double mutant embryo showing *Otx2* in the anterior region (white arrowhead)and *Gbx2* in the posterior (black arrowhead), in a complementary pattern. **D)** *Otx2* (red) and *Krox-20* (blue) in rhombomeres 3 and 5 of WT embryos at E8.5. **E)** *Cripto* null mutant showing *Otx2* expression but not *Krox-20*. **F)** double mutant embryo displaying *Krox-20* expression caudally to *Otx2* (black arrowheads). **G)** *Otx2* (red) and *Brachyury* (blue) expression pattern in the axial mesoderm and primitive streak in the WT embryo at E8.5. **H)** *Cripto* null mutant showing vestigial expression of *Otx2* and absence of *Brachyury* expression. **I)** double mutant embryo showing a small domain of *Otx2* expression in the tip of the embryo (black arrow) and proximal expression of *Brachyury* (black arrowhead). **J)** a different view of the same embryo as in **I** showing a notochord-like structure (white arrowhead). **K)** *Krox-20* (red) and *HNF3B/foxa2* (blue, white arrowheads) expression in WT embryos. **L)** *Cripto* null mutant displaying absence of both genes. **M)** lateral view of a double mutant embryo showing the expression of Krox-20 (red, black arrowhead) and. *HNF3B/foxa2* (blue, white arrow).

N) frontal view of the same embryo depicted in **M** showing *HNF3B/foxa2* specific expression in patches of cells (white arrow) and *Krox-20* in the anterior region of the embryo (black arrowheads). **O)** *Otx2* (red) and *Shh* (blue) in WT embryo of E9.5. **P)** *Cripto* null mutant showing absence of both markers. **Q)** double mutant embryo displaying a reduced embryonic axis with *Otx2* in one of the extremities (black arrowhead) and patches of *Shh* expressing cells (black arrow). **R)** Sagital section of the embryo M and N, showing expression of *HNF3B/foxa2* in the anterior endodermal layer of the double mutant (black arrow).

indicate that Cripto is not absolutely required for Nodal activity in the orientation of the A-P axis. We hypothesize that the removal of Cer-l increases the level of free Nodal protein and that this high Nodal level can bypass the absence of Cripto. However, even if A-P axis is correctly oriented, and the *Cer-l;Cripto* double mutants start to gastrulate normally, they fail to completely elongate the primitive streak and still lack trunk structures. These results suggest that although Cripto is dispensable for gastrulation to start, it is essential for its progression and for the complete development of the primitive streak and its derivatives. However, differently, from *Cripto*$^{-/-}$ embryos, *Cer-l;Cripto* double mutants develop anterior primitive streak structures (as shown by the expression of *Brachyury* and *Hnf3β/Foxa2*). Probably, the presence of these structures accounts for the formation of more caudal territories (identified by *Krox-20* expression) absent in *Cripto* null mutants.

Interestingly, the removal of one *Cer-l* allele in the context of the *Cripto* null mutation is sufficient for the partial rescue of the *Cripto* phenotype. The removal of the second copy of the *Cer-l* allele doesn't produce any additional phenotype, meaning that the level Nodal activity reached in the *Cer-l*$^{+/-}$*;Cripto*$^{-/-}$ is sufficient to drive the rescue of the A-P axis, but cannot be increased removing the second allele.

But how can *Cripto* and Cer*berus-like* interact in the embryo? It is interesting to notice that *Cer-l* and *Cripto* are not co-expressed in the mouse embryo. However during development they show adjacent/complementary domains of expression. At E5.5 *Cripto* is uniformly expressed in the epiblast (Ding et al, 1998) while *Cer-l* is expressed in the adjacent distal visceral endoderm (Belo et al, 1997). At the onset of gastrulation, *Cripto* domain is restricted to the proximal posterior epiblast (Ding et al, 1998) and *Cer-l* is confined to the anterior visceral endoderm (Belo et al, 1997) where it is required to inhibit Nodal signals secreted from the posterior epiblast (Perea-Gomez et al, 2002; Yamamoto et al, 2004). If we take into account that *Cer-l* is a secreted factor, it is plausible to propose that although not co-expressed, they may act on common cells. In

these discrete domains, the absence of both *Cer-l* and *Cripto* may raise the level of Nodal protein in the extracellular space and contribute to rescue the *Cripto* mutant phenotype.The outcome of this situation, according to our results, is a rescue of the positioning of the A-P axis, as demonstrated by the expression of *Lefty1/2* and *Brachyury*, at E6.5. This result suggests that Nodal activity in the double mutant embryos, before gastrulation, is sufficient to drive the anterior movement of the VE, eliciting the formation of the A-P axis. Probably, as a consequence of the high Nodal levels in the posterior epiblast, a primitive streak is formed, although it does not lengthen completely (as seen by the expression of *Brachyury* at E7.5). At neural plate stage both molecules are again expressed in adjacent domains. *Cripto* is essentially expressed along the primitive streak and the head process while *Cer-l* is expressed in the anterior definitive endoderm of the embryo that spans from the node vicinity to the rostral region of the embryo. This means that *Cer-l* and *Cripto* may exert their functions in the axial mesendoderm. Nodal activity is required in the anterior primitive streak and in the node in order to induce anterior definitive endoderm (Hoodless et al, 2001; Yamamoto et al, 2001), prechordal plate and notochord (Lowe et al, 2001, Norris et al, 2002). The fact that we may be generating high Nodal levels in this domain, may contribute to the rescue of notochord and anterior definitive endoderm in the double mutants at E8.5.

From our experiments we can conclude that in the *Cer-l;Cripto* double mutants there is the rescue of some embryonic structures that are absent in *Cripto* null mutants, but it is still not possible to determine the molecular mechanism by which it is occurring. However, several possibilities and discussed here.

The first possibility is that the increased Nodal levels generated in the double mutant, coupled to the inactivation of the Cripto-dependent pathway, may allow the binding of Nodal protein to a different Cripto-independent receptor or to a yet unidentified co-receptor that normally have a lower affinity for Nodal or is downregulated in the Wt embryo. One candidate receptor might be the activin type I receptor ALK7 which was shown to effectively transduce Nodal signals and activate phospho-Smad2 in both a Cripto-dependent and -independent fashions (Reissman et al, 2001). Unfortunately, very little is known about ALK7 expression, intracellular signaling and *in vivo* role in the mouse embryo.

In alternative, in the absence of Cripto, ALK4 may still be functional. In this case, in the *Cer-l;Cripto* double mutants Nodal proteins may act through ALK4, but elicit only a reduced level of Nodal activity.

However, we cannot exclude that the rescue obtained in the double mutants might be due to other signaling pathways, in addition to Nodal signaling. Thus, we can hypothesise that the molecular mechanism leading to the phenotypic rescue might involve the effective blockade of BMP signals, by formation of heterodimers. The direct binding between Nodal and BMP7 or BMP5 may cause mutual inhibition of both pathways (Yeo and Whitman, 2001). In the mouse, BMP7 and BMP5 are expressed at the onset of gastrulation in the primitive streak and have redundant functions (Solloway and Robertson, 1999). *Bmp5;Bmp7* double mutants do not display gastrulation defects but have abnormal neural tube closure in the forebrain. It was proposed that these defects are due to an increased cell growth (Solloway and Robertson, 1999). If *Bmp5* and *Bmp7* function as inducers of programmed cell death in the primitive streak region, the excess of Nodal molecules in the *Cer-l;Cripto* double mutant can inhibit BMP, and consequently, lead to a downregulation of cell death. The consequent effect of this may be the proliferation of primitive streak and posterior mesoderm that can account for the rescue observed in the *Cer-l;Cripto* double mutants.

A fourth hypothesis is that by inactivating *Cer-l* and *Cripto* we are generating not only the increase of free Nodal protein, but of another TGF-β ligand, such as GDF1. This molecule has been recently shown to signal through activin receptors and to be dependent on the activity of EGF-CFC co-factors (Cheng et al, 2003). GDF1 triggered signaling may be inhibited by *Cer-l* (our unpublished results). Although *GDF1* is expressed in a similar pattern to that of *Nodal* in the epiblast during gastrulation, genetic data showed that it is essential only at later stages for L-R axis specification. However we can't exclude that it plays a role during gastrulation, redundant with other genes, that can be unmasked only when other genes are simultaneously inactivated.

The hypothesis presented above are not mutually exclusive and a combination of them is, in theory, possible. Each of these scenarios requires further investigation. Nevertheless, our data favour the first two hypothesis in which the rescue is caused by an increased Nodal signaling that is tranduced via a Cripto-independent mechanism. The first reason to suggest this is the fact that the *Nodal* target genes *Lefty-1* and *Lefty-2* (which are absent in the *Cripto* null mutants) are expressed in the double mutants *Cer-l;Cripto*. This strongly indicates that Nodal signalling pathway is active and activating

its usual transcriptional targets. The second evidence comes from the fact that mutants for components of *Nodal* signaling cascade generate similar phenotypes to the one described here. In particular, the Nodal hypomorphic mutants (Lowe et al, 2001), asymmetric intronic enhancer (ASE) mutants (Norris et al, 2002) and the double ActRIIA/IIB mutants (Song et al, 1999) yield mutants with remarkable similarities to the *Cer-l;Cripto* double mutant, namely, the development outside the VYS and the presence of a rudimentary body axis with abnormal midline structures. These mutants were shown to display graded levels of Nodal signalling, where low levels are sufficient to reach the threshold required for gastrulation, notochord and hindgut formation but insufficient for node and prechordal plate formation, leading to an embryonic arrest at E8.5.

Our data provide strong evidence that in the *Cer-l;Cripto* double mutants, a Nodal signalling pathway is transducing the signals, although in a reduced level. The levels of Nodal activity achieved may fall into distinct categories: 1) insufficient to overcome gastrulation (class 4); 2) reach the threshold required to begin gastrulation, but display abnormal morphogenetic movements and develop outside the VYS (class 3); or 3) may develop inside the VYS, pattern the rostral and caudal brain domains, and induce some derivatives of the primitive streak (class 2). The fact that the rescue in *Cer-l;Cripto* double mutants does not occur in the totality of the embryos, but in only a percentage between 33 and 40% may indicate that in the remaining embryos the Nodal level is below the threshold required for gastrulation and mesoderm formation.

In conclusion, our data provide insight into an alternative Nodal signaling pathway that is Cripto-independent and accounts for a basal level of Nodal activity capable to overcome gastrulation in the mouse embryo. This work also highlights the importance of double mutant studies to uncover complex regulation networks occurring during mouse development, and the importance of antagonist and co-receptors to modulate Nodal signaling, in order to achieve optimal levels for embryonic development.

Chapter 6 – Results IV

Chapter 6 – Results IV

The activity of the Nodal antagonist *Cerl-2* in the mouse node is required for correct L-R body axis.

Sara Marques[1], Ana Cristina Borges[1,2], Ana Cristina Silva[1,2], Sandra Freitas[1], Michelangelo Cordenonsi[3] & José António Belo[1,2,#]

1. Instituto Gulbenkian de Ciência, Rua da Quinta Grande 6, Apartado 1781-901 Oeiras, Portugal.

2. Faculdade de Engenharia de Recursos Naturais, Universidade do Algarve, Campus de Gambelas, 8000-010 Faro, Portugal.

3. Department of Medical Biotecnologies University of Padua School of Medicine Viale Colombo 3, Padua, Italy.

Submited for publication (2004)

The specific contribution of A. C. Borges for this paper was the analysis of *Cerl-2* expression by histological analysis, study of the mutant phenotype and genetic interaction with Nodal, analysis of results and writing of the manuscript.

6.1. Abstract

Correct establishment of the L-R body asymmetry in the mouse embryo requires asymmetric activation of the evolutionary conserved *Nodal* signaling cascade in the left LPM. Furthermore, the presence of Nodal in the node is essential for its own expression in the left LPM. Here, we have characterized the function of *Cerberus-like-2 (Cerl-2)*, a novel Nodal antagonist, which displays a unique asymmetric expression on the right side of the mouse node. *Cerl-2* knock-out mice display multiple laterality defects including randomization of L-R axis. Strikingly, these defects can be partially rescued by removing one *Nodal* allele. Our results demonstrate that Cerl-2 plays a key role restricting the Nodal signaling pathway towards the left side of the mouse embryo by preventing its activity in the right side.

6.2. Introduction

Development of the internal organs proceeds across the left-right (L-R) axis and becomes apparent during organogenesis as a result of asymmetric activation of the conserved Nodal signaling cascade in the left lateral plate mesoderm (for review, see Beddington and Robertson. 1999; Capdevila et al. 2000; Hamada et al. 2002). Nodal signaling is a crucial player in the correct establishment of the vertebrate L-R body axis (Capdevila et al. 2000; Wright 2001; Hamada et al. 2002). *Nodal* expression in the perinodal region of the E7.0 mouse embryo has been shown to be required for its own activation in left LPM and thus generate the asymmetric expression of *Nodal* downstream genes (Brennan et al. 2002; Saijoh et al. 2003). Leftward flow in the mouse node (nodal flow) generated by specialized cilia (Nonaka et al. 1998) and intracellular calcium signaling (McGrath et al. 2003) has been recently implicated in the initial steps of lateralization. However, the exact mechanism behind the asymmetric Nodal activity in the node remains largely unexplained (for review, see Hamada et al. 2002).

We have identified a novel Cerberus/Dan family member, mouse *Cerberus-like2* (*Cerl-2*) that is asymmetrically expressed on the right side of the node. *Cerl-2* encodes for a secreted protein with the capability to bind directly to Nodal and to inhibit its signaling pathway in *Xenopus* assays. Inactivation of mouse *Cerl-2* resulted in a wide range of laterality defects including randomization of *Nodal* expression domain in the

LPM. These findings are consistent with an important role of *Cerl-2* in early events of L-R axis specification. In addition, the observed abnormalities can be partially rescued by the removal of one *Nodal* allele. Our results demonstrate that Nodal antagonism in the node, mediated by Cerl-2, is essential for proper specification of the mouse L-R axis.

6.3. Results

Using a sequence-similarity based search, we identified an incomplete EST sequence (GenBank - AA289243), later also designated *Dante* (Pearce et al. 1999) and mouse *Coco* (Bell et al. 2003) as the cDNA most related to mouse *Cerberus-like* (Belo et al. 1997) in the mammalian database. After cloning of the full-length cDNA, we observed that this gene, here designated *Cerberus-like2* (*Cerl-2*), is located in mouse chromosome 8, and is genomically organized into two exons, separated by an intron of 5,92 Kb. It encodes for a 20 kDa protein with a predicted signal peptide sequence and a cystein rich domain (CRD) containing 9 cysteins characteristic of Cerberus/DAN family (Fig. 6.1). The CRD domain is essential for the biological function of these proteins (Belo et al. 1997; Hsu et al.1998), so it is important to refer that only in Cerl-2 this complete domain is present, in contrast to what has been previously described for the incomplete sequence of Dante (Pearce et al, 1999).

Cerl-2 has close similarities to mouse *Cerberus-like* (I=35%, P=47%), cCaronte (I=34%, P=51%), *Xcoco* (I=38%, P=53%), and to a hypothetical human protein (I=57%, P=65%, Fig. 6.1). The latter is probably the human homologue of mouse Cerl-2, and we named it human Cer2. It also shares some similarities with the recently described zebrafish Charon (I=33%, P=55%).

As shown by whole mount *in situ* hybridization (WISH), *Cerl-2* transcripts can be firstly detected in a horse-shoe shaped expression pattern in the perinodal region of the early headfold stage of the mouse embryo (E7.0; Fig. 6.2.A,A'), resembling *Nodal* expression at this stage (Lowe et al. 1996; Collignon et al. 1996). However, by late

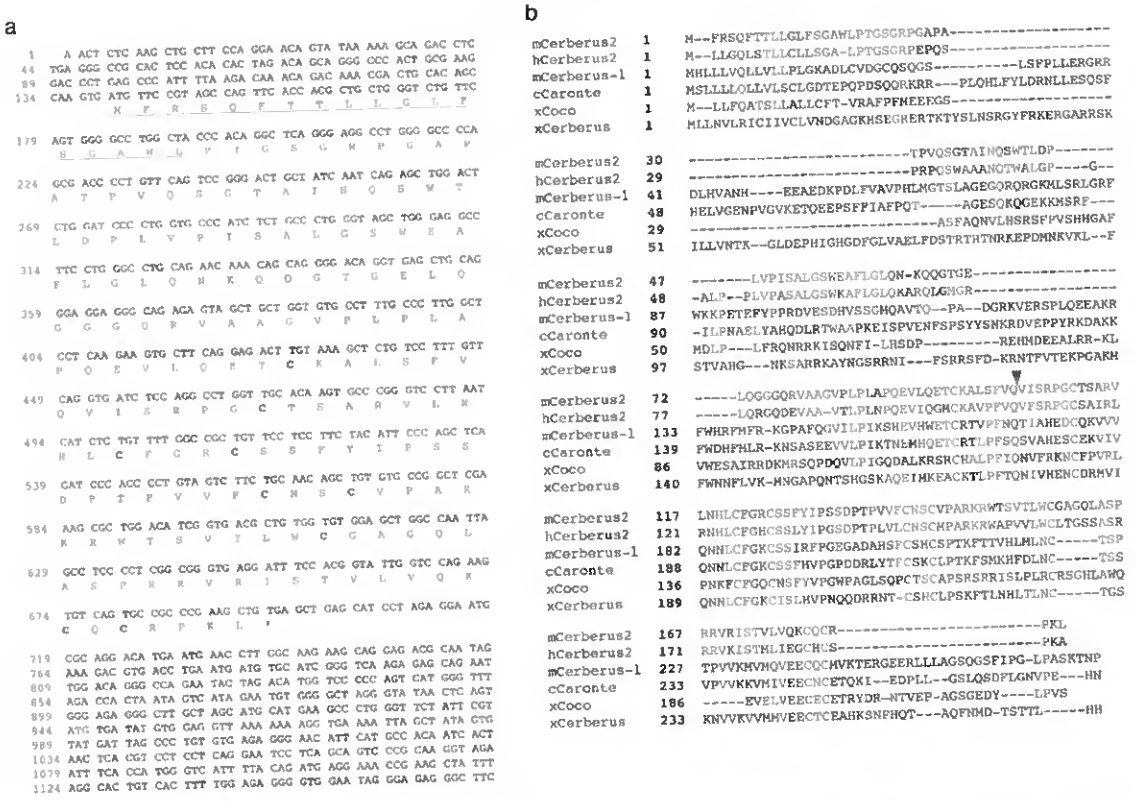

Figure 6.1. Identification of the Nodal inhibitor Cerberus-like 2. **a**, nucleotide sequence of mouse *Cerl-2* and deduced protein sequence. **b,** Alignment at the amino acid level of Cerl-2 related proteins. In the most conserved domain, Cerl-2 shares 57% identities with its human counterpart hCerl2, 34% with cCaronte, 38% with Xcoco, and 34% with Xcerberus. Indicated in red are the 9 cysteins characteristic of the DAN family of proteins; in blue identical aa; and blue arrowhead indicates the exon boundary between aa 104 and 105.

headfold stage (E7.5), expression of *Cerl-2* begins to decrease in intensity on the left side (Fig. 6.2B,B') and by early somitogenesis (E8.0), it can be strongly detected in the right side of the node (Fig. 6.2C,C'), assuming a complementary expression pattern to that of *Nodal* (Lowe et al. 1996; Collignon et al. 1996). Thus, *Cerl-2* is expressed at the proper time and place to be involved in an early L-R symmetry-breaking event in the mouse gastrula.

Cerl-2 belongs to a family of secreted antagonists, that are inhibitors of TGF-ß proteins like Nodal and BMPs, and also of Wnts, whose specificity can be unveiled by heterologous assays in the frog embryo (Piccolo et al. 1999; Belo et al. 2000). To assay Cerl-2 activity against endogenous signals we injected *Cerl-2* mRNA (750 pg) in the marginal zone of *Xenopus* embryos at the 4 cell stage and then performed WISH for a mesodermal marker (*Xbra*) at stage 11. We found that embryos injected with *Cerl-2*

mRNA fail to properly gastrulate and form mesoderm (data not shown) indicating a possible interference with endogenous *Nodal* signals. To test this hypothesis, *Cerl-2* and *mNodal* mRNAs were co-injected in the animal pole of 4-cell stage embryos, animal caps were explanted at blastula stage, harvested at stage 10.5 and analyzed by RT-PCR for *Xbra* and *Sox17ß* (pan-endoderm marker), two prototypic Nodal target genes (Belo et al. 2000). To test whether inhibition of *mNodal* took place upstream or downstream of the Nodal receptor we performed epistatic experiments with a constitutively active form of the activin receptor (ca*Alk5*). Microinjection of animal caps with either *mNodal* (50pg) or ca*Alk5* (800pg; Fig. 6.2D, lanes 5 and 8) induced expression of both *Xbra* and *Sox17ß*. Coinjection of *mNodal* with *Cerl-2* (1ng) mRNA completely blocked mNodal signal (Fig. 6.2D, lane 6). However, these inductions could not be prevented when *Cerl-2* was coinjected along with ca*Alk5*, showing that it acts upstream of this Nodal receptor. (Fig. 6.2D, lane 9).

A similar experiment was performed to test if *Cerl-2* could also inhibit BMP4 signaling (Fig. 6.2F). For this experiment, animal caps were harvested at stage 11 and the downstream targets, *Szl1* and X*vent1*, were analyzed by RT-PCR. Microinjection of X*BMP4* (300pg) or ca*Br* (a constitutively active BMP4 receptor used for the epistatic experiment) alone induced the expression of both *Szl1* and X*vent1* (Fig. 6.2F, lanes 5 and 8). Coinjection of *Cerl-2* (1ng) with caBr (480pg) did not prevent *Szl1* and X*vent1* expression (Fig. 6.2F, lane 9) while coinjection of Cerl-2 with X*BMP4* inhibited the expression of both markers (Fig. 6.2F, lane 6). In both experiments X*cer* (800pg) was injected as a control as it is known to inhibits both *Nodal* and *BMP4* signaling. Taken together these results show that full-length *Cerl-2* inhibits *Nodal* and *BMP4* but not ca*Alk5* or ca*Br* signaling (Fig. 6.2D and 6.2F), suggesting that Cerl-2 might antagonize Nodal and BMP4 extracellularly.

In order to determine whether Cerl-2 is able to physically interact with TGF-β proteins, we co-injected into animal poles synthetic mRNAs encoding a Flag-tagged version of Cerl-2 together with a HA-tagged version of Xnr1. Extracts were immunoprecipitated with anti-Flag antibody and the co-precipitating proteins were analysed by anti-HA western blotting. As shown in Figure 6.2E, HAXnr1 protein was found in a complex with FlagCerl2.

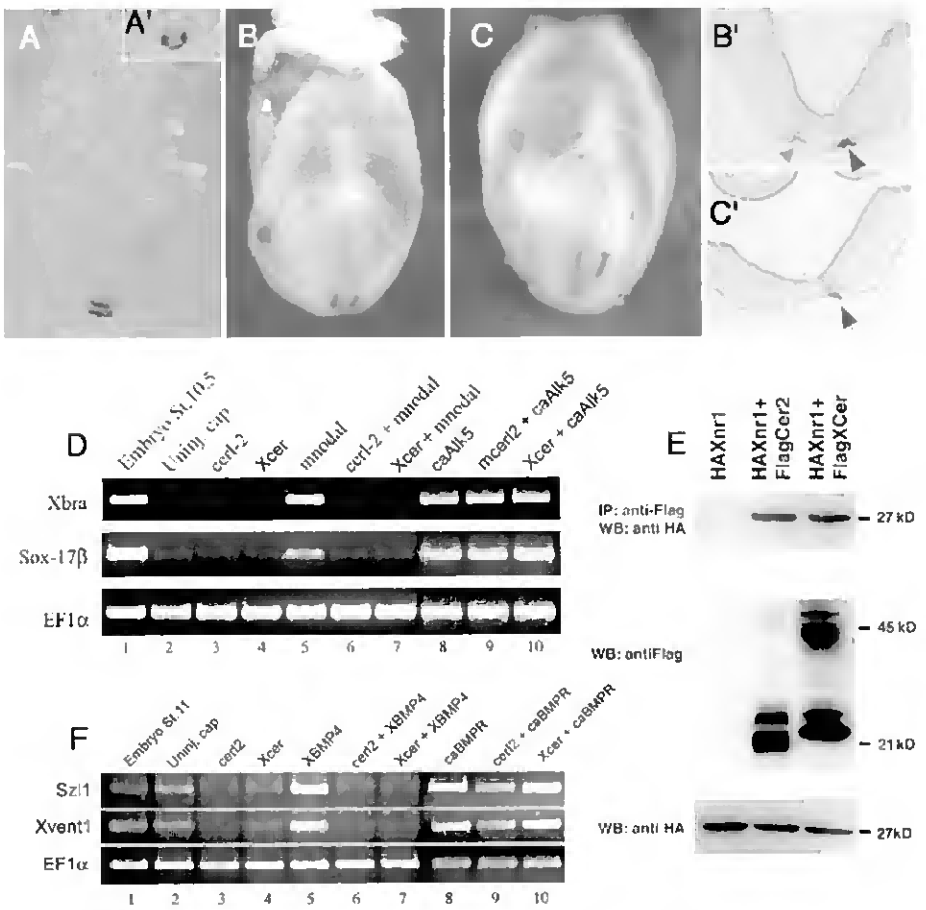

Figure 6.2. Biological activity of the asymmetrically expressed *Cerl-2*. **A-C,** *Cerl-2* expression pattern during early mouse development. **A, A',** Lateral and anterior views, respectively, of *Cerl-2* expression in the node at E7.0. **B,** At E7.5, *Cerl-2* starts to be asymmetrically upregulated on the right side of the node and at E8.0 **(C)** the asymmetry becomes more evident. **B', C',** Frontal sections of the embryos in **B** and **C**, respectively, and provide a detailed view of the perinodal region where *Cerl-2* is expressed (arrowheads). **D-F,** Inhibitory effects of Cerl-2 on Nodal and BMP signaling. **D,** *Cerl-2* inhibits m*Nodal* but not ca*ALK5* mRNA, as assayed by the induction their target genes *Xbra* and *Sox-17ß*. **E,** Co-immunoprecipitation experiments showing direct binding of Cerl-2 and Xcer to Xnr1. **F,** *Cerl-2* inhibits X*BMP4* but not ca*Br* mRNA, as assayed by the induction their target genes *Szl1* and *Xvent1*.

In order to determine whether Cerl-2 is able to physically interact with TGF-β proteins, we co-injected into animal poles synthetic mRNAs encoding a Flag-tagged version of Cerl-2 together with a HA-tagged version of Xnr1. Extracts were immunoprecipitated with anti-Flag antibody and the co-precipitating proteins were analysed by anti-HA western blotting. As shown in Figure 6.2E, HAXnr1 protein was found in a complex with FlagCerl2.

All the *in vitro* experiments: 1) the inhibition of Nodal and its downstream targets by Cerl-2; 2) its activity being upstream of Nodal receptor; and 3) the biochemical assay showing a physical interaction between the two proteins; suggest that Cerl2 is a novel Nodal antagonist.

To determine the *in vivo* role of *Cerl-2* we inactivated this gene in ES cells by replacing the second exon (containing the core CRD) with a LacZ reporter cassette (Fig. 6.3A). WISH in E7.5 *Cerl-2*$^{+/-}$ embryos using a *LacZ* probe, revealed that its expression is also asymmetric in the right side of the node (Figs. 6.3D,E). The offspring of *Cerl-2*$^{+/-}$ intercrosses were born according to the correct mendelian ratio. We observed that 35% of the homozygous mutants (33/94) died within the first 48 hours after birth. From those animals that died perinatally (n=33), 18% (6/33) showed left pulmonary isomerism (Fig 6.3G), 18% (6/33) thoracic *situs inversus* (Fig. 6.3H), and the remaining 64% (21/33) failed to show any apparent laterality defect. However when these apparently unaffected animals were examined carefully by histological analysis it was observed that they displayed cardiovascular malformations (Fig 6.3J,L), these being their probable cause of death. These defects include incomplete atrial (Fig. 6.3L) and ventricular septation (not shown). Of the 65% mutant animals that survived (61/94), 40% become normal adults (37/94), and the remaining 25% (24/94) die between weaning age and 3 months old, most of them showing heterotaxia of the abdominal organs (Fig. 6.4).

Due to its expression pattern and to its Nodal inhibitory activity, together with the observed laterality defects, we decided to investigate the effect of the loss of *Cerl-2* in the expression of left-right determinant genes. At early somite stages, *Nodal*, *Lefty1*, *Lefty2* and *Pitx2* are expressed in the left side of the embryo and are part of an evolutionary conserved signaling cascade essential for correct L-R morphogenesis (Capdevila et al. 2000; Wright 2001; Hamada et al.2002). At E8.0, *Nodal* is expressed in the node and in the left LPM of WT embryos (Fig. 6.5A). WISH in *Cerl-2*$^{-/-}$ embryos (N=60) using a *Nodal* probe revealed that although 40% of the embryos showed normal expression, 50% displayed bilateral and, 10% had an inverted pattern of expression in the right LPM (Fig. 6.5B-D). Interestingly, *Nodal* expression in the node remains unaffected in these three situations, being always stronger in the left side (red arrows in Fig. 6.5A-D). This evidence supports previously described work in which *Nodal* asymmetric expression in the node is not necessary or linked to its later expression

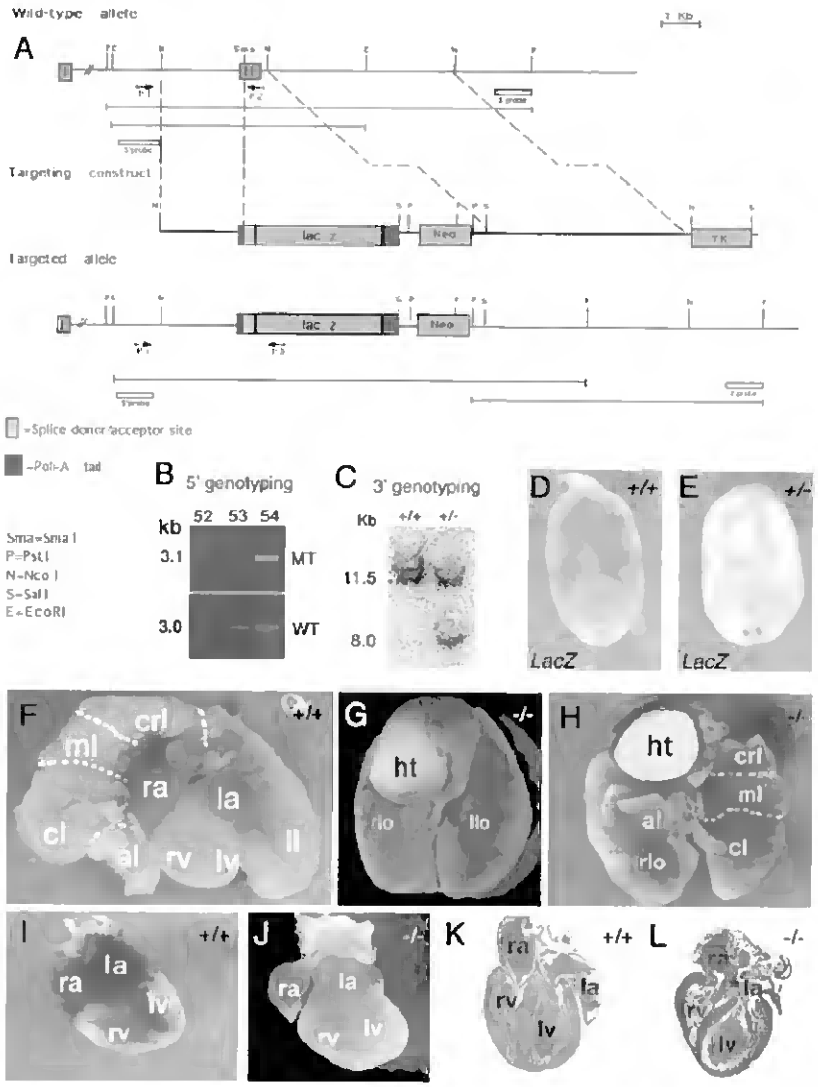

Figure 6.3. Targeted inactivation of *Cerl-2* gene. **A,** Schematic representation of the wild-type *Cerl-2* locus, targeting vector and targeted allele. Positions of primers, restriction enzyme sites and the probe used for PCR and Southern-blot analysis, respectively are shown. **B**, PCR-based 5' genotyping of WT and targeted ES cell DNA. **C,** Genomic Southern blot of PstI-digested tail DNA, prepared from newborn offspring of a mating of heterozygous mice. **D, E,** *LacZ in situ* hybridization in WT (**D**) and heterozygous (**E**) embryos. **F-H,** Thoracic organs of newborn WT (**F**) and *Cerl-2* $^{-/-}$ littermates displaying left lung isomerism (**G**) or inverted *situs* (**H**). **I, J,** Hearts of newborn WT and *Cerl-2*$^{-/-}$ littermates, respectively. **K, L,** Frontal sections of the hearts depicted in **I** and **J**, respectively, showing the atrial septal defects (asterisk) in *Cerl-2*$^{-/-}$. **al**, acessory lobe; **cl**, caudal lobe; **crl,** cranial lobe; **ht**, heart; **ml**, middle lobe **la**, left atrium; **llo**, left lobe, **lv**, left ventricle; **ra**, right atrium; **rlo**, right lobe; **rv**, right ventricle;

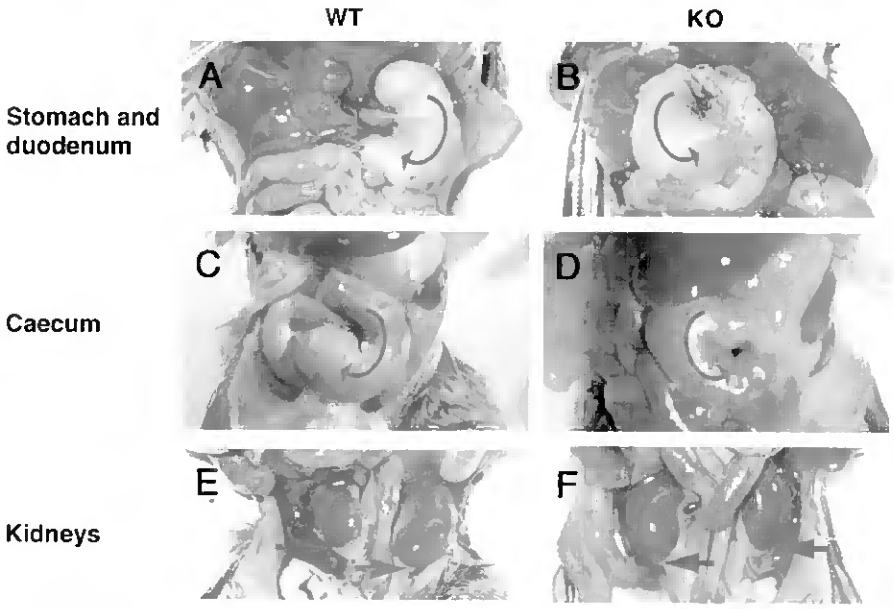

Figure 6.4. Reversal of the orientation of abdominal organs in *Cerl-2*$^{-/-}$ mutants. **A**) and **B**) Reversal of orientation of stomach and duodenum (directions indicated by green arrows) ; **C**) and **D**) Reversal of caecum loop (green arrows); **E**) and **F**) reversal of the rostro-caudal arrangement of the kidneys (green arrows) in *Cerl-2*$^{-/-}$ mutants.

domain in the left LPM (Brennan et at, 2002, Saijoh et al, 2003). At this same developmental stage, *Lefty1* is expressed along the ventral midline in the prospective floor plate of the WT embryo (Fig. 6.5E), while *Lefty2* expression can be detected in the left LPM (Meno et al. 1996, 1997; Fig. 6.5E). Both genes, *Lefty1* and *Lefty2*, have been described to be downstream targets of *Nodal* and also its inhibitors (for review, Hamada et al. 2002). By performing WISH using a riboprobe that detects both *Lefty* genes, we found that in *Cerl-2*$^{-/-}$ embryos, *Lefty-2* expression in the LPM is very similar to the one of *Nodal* as it would be expected. It can be detected in the left LPM, bilaterally or in the right LPM (Fig. 6.5F-H). We could also observe that, in *Cerl-2* null mutants, *Lefty1* expression in the midline is not affected (Fig. 6.5F-H). *Lefty1* was proposed to function as a midline barrier to prevent the diffusion of *Nodal*-induced signals emanating from the left to the right LPM (Meno et al. 1998). The proper expression of *Lefty1* (Fig 6.5F-H) and *Shh* (data not shown) in the prospective floorplate in *Cerl-2*$^{-/-}$ embryos leads us to conclude that the abnormal expression of left determinant genes in *Cerl-2*$^{-/-}$ embryos is not due to midline defects. Furthermore, 10% of *Cerl-2*$^{-/-}$ embryos show right-sided ectopic expression of *Nodal* (Fig.6.5D). In addition, in embryos with bilateral *Nodal*

expression in LPM, this expression starts at the level of the node (Fig 6.5C). Taken together, these results strongly indicate that the leaking of left side determinants takes place at the level of the node, and not later through to a defectively patterned midline.

Pitx2 is a downstream target of *Nodal* that is responsive to Nodal signaling through an asymmetric enhancer (Shiratori et al. 2001), similar to *Lefty2* and *Nodal* (Adachi et al. 1999; Norris and Robertson, 1999; Saijoh et al. 1999). At E8.5 *Pitx2* expression can be detected in the left LPM (Ryan et al. 1998; Figs. 6.5I,J) and it has been shown to be required for asymmetric development of organ *situs* (Kitamura et al. 1999; Gage et al. 1999; Lu et al. 1999; Lin et al. 1999). In *Cerl-2*$^{-/-}$ embryos, *Pitx2* expression in the LPM (N=11) could be detected bilaterally (38%), in the left (55%), or in the right side (9%) (Figs 6.5K-M).

The L-R determining genetic cascade leads to morphological consequences in the positioning of internal organs, and the first morphological manifestation of L-R axis determination is the orientation of embryonic heart looping (Fujinaga 1997). In wild type mouse embryos, the linear heart tube loops rightwards, while 50% (N=14) of *Cerl-2*$^{-/-}$ exhibited leftward or ventral heart looping (Fig. 6.5K-L). This comes in agreement with the previous experiments in which we show that Cerl-2 activity is essential for the correct establishment of the left side determinant genes and therefore, it is also necessary for the correct asymmetric development of the organ *situs*. In fact besides the mentioned defects in heart looping, later developmentally–associated phenotypes like left isomerism, situs inversus, and cardiac malformation were also observed (Fig 6.3F-L and Fig. 6.4). The phenotype of *Cerl-2* mutants suggests that Nodal activity is increased in the node, leading to abnormal expression of *Nodal* and downstream targets in the LPM. Therefore we hypothesized that by removing one copy of *Nodal* gene, in the context of the *Cerl-2* mutant, Nodal activity in the node would be lowered to a condition more similar to the WT. To test this, we intercrossed *Cerl-2*$^{-/-}$ with *Nodal*$^{+/-}$ animals (Lowe et al, 1996), recovered the embryos at E9.5 and scored them according to the heart loop direction. Indeed, we could observe that in *Cerl-2*$^{-/-}$; *nodal*$^{+/-}$ embryos (N=17), the abnormal heart-looping phenotype is reduced by 30% (6/17; Fig. 6.5P). These results strongly suggest that the phenotypes in L-R axis determination observed in *Cerl-2*$^{-/-}$ embryos result from an excess of Nodal signaling due to the lack of the Cerl-2 anti-Nodal activity in the mouse node.

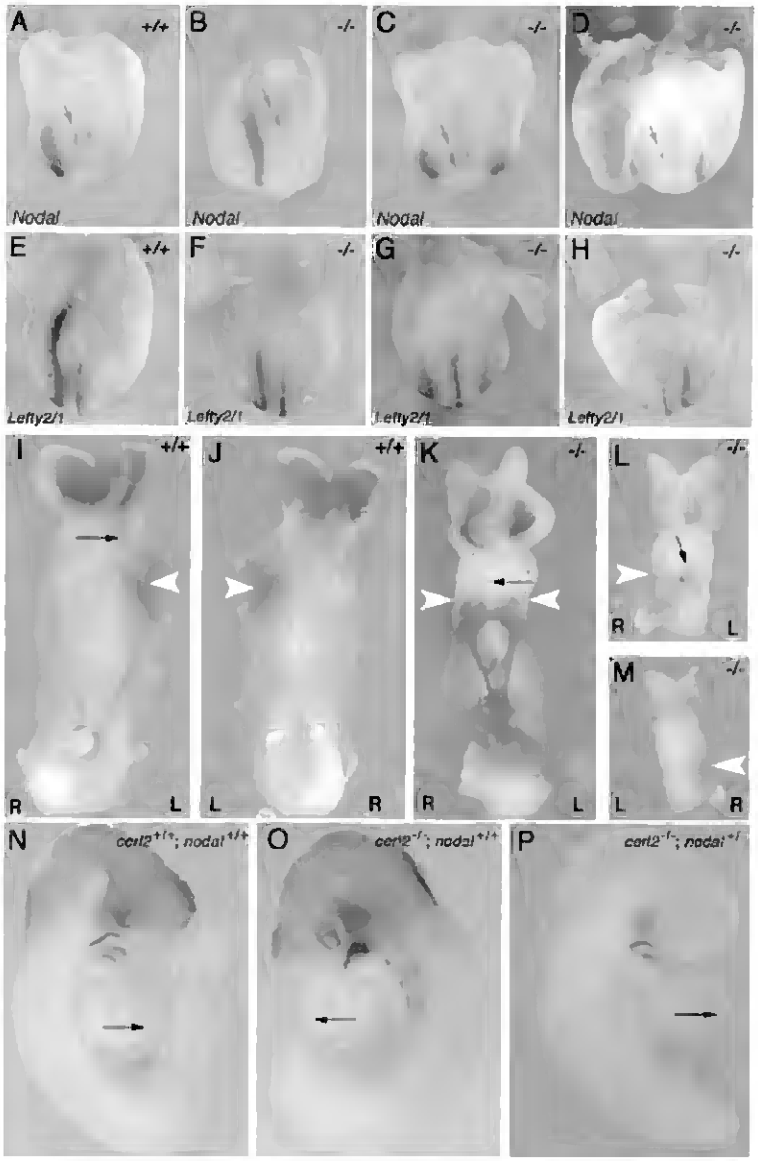

Figure 6.5. *Cerl-2* null mutants display a range of L-R defects. **A-H,** posterior views of E8.0 embryos. **A,** WT *Nodal* expression in the node and left LPM. **B-D,** *Cerl-2*$^{-/-}$ embryos showing normal **(B)**, bilateral **(C)** and right sided expression of *Nodal* in the LPM **(D)**. **E,** WT *Lefty2/1* expression in the left LPM and floorplate. **F-H,** *Cerl-2*$^{-/-}$ embryos displaying normal (**F**), bilateral (**G**) and right sided expression of *Lefty-2* in the LPM (**H**). **I, J,** ventral and dorsal views, respectively, of E8.5 WT embryos showing Pitx2 on the left LPM. **K-M,** *Cerl-2*$^{-/-}$ embryos presenting bilateral (**K**) and right sided expression of *Pitx2* in the LPM (**L, M**). White arrowheads indicate expression domain of *Pitx2*. **N-P,** Rescue of *Cerl-2* phenotype by reduced Nodal activity. **N,** E9.5 WT embryo showing rightward looping of the heart. **O,** *Cerl-2*$^{-/-}$ littermate with a reversed heart loop. **P,** *Cerl-2* $^{-/-}$;*nodal*$^{+/-}$ compound mutant with normal looping of the heart.

6.4. Discussion

Cerl-2 appears to have the capability to inhibit BMP4, however, this is unlikely to be correlated with the observed phenotypes. Analysis of targeted inactivation of a number of dedicated BMP4 antagonists like Chordin (Bachiller et al. 2003) and Noggin (McMahon et al. 1998), expressed in the mouse node, did not uncover defects in the correct establishment of the left-side determinant genes.

It has been recently described in zebrafish a gene named *Charon* that may be an orthologue of *Cerl-2*. In zebrafish, the expression patterns of *Southpaw* and *Charon* are not asymmetric. Nevertheless, knockdown of *Charon* using a morpholino oligonucleotide produces a similar phenotype to that of *Cerl-2* mutants (Hashimoto et al, 2004). Although in zebrafish the breaking of L-R symmetry is still not very well understood, this unveils a possible conserved evolutionary mechanism of Nodal antagonism in the node, mediated by Cerberus/DAN family members, essential for the correct development of L-R axis.

In the mouse, *Nodal* activity in the node is required for *Nodal* expression in the left LPM (Brennan et al. 2002; Saijoh et al. 2003) and subsequent activation of *Lefty2* and *Pitx2*. In the *Cerl-2* null mutant, we observed a perturbation in this mechanism of asymmetric information transfer from the node to the left LPM. According to our data, the role we propose for *Cerl-2* is to restrict Nodal activity to the left side of the node. The consequent effect of such inhibition is to prevent additional activation of *Nodal*, *Lefty*-2 and *Pitx-2* in the right LPM (Fig. 6.6). In the absence of Cerl-2 antagonistic activity on the node, *Nodal* may be also activated in the right LPM, leading to bilateral, or ectopic expression of this genetic cascade in the right LPM. In addition, we noticed that *Nodal* expression on the node is still asymmetric on the left side of *Cerl-2* mutants, indicating that randomization of *Nodal* expression in the LPM may be uncoupled from asymmetric gene expression within the node, as previously described (Brennan et al. 2002; Saijoh et al. 2003). Although this remains unexplained, our data highlights the importance of tight regulation of Nodal activity in the node by the extracellular antagonism mediated by Cerl-2 as an integral part of the L-R program.

The first known event for inducing asymmetry in *Nodal* expression is the concerted rotational movement of cilia of the node pit cells (the nodal flow); indeed, in *iv/iv* mice that lack such oriented fluid flow, *Nodal* has a randomized asymmetric

expression in the node (Supp et al. 1999). Paradoxically, despite the different expression pattern of *Nodal* in the node, of the *iv/iv* (Supp et al. 1999) and *Cerl-2* mutants, they end-up displaying a very similar type of randomization, characterized by left-, right- or bilateral activation of the "leftness" program in the LPM. This indicates that Cerl-2 plays an important role in the early events of simetry-breaking that take place in the node. Our data suggests a possible explanation in which the L-R asymmetry is controlled by a double-assurance mechanism consisting of two parallel systems, one relying on the leftward nodal-cilia flow and the other, on the antagonism between Cerl-2 and Nodal described by the proposed model (Fig. 6.6).

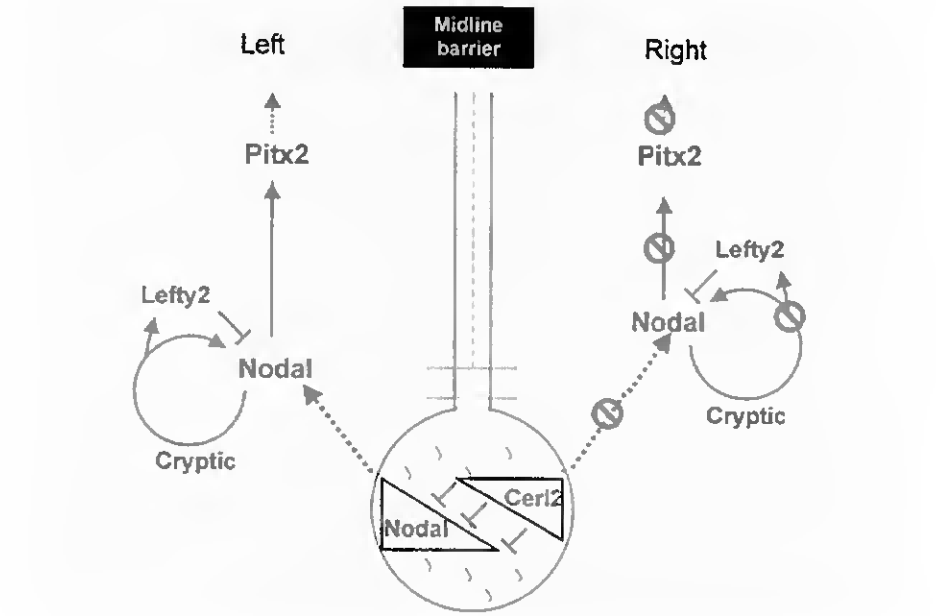

Figure 6.6. Proposed model for the role of *Cerl-2* in the generation of asymmetric gene expression. *Cerl-2* restricts Nodal activity to the left side of the node preventing additional activation of *Nodal*, *Lefty*-2 and *Pitx-2* in the right LPM .

Chapter 7 - Discussion

Chapter 7 - Discussion

7.1 Cerberus-like and BMP inhibition

Cerberus/Dan family is characterized by the presence of a cystein rich domain (CRD; Pearce et al, 1999). This domain, containing 9 cysteins, is essential for the biological role of these proteins that are TGF-β inhibitors. In particular, mouse Cer-l and Cerl-2 function as BMP and Nodal antagonists. BMP inhibition was shown to have an important role in embryonic development as revealed by the gene targeting of the BMP antagonists *Chordin* (Bachiller et al, 2003), *Noggin* (McMahon et al, 1998), and the *chordin;noggin* double mutants (Bachiller et al, 2000). Although *in vitro* experiments show that Cer-l is able to physically bind BMP-4, the mouse *in vivo* role, has not yet been demonstrated. Neither the targeted inactivation of *Cer-l* (Belo et al, 2000), nor the double mutants *Cerberus-like; Noggin* (chapter 3; Borges et al, 2001), *Cerberus-like;Goosecoid* (chapter 4; Borges et al, 2002), or *Cerberus-like;Chordin* (E. M. De Robertis, personal communication) revealed a requirement of *Cerberus-like* for BMP inhibition in the mouse. This may indicate that in the mouse embryo Cer-l mediated BMP-4 inhibition does not seem to be present at physiological conditions. An alternative explanation might be related to the presence of other redundant molecules that are yet to be identified.

7.2 Cerberus-like and Nodal signaling

Nodal pathway plays important roles during early mouse development. Nodal signals are required before gastrulation to specify the proximo-distal axis of the embryo, then, are essential for the displacement of the AVE, and correct positioning of the A-P axis. During gastrulation, Nodal is necessary for the formation of the primitive streak and specification of the node derivatives. After gastrulation, at early somite-stages Nodal signals are crucial for the correct determination of the L-R axis. Both Cerberus-like and Cerberus-like2 factors are required for the modulation of Nodal activity in the mouse embryo.

Cerberus-like has previously been shown to have redundant roles with *Lefty-1* (Perea-Gomez et al, 2002; Yamamoto et al, 2004), thereby, being implicated in Nodal

inhibition. Here, we reported the generation of *Cerberus-like;Cripto* double mutants in order to study Nodal signaling activities in the mouse embryo. This study led us to uncover the existence of a Cripto-independent pathway that effectively transduces Nodal signals and accounts for the displacement of the AVE towards the anterior region of the embryo, and partially rescues gastrulation. *Cer-l;Cripto* double mutants closely resemble *Nodal* hypomorphic mutants (Lowe et al, 2001), *Nodal* $^{\Delta 600/-}$ (Norris et al, 2002), and *ActRIIA/ActRIIB* double mutants (Song et al, 1999). In these mutant embryos, Nodal signaling is diminished and the mutants present several degrees of defects that correspond to the thresholds needed to accomplish the different Nodal biological functions (figure 1.4). The *Cer-l;Cripto* double mutant phenotypes can be positioned within the range of defects produced by defective Nodal activity.

Interestingly, in *Nodal* hypomorphs and *Nodal* $^{\Delta 600/-}$ animals, where Nodal signaling pathway components are intact (only Nodal protein levels are impaired), Nodal signals can be effectively transduced by the "canonical" pathway. In contrast, in the *Cer-l;Cripto* double mutants, the "canonical" pathway is disrupted, due to the absence of the EGF-CFC factor Cripto. Despite these differences, in both cases the phenotypes are remarkably similar, suggesting that in the *Cer-l;Cripto* double mutants, Nodal signals bypass the Cripto-dependent receptor complex and can elicit some Nodal–dependent biological functions. This contrasts with the general accepted view that EGF-CFC factors are essential for Nodal signaling. This alternative pathway may be mediated by ALK7, a receptor that was shown to transduce Nodal signals in a Cripto-independent fashion.

Nodal expression in the proximal posterior epiblast, driven by the PPE enhancer element can induce posterior epiblast fates and VE markers in a Cripto- and Smad-2-independent mechanism (Brennan et al, 2001; Norris et al, 2002). In the light of our recent results, we may hypothesize that these *Nodal* functions may be mediated via the same molecular mechanism that drives gastrulation in *Cer-l;Cripto* double mutants. Surprisingly, this mechanism can be uncovered in the absence of only one *Cer-l* copy, highlighting the critical balance existent between Nodal proteins and its antagonists. This underscores the importance of modulating Nodal signals, namely through the presence of specific antagonists and co-receptors, that are fundamental to accomplish Nodal biological functions.

It was shown that Lefty physically binds to Nodal and also to Cripto (Chen and Shen, 2004; Cheng et al, 2004). One possibility that can account for the rescue observed in *Cer-l*$^{+/-}$;*Cripto*$^{-/-}$ is the direct interaction between Cer-l and Cripto, contributing to one additional level of regulation of Nodal cascade. In this case, in the *Cripto* null mutant, all the Cer-l molecules would be targeted to Nodal inhibition, thereby, almost inactivating Nodal signaling. In the *Cer-l*$^{+/-}$;*Cripto*$^{-/-}$, due to the absence of one *Cer-l* allele, some Nodal molecules may be released from Cer-l inhibition, and elicit some cellular responses. To gain insight into this mechanism, biochemical and functional studies have to be performed.

7.3 Cerberus-like 2 and L-R development

In chapter 6, we showed that the Cerberus/Dan family member Cerberus-like 2 is a novel Nodal antagonist required for the proper development of the L-R axis. Cerl-2 plays an important role in regulating Nodal activity in the node, a mechanism that is indispensable for the correct transfer of left-biased information from the node to the left LPM. In the absence of *Cerl-2*, left-side specific genes may be ectopically expressed either on the right LPM or bilaterally.

Interestingly, is the fact that symmetric *Nodal* expression in the node is sufficient to drive *Nodal* expression in the left LPM (Norris et al, 2002; Saijoh et al, 2003), suggesting that asymmetries in the node are not required for the proper L-R development. Our results may shed light into this subject, since the data suggest that Cerl-2 may block or attenuate Nodal signals on the right side of the node and therefore Cerl-2 may perform a key role in maintaining the asymmetries generated by the node monocilia. According to our model (figure 6.6), Cerl-2 activity assures that the Nodal signals on the right side of the node do not reach the threshold required to transfer the left-side information to the right LPM, therefore allowing the transfer of Nodal signals, unilaterally from the node to the left LPM.

While the downstream events of Cerl-2 activity were characterised, the mechanisms that control *Cerl-2* expression in the node remain unclear. In fact, at the moment, one the most challenging questions in the field is: how is the bilateral symmetry broken in the embryo and how is it translated into asymmetric gene expression?

In the mouse, the nodal flow is the first mechanism known to generate L-R molecular asymmetries. However, the role of the Nodal flow is not consensual. It has been evoked as a mechanism that displaces a morphogen that would accumulate in the left side of the node and trigger asymmetric gene expression (reviewed in Hamada, 2002), but more recent studies have attributed to the node monocilia, a mechanosensor role that senses the flow and transduces it as a calcium influx in the left cells of the node (McGrath et al, 2003). Although there are evidences supporting both roles, at the moment it is not possible to discern between the two hypothesis.

In *iv/iv* mutants, in which the nodal flow is defective due to immotile cilia, the expression of *Nodal* and *Cerl-2* genes in the node is randomised (H. Hamada personal communication). This clearly positions asymmetric gene expression in the node downstream of the nodal flow. In addition, *Nodal* symmetric expression in the node is dependent on Notch/Delta activation (Krebs et al, 2003; Raya et al, 2003). Therefore, it seems that the node monocilia act as an inducer of asymmetric gene expression in the node, by regulating the distribution of previously symmetric molecules. Whether *Cerl-2* is also a target gene of Notch/Delta cascade remains uncertain.

Cerl-2 ortholog genes were described in other vertebrate classes: *Charon* in zebrafish and *Caronte* in chick. *Charon* is expressed in the region that contains specialised monocilia, the Kupfer´s vesicle (Essner et a, 2002; Hashimoto et al, 2004). Although symmetric, it was shown that *Charon* is essential for the correct L-R specification in the fish embryo. Moreover, it functions as a Nodal antagonist, suggesting the existence of high similarities with *Cerl-2,* at structural and functional levels. Chick *Caronte* is an important element in the L-R cascade, but it seems that its biological function and mechanism of action are different from those of *Cerl-2* and *Charon* (Rodriguez-Esteban et al, 1999; Yokouchi et al, 1999). *Caronte* is essential for the transfer of left-side signals from the Hensen´s node to the left LPM, and it acts as a *Nodal* inducer, contrarily to its mouse and fish counterparts. Interestingly, Caronte induces Nodal through BMP inhibition, and Cerl-2 is also a BMP antagonist. The functional role of this biochemical activity of Cerl-2 is unknown, but its role in mediating L-R development may be important.

Together, these results suggest essential roles for *Cerl-2*-related genes in the correct specification of the L-R axis. Although the data point to divergent roles of these genes in the L-R cascade, reflecting the functional adaptation of these molecules to the different cascades that generate L-R asymmetry among vertebrate species.

7.4 Cerberus-like 2 and heart development

Cerl-2 null mutants are not embryonic lethal, their primary cause of death is the presence of cardiovascular defects (incomplete atrial and ventricular septation, transposition of the great arteries and persistent truncus arteriosus). The type of defects observed in *Cerl-2* mutants may be found in almost all mutations for genes with essential roles in L-R axis development. The functions of these genes converge in the regulation of the Nodal activity, and consequently, its target gene *Pitx2*. L-R patterning processes controlled by *Pitx2* are important for the rightward looping of the heart and the asymmetric remodelling of the aortic arches. These asymmetric processes must occur normally to establish the correct spatial relashionships among the cardiac chambers and to align the heart and vasculature (Franco and Campione, 2003). In *Cerl-2* null mutants, *Pitx2* expression is randomised in the left LPM at E8.5, leading to an abnormal cardiovascular morphogenesis.

In humans, the frequency of cardiac abnormalities accompanied by aberrant L-R asymmetry is quite significant, affecting 1 in 7000 live births (Ahmad et al, 2004). This figure reveals the importance of L-R patterning defects in the etiology of congenital heart disease and underscores the necessity of developing mammalian model systems to elucidate the molecular basis of L-R asymmetry. The study of these models will make it possible to develop screening tests for specific heart or laterality syndromes and, perhaps, will enhance understanding of the risk factors. Therefore, mouse *Cerl-2* null mutants may provide a powerful system to study the genetics and embryology of L-R asymmetry and the associated cardiovascular defects.

Chapter 8 - Conclusion

Chapter 8 - Conclusion

The results presented in this thesis shed light on the function of mouse *Cerberus-like* genes during embryonic development. Both *Cerberus-like* and *Cerberus-like 2* were shown to be important Nodal antagonists, required for the correct establishment of body axes. By the generation of *Cer-l;Cripto* double mutants, we showed the importance of *Cerberus-like* in the control of Nodal signaling before and during gastrulation, for the definition of the A-P embryonic axis. Cerberus-like2 functions as a Nodal inhibitor essential for the establishment of the L-R axis in the mouse embryo. Collectively these results provide evidence for the requirement of temporal and spatial control of Nodal signals by Cerberus-like genes during embryogenesis

Concerning the anti-BMP activity of Cerberus-like factors, their biological meaning are not yet clear. Since BMP signaling is also involved in the establishment of the three main body axes, it is conceivable that *Cerberus-like* genes may also be required to modulate this signaling pathway. More functional studies are required to test this hypothesis.

Cerberus-related genes were not described in non-vertebrate species, indicating a possible role in a high level of complexity in the regulation of the vertebrate genomes. *Nodal* genes are also restricted to the vertebrate classes, contrarily, for example to BMPs (the homolog *Dpp* is present in *Drosophila melanogaster*), suggesting that *Nodal* genes evolved to regulate specific features of vertebrate development. Therefore, *Cerberus-like* genes may have arisen as a developmental novelty to fulfil the need of fine-tuning the powerful Nodal signaling activities. Interestingly, the Wnt signaling antagonist Dkk is also restricted to vertebrate species, albeit Wnt pathway being present in invertebrates such as *Drosophila*. Thus, *Cerberus-like* secreted antagonists are part of an extensive network of regulatory molecules with important roles in vertebrate embryonic development.

Genetic networks that control embryogenesis have been continuously uncovered through the generation of double mutants and are giving a contribution to the integration of different pathways in common biological functions. With this aim, genetic studies should be systematically used, in a combination with biochemical, embryological and cell biology approaches, in order to increase the understanding of the complexity of vertebrate systems.

Chapter 9 - Perspectives

Chapter 9 - Perspectives

The functional studies of mouse *Cerberus-like* genes presented in this thesis strongly suggest an important role for these genes in Nodal antagonism required for the patterning of A-P and L-R axes. However, there are missing links that would provide a better understanding of embryonic development regulation. Here, some prospective experiments are summarized in order to further increase the knowledge about the functions of *Cerberus-like* genes during development.

9.1.Cerberus-like

In the *Cer-l;cripto* system, we found that *Cripto* phenotype was rescued, probably due to the rescue of Nodal signalling. It would be interesting to determine 1) the *in vivo* levels of *Nodal* expression in the double mutants (by *in situ* hybridisation or RT-PCR); 2) the Nodal signalling activity, by monitoring phospho-Smad2 (by western blot); and 3) the receptors or co-receptors involved in the mechanism of Nodal transduction, (by assessing for the expression of candidate alternative receptors or co-receptors, such as ALK7 or Cryptic).

To assess accurately the embryonic structures and tissues that are present in the double mutant embryos, a detailed histological analysis has to be performed at several stages of development. Since cell proliferation plays an important role in the migration of the VE cells and establishment of A-P axis, it could be interesting to compare the levels of proliferative activity in *cripto* null mutants and *Cer-l;cripto* double mutants.

To gain more insight into the biochemical capabilities of Cerberus in binding to Cripto, the physical interaction between the two proteins has to be assayed *in vitro*, as well as the functional relevance of this mechanism *in vivo*.

In order to assess the anti-BMP activity of *Cer-l* it will be of interest to generate double mutants with another BMP inhibitor that shows domains of co-expression. In this sense, *Cerl-2* emerges a good candidate, since it is expressed in the node, while *Cer-l* is expressed in the node derivatives, such as notochordal, prechordal plates, and anterior definitive endoderm. Since both mouse *Cerberus-like* genes have the same biochemical capability of inhibiting BMP4 and are expressed in adjacent regions, they

might have redundant functions, that could be unmasked by the generation of compound mutants.

9.2. Cerberus –like 2

Since Nodal activity regulation in the node seems to be of major importance in order to proper establish the L-R axis, it would be interesting to monitor Cerl-2 protein levels in the node of the mouse embryo. This has to await the production of specific Cerl-2 antibody.

The fact that Nodal initial expression in the node is dependent on the activation by the Notch pathway, it would be relevant to determine if Cerl-2 is also a target of that pathway. For that, it is necessary to study the Cerl-2 transcriptional regulatory elements.

Since the relation between the node cilia and the asymmetric gene expression in the node is of major interest, some genetic studies may be performed to see if both mechanisms act synergistically. For that double mutants may be produced in which both functions are affected. As an example, *Cerl-2; iv/iv* mutants could be generated with the aim to assess for the existence of asymmetries in the node and LPM. If these genes function to establish and consequently to maintain molecular asymmetries, their loss of function should elicit a more severe phenotype than the one displayed by the *iv/iv* mutants.

Answers to these questions would definitely contribute to a better understanding of the events that control *Cerl-2* function and L-R asymmetry in the mouse.

References

REFERENCES

ACAMPORA, D., MAZAN, S., LALLEMEND, Y., AVANTAGGIATO, V., MAURY, M., SIMEONE, A. AND BRULET, P. (1995). Forebrain and midbrain regions are deleted in Otx2-/- mutants due to a defective anterior neuroectoderm specification during gastrulation. *Development.* 121: 3279-3290.

ADACHI, H., SAIJOH, Y., MOCHIDA, K., OHISHI, S., HASHIGUCHI, H., HIRAO, A., AND HAMADA, H. (1999). Determination of left/right asymmetric expression of nodal by a left side-specific enhancer with sequence similarity to a lefty-2 enhancer. *Genes & Dev.* 13: 1589-1600.

ADAMSON, E. D., MINCHIOTTI, G. AND SALOMON, D. S. (2002). Cripto: A tumor growth factor and more. *J. Cell Physiol.* 190: 267-278.

AHMAD, N., LONG, S. AND REBAGLIATI, M. (2004). A Southpaw joins the roster: the role of the zebrafish nodal-related gene southpaw in cardiac LR asymmetry. *Trends in Med.* 14: 43-49-

AMACK, J. D. AND YOST, H. J. (2004). The T box trancription factor No Tail in ciliated cells controls zebrafish left-right asymmetry. *Curr. Biol.* 14:685-690.

ANG, S.-L. AND ROSSANT, J. (1994). HNF-3β is essential for node and notochord formation in mouse development. *Cell.* 78: 561-574.

ANG, S.-L., JIN, O., RHINN, M., DAIGLE, N., STEVENSON, L. AND ROSSANT, J. (1996). A targeted mouse Otx2 mutation leads to severe defects in gastrulation and formation of axial mesoderm and to deletion of rostral brain. *Development.* 122: 243-252.

BACHILLER, D., KLINGENSMITH, J., KEMP., C.,BELO, J.A., ANDERSON, MAY, S.R., MCMAHON, J.A., MCMAHON, A.P., HARLAND, R.M., ROSSANT, J. AND DE ROBERTIS, E.M. (2000). The organizer factors Chordin and Noggin are required for mouse forebrain development. *Nature.* 403: 658-661.

BACHILLER, D., KLINGENSMITH, J., SHANEYDER, N., TRAN, U., ANDERSON, R., ROSSANT, J, AND DE ROBERTIS, E. M. (2003). The role of chordin/Bmp signals in mammalian pharyngeal development and DiGeorge syndrome. *Development.* 130: 3567-3578.

BARRANTES, I.B., DAVIDSON, G., GRONE, H.-J., WESTPHAL, H. AND NIEHRS, C. (2003). Dkk1 and noggin cooperate in mammalian head induction. *Genes & Dev.* 17: 2239-2244.

BEDDINGTON, R. S. (1994). Induction of a second neural axis by the mouse node. *Development.* 120: 613-620.

BEDDINGTON, R.P AND ROBERTSON, E. J. (1989). An assessment of the developmental potential of embryonic stem cells in the midgestation mouse embryo. *Development.* 105: 733-737.

BEDDINGTON, R. P. AND ROBERTSON, E. J. (1998). Anterior patterning in the mouse. *Trends Genet.* 14: 277-284.

BEDDINGTON, R.S. AND ROBERTSON,E.J. (1999). Axis development and early asymmetry in mammals. *Cell* 96: 195-209.

BELL, E., MUNOZ-SANJUAN, I., ALTMANN, C.R., VONICA, A., AND BRIVANLOU, A.H. (2003). Cell fate specification and competence by Coco, maternal BMP, TGFbeta and Wnt inhibitor. *Development* 130: 1381-1389.

BELO, J.A., BACHILLER, D., AGIUS, E., BORGES, A.C, MARQUES, S., PICCOLO, S., AND DE ROBERTIS, E.M. (2000). Cerberus-like is a secreted BMP and Nodal antagonist not essential for mouse development. *Genesis.* 26: 265-270.

BELO, J.A., BOUWMEESTER, T., LEYNS, L. KERTESZ, N., GALLO, M., AND DE ROBERTIS, E.M. (1997). Cerberus-like is a secreted factor with neuralizing activity expressed in the anterior primitive streak endoderm of the mouse gastrula. *Mech. Dev.* 68: 45-57.

BELO, J.A., LEYNS, L., YAMADA, G. AND DE ROBERTIS, E.M. (1998). The prechordal midline of the chondrocranium is defective in Goosecoid-1 mouse mutants. *Mech. Dev.* 72: 15-25.

BERTOCCHINI, F. AND STERN, C. D. (2002). The hypoblast of the chick embryo positions the primitive streak by antagonizing nodal signalling. *Dev. Cell.* 3: 735-744.

BIBEN, C., STANLEY, E., FABRI L., KOTECHA, S., RHINN, M., DRINKWATER, C., LAH, M., WANG, C-C., NASH, A., HILTON, D. , ANG, S-L., MOHUN, T., AND HARVEY, R.P. (1998). Murine Cerberus homologue mCer-1: a candidate anterior patterning molecule. *Dev Biol.* 194: 135–151.

BISGROVE, B. W., ESSNER, J. J. AND YOST, H. J. (1999). Regulation of midline development by antagonism of lefty and nodal signalling. *Development.* 126: 3253-3262.

BLUM, M., GAUNT, S. J., CHO, K. W. Y., STEINBEISSER, H., BLUMBERG, B., BITTNER, D. AND DE ROBERTIS, E. M. (1992). Gastrulation in the mouse: The role of the homeobox gene *goosecoid. Cell.* 69: 1097-1106.

BOETTGER, T., WITTLER, L. AND KESSEL, M. (1999). FGF8 functions in the specification of the right body side of the chick. *Curr. Biol.* 9 : 277-280.

BOORMAN, C. J. AND SHIMELD, S. M. (2002). The evolution of left-right asymmetry in chordates. *Bioessays.* 24: 1004-1011.

BORGES, A. C., MARQUES, S., AND BELO, J. A. (2001). The BMP antagonists cerberus-like and noggin do not interact during mouse forebrain development. *Int. J. Dev. Biol.* 45: 441-443.

BOUWMEESTER, T., KIM, S., SASAI, Y., LU ,B., AND DE ROBERTIS, E.M. (1996). Cerberus is a head-inducing secreted factor expressed in the anterior endoderm of Spemann's organizer. *Nature* 382: 595-601.

BRENNAN, J, LU, C. C., NORRIS, D. P., RODRIGUEZ, T. A., BEDDINGTON, R. S. AND ROBERTSON, E. J. (2001). Nodal signaling in the epiblast patterns the early mouse embryo. *Nature.* 411: 965-969.

BRENNAN, J., NORRIS, D.P., AND ROBERTSON ,E.J. (2002). Nodal activity in the node governs left-right asymmetry. *Genes & Dev.* 16: 2339-2344.

BRUNET, L.J., MCMAHON, J.A., MACMAHON, A.P. AND HARLAND, R.M. (1998). Noggin, Cartilage Morphogenesis and joint formation in the mammalian skeleton. *Science.* 280: 1455-1457.

CAMPIONE, M., STEINBEISSER, H., SCHWEICKER, A., DEISSLER, K., VAN BEBBER, F., LOWE, L., NOWOTSCHIN, S., VIEBAHN, C., HAFFTER, P., KUHEN, M. R. AND BLUM, M. (1999). The homeobox gene Pitx2: mediator of asymmetric left-right signalling in vertebrate heart and gut loop. *Development.* 126: 1225-1234.

CAMUS, A., DAVIDSON, B. P., BILLIARDS, S., KHOO, P.-L., RIVERA-PEREZ, J. A., WAKAMIYA, M., BEHRINGER, R. R. AND TAM, P. P. (2000). The morphogenetic role of midline mesendoderm and ectoderm in the development of the forebrain and midbrain of the mouse embryo. *Development.* 127: 1799-1813.

CAPDEVILA ,J., VOGAN, K.J., TABIN ,C.J. AND IZPISUA-BELMONTE, J.C. (2000). Mechanisms of left-right determination in vertebrates . *Cell.* 101: 9-21.

CARSON, D. D., TANG, J-P. AND JULIAN, J. (1993). Heparan sulphate proteoglycan (perlecan) expression by mouse embryos during acquisition of attachment competence. *Dev. Biol.* 155: 97-106.

CARTWRIGHT, J. H. E., PIRO, O. AND TUVAL, I. (2004). Fluid-dynamical basis of the embryonic development of left-right asymmetry in vertebrates. *Proc. Nac. Acad. Sci.* 101: 7234-7239.

CHEN, C. AND SHEN, M. M. (2004). Two modes by which Lefty proteins inhibit Nodal signalling. *Curr. Biol.* 14: 618-624.

CHENG, S. K., OLALE, F., BRIVANLOU, A. H. AND SCHIER, A. F. (2004). Lefty blocks a subset of TGFβ signals bt antagonizing EGF-CFC coreceptors. *Plos Biol.* 2: 215-226.

CHENG, S. K., OLALE, F., BENNET, J. T., BRIVANLOU, A. H. AND SCHIER, A. F. (2003). EGF-CFC PROTEINS ARE ESSENTIAL CORECEPTORS FOR THE TGF-BETA SIGNALS VG1 AND GDF1. *Genes Dev.* 17: 31-36.

COLLIGNON, J., VARLET, I., AND ROBERTSON, E.J. (1996). Relashionship between asymmetric nodal expression and the direction of embryonic turning. *Nature.* 381: 155-158.

CONLON, F., LYONS, K. M., TAKAESKU, N., BARTH, K. S., KISPERT, A., HERRMANN, B. AND ROBERTSON, E. J. (1994). A primary requirement for nodal in the formation and maintenance of the primitive streak in the mouse. *Development.* 120: 1919-1928.

COUCOUVANIS, E. AND MARTIN, G. R. (1995). BMP signaling plays a role in visceral endoderm differentiation and cavitation in early mouse embryo. *Development.* 126: 535-546.

DANOS, M. C. AND YOST, H. J. (1996). Role of notochord in specification of cardiac left-right orientation in zebrafish and Xenopus. *Dev. Biol.* 177: 96-103.

DE ROBERTIS, E. M, WESSLEY, O., OELGESCHLAGER, M., BRIZUELA, B., PERA, E., LARRAIN, J., ABREU, J. AND BACHILLER, D. (2001). Molecular mechanisms of cell-cell signalling by the SpemNN-Mangold organizer. *Int. J. Dev. Biol.* 45 : 189-197.

DE ROBERTIS, E.M. AND SASAI, Y. (1996). A common plan for dorsoventral patterning in Bilateria. *Nature.* 380: 37-40.

DE ROBERTIS, E.M., KIM, S.H., LEYNS, L., PICCOLO, S., BACHILLER, D., AGIUS. E., BELO, J.A., YAMAMOTO, A., HAINSKI-BROUSSEAU, A., BRIZUELA, B., WESSELY, O., LU, B. AND BOUWMEESTER, T. (1997). Patterning by genes expressed in the Spemann's organizer. *Cold Spring Harbour Symp. Quant. Biol.* 62: 169-175.

DING, J., YANG, L., YAN, Y.-T., CHEN, A., DESAI, N., WYNSHJAW-BORIS, A. AND SHEN, M. M. (1998). Cripto is required for correct orientation of the anterior-posterior axis in the mouse embryo. *Nature.* 395: 702-707.

DONO, R., SCALERA, L., PACIFICO, F., ACAMPORA, D., PERSICO, M- G. AND SIMEONE, A. (1993). The murine gene cripto gene: expresión during mesoderm induction and early heart morphogenesis. *Development.* 118: 1157-1168.

ECHELARD, Y., EPSTEIN, D.J., ST-JACQUES, B., SHEN, L., MOHLER, J., MCMAHON, J.A. AND MCMAHON, A.P. (1993). Sonic Hedgehog, a Member of a Family of Putative Signaling Molecules, Is Implicated In the Regulation of CNS Polarity. *Cell.* 75: 1417.

ESSNER, J. J., VOGAN, K. J., WAGNER, M. K., TABIN, C. J., YOST, H. J. AND BRUECKNER, M. (2002). Conserved function for embryonic nodal cilia. *Nature.* 418: 37-38.

FAINSOD, A., STEINBEISSER, H. AND DE ROBERTIS, E. M. (1994). On the function of BMP-4 in patterning the marginal zone of the *Xenopus* embryo. *EMBO J.* 13: 5015-5025.

FELDMAN, B., GATES, M. A., EGAN, E. G., DOUGAN, S. T., RENNEBECK, G. (1998). Zebrafish organizer development and germ-layer formation require nodal-related signals. *Nature.* 395: 181-185.

FILOSA, S., RIVERA-PEREZ, J. A., PEREA-GOMEZ, A., GANSMULLER, A., SASAKI, H., BEHRINGER, R. R. AND ANG, S-L. (1997). goosecoid and HNF-3β genetically interact to regulate neural tube patterning during mouse embryogenesis. *Development.* 124: 2843-2854.

FRANCO, D. AND CAMPIONE, M. (2003). The role of Pitx2 during cardiac development. *Trends in Med.* 13: 157-163.

FUJINAGA, M. (1997). Development of sidedness of asymmetric body structures in vertebrates. *Int. J. Dev. Biol.* **41**: 153-186.

FUJIWARA, T., DEHART, D. B., SULIK, K. K. AND HOGAN, B. L. (2002). Distinct requirements for extra-embryonic bone morphogenetic protein 4 in the formation of the node and primitive streak and coordination of left-right asymmetry in the mouse. *Development.* 129: 4685-4696.

GAGE, P.J., SUH, H., AND CAMPER, S.A. (1999). Dosage requirement of Pitx2 for development of multiple organs. *Development* . **126**: 4643-4651.

GALILI, N., BALDWIN, H. S., LUND, J., REEVES, R., GONG, W., WANG, Z., ROE, B. A., EMANUEL, B. S., NAYAK, S., MICKANIN, C., BUDARF, M. L. AND BUCK, C. A. (1997). A region of mouse cromosome 16 is synthetic to the DiGeorge, velocraniofacial syndrome minimal critical region. *Genome Research* 7: 17-26.

GARDNER, R. L. (2001). Specification of embryonic axes begin before cleavage in normal mouse development. *Development.* 128: 839-847.

GAUNT, S. J., BLUM, M. AND DE ROBERTIS, E. M. (1993). Expression of the mouse *goosecoid* gene during mid-embryogenesis may mark mesenchymal cell lineages in the developing head, limbs and body wall. *Development.* 117: 769-778.

GLINKA, A., WU, WEI, DELIUS, H., MONAGHAN, P., BLUMENSTOCK, C. AND NIEHRS, C. (1998) Dickkopf-1 is a member of a new family of secreted proteins and functions in head induction. *Nature.* 391: 357-362.

GRITSMAN, K., ZHANG, J., CHENG, S., HECKSCHER, E., TALBOT, W. S. AND SHIER, A. F. (1999). The EGF-CFC protein one-eye-pinhead is essential for nodal signalling. *Cell.* 97: 121-132.

GU, Z. Y., REYNOLDS, E. M., SONG, J. H., LEI, H., FEIJEN, A. (1998). The type I serine/threonine kinase receptor ActRIA (ALK2) is required for gastrulation of the mouse embryo. Development. 126: 2551-2561.

HAMADA, H., MENO, C., WATANABE, D., AND SAIJOH, Y. (2002). Establishment of vertebrate left-right asymmetry. *Nature Reviews Genetics.* 31: 103-113.

HARLAND, R. AND GERHART, J. (1997). Formation and function of Spemann's Organizer. *Ann. Rev. Cell Dev. Biol.* 13: 611-667.

HASHIMOTO, H., REBAGLIATI, M., AHMAD, N., MURAOKA, O., KUROKAWA, T., HIBI, M., AND SUZUKI, T. (2004). The Cerberus/Dan-family protein Charon is a negative regulator of Nodal signaling during left-right patterning in zebrafish. *Development* **131**: 1741-1753.

He, X., Semenov, M., Tamai, K. and Zeng, X. (2004). LDL receptor-related proteins 5 and 6 in Wnt/β-catenin signalling: Arrows point the way. *Development.* 131: 1663-1677.

HERMESZ, E., MACKEM, S. AND MAHON, K. A. (1996). Rpx: A novel anterior-restricted homeobox gene progressively activated in the prechordal plate, anterior neural plate and Rathke's pouch of the mouse embryo. Development. 122: 41-52.

HOODLESS, P. A., PYE, M., CHAZAUD, C., LABBÉ, E., ATTISANO, L., ROSSANT, J. AND WRANA, J. (2001). FoxH1 (Fast) functions to specify the anterior primitive streak in the mouse. *Genes & Dev.* 15: 1257-1271.

HSU, D.R., ECONOMIDES, A.N., WANG, X., EIMON P.M., AND HARLAND, R.M. (1998). The Xenopus dorsalizing factor Gremlin identifies a novel family of secreted proteins that antagonize BMP activities. *Mol Cell.* 1:673-683.

HUELSKEN, J., VOGEL, R., BRINKMANN, V., ERDMANN, B, BIRCHMEIER, C AND BIRCHMEIER, W. (2000).Requirement of β-catenin in anterior-posterior axis formation in mice. *J. Cell Biol.* 148: 567-578.

IEMURA, S., YAMAMOTO, T.S., TAKAGI, C., UCHIYAMA, H., NATSUME, T., SHIMASAKI, S., SUGINO, H. AND UENO, N. (1995). Direct binding of follistatin to a complex of bone-morphogenetic protein and its receptor inhibits ventral and epidermal cell fates in early *Xenopus* embryo. *Proc. Natl. Acad. Sci.* 95: 9337-9342.

JONES, M., KUHEN, M. R., HOGAN, B., SMITH, J. C. AND WRIGHT, C. V. (1995). Nodal-related signals induce axial mesoderm and dorsalize mesoderm during gastrulation. Development. 121: 3651-3662.

JOYNER, A.L. AND MARTIN, G.R. (1987). En-1 and En-2, two mouse genes with sequence homology to the Drosophila engrailed gene: expression during embryogenesis. *Genes Dev.* 1: 29-38.

KIECKER, C AND NIEHRS, C. (2001). The role of prechordal mesendoderm in neural patterning. *Curr. Opin. Neurobiol.* 11: 27-33.

KIMURA, C., YOSHINAGA, K., TIAN, E., SUZUKI, M., AIZAWA, S AND MATSUO, I. (2000). Visceral endoderm mediates forebrain development by suppressing posteriorizing signals. *Dev. Biol.* 225: 304-321.

KIMURA,C., SHEN, M. M., TAKEDA, N., AIZAWA, S. AND MATSUO, I. (2001). Complementary functions of Otx2 and Cripto in initial patterning of mouse epiblast. *Dev. Biol.* 235: 12-32.

KINDER, S. J., TSANG, T. E., QUINLAN, G. A. HADJANTONASKIS, A. K., NAGY, A. AND TAM, P. P. (1999). The orderly allocation of mesodermal cells to the extraembryonic structures and the anteroposterior axis during gastrulation of the mouse embryo. *Development.* 126: 4691-4701.

KITAMURA, K., MIURA, H., MIYAGAWA-TOMITA, S., YANAZAWA, M., KATOH-FUKUI, Y., SUZUKI, R., OHUCHI, H., SUEHIRO, A., MOTEGI, Y., NAKAHARA, Y., KONDO, S., AND YOKOYAMA, M. (1999). Mouse Pitx2 deficiency leads to anomalies of the ventral body wall, heart, extra- and periocular mesoderm and right pulmonary isomerism. *Development.* 126: 5749-5758.

KREBS, L. T., IWAI, N., NONAKA, S., WELSH, I. C., LAN, Y., JIANG, R., SAIJOH, Y., O'BRIEN, T. P., HAMADA, H. AND GRIDLEY, T. (2003). Notch signalling regulates left-right asymmetry determination by inducing Nodal expression. *Genes & Dev.* 17: 1207-1212.

LAWSON, K. A., MENESES, J. J. AND PEDERSEN, R. A. (1991). Clonal analysis of epiblast fate during germ layer formation in the mouse embryo. *Development.* 113: 891-911.

LEMAIRE, L., ROESER, T., IZPISÚA-BELMONTE, J. C. AND KESSEL, M. (1997). Segregating expression domains of two goosecoid genes during the transition from gastrulation to neurulation in chick embryos. *Development.* 124: 1443-1452.

LEMAIRE, P. AND KODJABACHIAN, L. (1996). The vertebrate organizer: structure and molecules. *Trends in Genet.* 12: 525-531.

LEVIN, M. AND MERCOLA, M. (1998). Gap junctions are involved in the early generation of left-right asymmetry. *Dev. Biol.* 202: 90-105.

LEVIN, M. AND MERCOLA, M. (1999). Gap junction-mediated transfer of left-right asymmetry patterning signals in the early chick blastoderm is upstream of Shh asymmetry in the node. *Development.* 126: 4703-4714.

LEVIN, M., THORLIN, T., ROBINSON, K. R., NOJI, T. AND MERCOLA, M. (2002). Asymmetries in H+/K+-ATPase and cell membrane potentials comprise a very early step in left-right patterning. *Cell.* 111: 77-89.

LIGUORI, G., L., ECHEVARRIA, D., IMPROTA, R., SIGNORE, M., ADAMSOM, E., MARTINEZ, S. AND PERSICO, M. G. (2003). Anterior neural plate regionalization in cripto null mutant mouse embryos in the absence of node and primitive streak. *Dev. Biol.* 264: 537-549.

LIN C.R., KIOUSSI, C., O'CONNELL, S., BRIATA, P., SZETO, D., LIU, F., IZPISUA-BELMONTE, J.C., AND ROSENFELD, M.G. (1999). Pitx2 regulates lung asymmetry, cardiac positioning and pituitary and tooth morphogenesis. *Natur.e* 401: 279-282.

LIU, P, WAKAMIYA, M., SHEA, M. J., ALBRECHT, U., BEHRINGER, R. R. AND BRADLEY, A. (1999). Requirement for Wnt 3 in vertebrate axis formation. *Nature Genet.* 22: 361-365.

LOGAN, M., PAGAN-WESTPHAL, S. M., SMITH, D. M., PAGANESSI, L. AND TABIN, C. J. (1998). The transcription factor Pitx2 mediates situs-specific morphogenesis in response to left-right asymmetric signals. *Cell.* 94: 307-317.

LOHR, J. L., DANOS, M. C. AND YOST, M. J. (1997). Left-right asymmetry of a nodal-related gene is regulated by dorsoanterior midline structures during Xenopus development. *Development.* 1465-1472.

LOWE, L., YAMADA, S. AND KUEHN. (2001). Genetic dissection of nodal function in patterning the mouse embryo. *Development.* 128: 1831-1843.

LOWE, L.A., SUPP, D.M., SAMPATH, K., YOKOYAMA, T., WRIGHT, C.V., POTTER, S.S., OVERBEEK, P., AND KUEHN, M.R. (1996). Conserved left-right asymmetry of nodal expression and alterations in murine situs inversus. *Nature.* 381: 158-161.

LU M.F., PRESSMAN C., DYER R., JOHNSON R.L., AND MARTIN J.F. (1999). Function of Rieger syndrome gene in left-right asymmetry and craniofacial development. *Nature.* 401: 276-278.

MARSZALEK, J. R., RUIZ-LOZANO, P., ROBERTS, E., CHIEN, K. R. AND GOLDSTEIN, L. S. (1999). Situs inversus and embryonic ciliary morphogenesis defects in mouse mutants lacking KIF3A subunit of kinesin-II. *Proc. Nat. Acad. Sci.* 96: 5043-5048.

MATZUK, M. M., KUMAR, T. R., SHOU, W., COERVER, K. A., LAU, A. L., BEHRINGER, R. R. AND FINEGOLD, M. .(1996). Transgenic models to study the roles of inhibins and activins in reproduction, oncogenesis, and development. *Recent Prog. Horm. Res.* 51: 123-154.

MCGRATH, J., SOMLO, S., MAKOVA, S., TIAN, X. AND BRUECKNER, M. (2003). Two populations of node monocilia initiate left-right asymmetry in the mouse. *Cell.* 114: 61-73.

MCMAHON, J.A., TAKADA, S., ZIMMERMAN, L.B., FAN, C., HARLAND, R.M. AND MCMAHON, A.P. (1998). Noggin-mediated antagonism of BMP signalling is required for growth and patterning of the neural tube and somite. *Genes Dev.* 12: 1438-1452.

MENO, C., SAIJOH, Y., FUJII, H., MASAKO, I., YOKOYAMA, T., YOKOYAMA, M., TOYODA, Y. AND HAMADA, H. (1996). Left-right asymmetric expression of the tgfβ-family member lefty in mouse embryos. *Nature.* 381: 151-155.

MENO, C., GRITSMAN, K., OHISHI, S., OHFUJI, Y. HECKSHER, E. (1999). Mouse Lefty-2 and zebrafish antivin are feedback inhibitors of nodal signalling during vertebrate gastrulation. *Mol. Cell.* 4: 287-298.

MENO, C., ITO, Y. SAIJOH, Y., MATSUDA, Y., TASHIRO, K., KUHARA, S., AND HAMADA, H. (1997). Two closely-related left-right asymmetrically expressed genes, lefty-1 and lefty-2: their distinct expression domains, chromosomal linkage and direct neuralizing activity in Xenopus embryos. *Genes Cells* 2: 513-524.

MENO, C., SHIMONO, A., SAIJOH, Y., YASHIRO, K., MOCHIDA, K., OHISHI, S., NOJI, S., KONDOH, H., AND HAMADA, H. (1998). Lefty-1 is required for left-right determination as a regulator of lefty-2 and nodal. *Cell.* 94: 287-297.

MENO, C., TAKEUCHI, J. SAKUMA, R., KOSHIBA-TAKEUCHI, K., OHISHI, S. AND HAMADA, H. (2001). Diffusion of nodal signalinging activity in the absence of the feedback inhibitor Lefty-2. *Dev. Cell.* 1: 127-138.

MERCOLA, M. AND LEVIN, M. (2001). Left-right asymmetry determination in vertebrates. *Annu. Rev. Cell Dev. Biol.* 17: 779-805.

MEYERS, E. N. AND MARTIN, G. R. (1999). Differences in left-right axis pathways in mouse and chick: functions of FGF8 and SHH. *Science.* 285: 403-406.

MINCHIOTTI, G., PARISI, S., LIGUORI, G., SIGNORE, M., LANIA, G., ADAMSON, E. D., LAGO, C. T. AND PERSICO, M. G. (2000). Membrane-anchorage of Cripto protein by glycosylphosphatidylinositol and its distribution during early mouse development. *Mech. Dev.* 90: 133-142.

MISHINA, Y., SUZUKI, A., UENO, N. AND BEHRINGER, R. R. (1995). Bmpr encodes a type I bone morphogenetic protein receptor that is essential for gastrulation during mouse embryogenesis. *Genes & Dev.* 9: 3027-3037.

MOCHIZUKI, T., SAIJOH, Y., TSUCHIYA,K., SHIRAYOSHI, Y., TAKAI, S., TAYA, C. YONEKAWA, H., YAMADA, K., NIHEI, H., NAKATSUJI, N., OVERBEEK, P. A., HAMADA, H. AND YOKOYAMA, T. (1998). Cloning of *inv*, a gene that controls left/right asymmetry and kidney development. *Nature.* 395: 177-181.

MORGAN, D., TURNPENNY, L., GOODSHIP, J., DAI, W., MAJUMDER, K., MATTEWS, L., GARDNER, A., SCHUSTER, G., VIEN, L., HARRISON, W., ELDER, F. F., PENMAN-SPLITT, M., OVERBEEK, P. AND STRACHAN, T. (1998). Inversin, a novel gene in the vertebrate left-right axis pathway, is partially deleted in the *inv* mouse. *Nature Genet.* 20: 149-156. erratum: 20: 312.

MUKHOPADHYAY, M., SHTROM, S., RODRIGUEZ-ESTEBAN, C., CHE, L., TSUKUI, T., GOMER, L., DORWARD, D.W., GLINKA, A., GRINBERG, A.,HUANG, S.-P., NIEHRS, C., IZPISUA-BELMONTE, J.C. AND HEIFNER WESTPHAL. (2001). Dickkopf1 is required for embryonic head induction and limb morphogenesis in the mouse. *Dev. Cell.* 1: 423-434.

NOMURA, M. AND LI, E. (1998). Smad2 role in mesoderm formation, left-right patterning and craniofacial development. *Nature.* 393: 786-780.

NONAKA, S., SHIRATORI, H., SAIJOH, Y. AND HAMADA, H. (2002). Determination of left-right patterning of the mouse embryo by artificial nodal flow. *Nature.* 418: 96-99.

NONAKA, S., TANAKA, Y., OKADA, Y., TAKEDA, S., HARADA, A., KANAI, Y., KIDO, M., AND HIROKAWA, N. (1998). Randomization of left-right asymmetry due to loss of nodal cilia generating leftward flow of extraembryonic fluid in mice lacking KIF3B motor protein. *Cell.* 95: 829-837.

NORRIS, D. P., BRENNAN, J., BIKOFF, E. K AND ROBERTSON, E. J. (2002). The FoxH1-dependent autoregulatory enhancer controls the level of nodal signals in the mouse embryo. *Development.* 129: 3455-3468.

NORRIS, D. P.AND ROBERTSON, E.J. (1999). Asymmetric and node-specific nodal expression patterns are controlled by two distinct *cis*-acting regulatory elements. *Genes & Dev.* 13:1575-1588.

Okada, Y. Okada, Y., Nonaka, S., Tanaka, Y. Saijoh, Y., Hamada, H. and Hirokawa, N (1999). Abnormal nodal flow precedes situs inversus in *iv* and *inv* mice. Mol. *Cell.* 4: 459-468.

Oliver, G., Mailhos, A., Wher, R., Copeland, N.G., Jenkins, N.A. and Gruss, P. (1995). *Six-3,* a murine homologue of the *sine oculis* gene, demarcates the most anterior border of the developing neural plate and is expressed during eye development. *Development.* 12: 4045-4055.

Parameswaran, M. and Tam, P. P. (1995). Regionalization of cell fate and morphogenetic movement of the mesoderm during mouse gastrulation. *Dev. Genet.* 17: 16-28.

Parisi, S., D'Andrea, D., Lago, C. T., Adamsom, E. D. and Persico, M. G. (2003). Nodal-dependent cripto signalling promotes cardiomyogenesis and redirects the neural fate of embryonic stem cells. *J. Cell. Biol.* 163: 303-314.

Pearce, J.J., Penny, G. and Rossant, J. (1999). A mouse cerberus/Dan-related gene family. *Dev. Biol.* 209: 98-110.

Pedersen R A Wu K and Batakier H. (1986). Origin of the inner cell mass in mouse embryos: cell lineage by microinjection. *Dev. Biol.* 117: 581-595.

Perea-Gomez, A., Rhinn, M. And And, S.-L. (2001). Role of the anterior visceral endoderm in restricting posterior signals in the mouse embryo. *Int. J. Dev. Biol.* 45 : 311-320.

Perea-Gomez, A., Vella, F.D.J., Shawlot, W., Oulad-Abdelghani, M., Chazaud, C., Meno, C., Pfister, V., Chen, L., Robertson, E. J., Hamada, H., Behringer, R. R. and Ang, S.-L. (2002). Nodal antagonists in the anterior visceral endoderm prevent the formation of multiple primitive streaks. *Dev. Cell.* 3 : 745-756.

Perona, R. M. and Wasserman, P. M. (1986). Mouse blastocysts hatch in vitro by using a trypsin-like proteinase associated with cells of mural trophoectoderm. *Dev. Biol.* 114: 42-52.

PICCOLO, S., AGIUS, E., LEYNS, L., BHATTACHARYYA, S., GRUNZ, H., BOUWMEESTER, T. AND DE ROBERTIS, E.M. (1999). The head inducer Cerberus is a multifunctional antagonist of Nodal, BMP and Wnt signals. *Nature*. 397: 707-710.

PICCOLO, S., SASAI,Y., LU, B., AND DE ROBERTIS, E.M. (1996). Dorsoventral patterning in *Xenopus*: inhibition of ventral signals by direct binding of chordin to BMP-4. *Cell*. 86: 589-598.

PIEDRA, M. E., ICARDO, J. M., ALBAJAR, M., RODRÍGUEZ-REY, J. C. AND ROS, M. (1998). Pitx2 participates in the late phase of the pathway controlling left-right asymmetry. *Cell*. 94: 319-324.

PIKO, L AND CLEGG, K. B.(1982) Quantitative changes in total Rna, total poly(A), and ribossomes in early mouse embryos. *Dev. Biol.* 89:362-378.

PIOTROWSKA, K. AND ZERNICKA-GOETZ, M. (2001). Role of sperm in spatial patterning of the early mouse embryo. *Nature*. 409: 517-521.

PIOTROWSKA, K. AND ZERNICKA-GOETZ, M. (2002). Early patterning of the mouse embryo – contributions of sperm and egg. *Development*. 129: 5803-5813.

PIOTROWSKA, K., WIANNY, F., PEDERSEN, R. AND ZERNICKA-GOETZ, M. (2001). Blastomeres arising from the first cleavage division have distinguishable fates in normal mouse development. *Development*. 128: 3739-3748.

PLUSA, B., GRABAREK, J., POTROWSKA, K., GLOVER, D. M. AND ZERNICKA-GOETZ, M. (2002). Site of the previous meiotic division defines cleavage orientation in the mouse embryo. *Nature Cell Biol.* 4: 811-815.

RANKIN, C. T., BUNTON, T., LAWLER, A. M. AND LEE, S.-J. (2000). Regulation of left-right patterning in mice by growth/differentiation factor-1. *Nature Genet*. 24: 262-265.

RAYA, A., KAWAKAMI, Y., RODRIGUEZ-ESTEBAN, C., IBANES, M., RASSKIN-GUTMAN, D., RODRÍGUEZ-LEON, J, BUSHER, D., FEIJÓ, J. A. AND IZPISUA-BELMONTE, J. C. (2004). Notch activity acts as a sensor for extracellular calcium during vertebrate left-right determination. *Nature*. 427: 121-128.

RAYA, A., KAWAKAMI, Y., RODRIGUEZ-ESTEBAN, C., BUSHNER, D., KOTH, C. M., ITOH, T., MORITA, M., RAYA, R. M., DUBOVA, I., BESSA, J. G., DE LA POMPA, J. L. AND IZPISUA-BELMONTE, J.C. (2003). Notch activity induces Nodal expression and mediates the establishment of left-right asymmetry in vertebrate embryos. *Genes Dev.* 17: 1213-1218.

REISSMAN, E., JORNVALL, H., BLOKZIJL, A., ANDERSSON, O., CHANG, C., MINCHIOTTI, G., PERSICO, M. G., IBANEZ, C. AND BRIVANLOU, A. (2001). The orphan receptor ALK7 and the activin receptor ALK4 mediate signalling by nodal proteins during vertebrate development. *Genes & Dev.* 15: 2010-2022.

RHINN, M., DIERICH, A., SHAWLOT, W., BEHRINGER, R. R., LE MEUR, M. AND ANG, S.-L. (1998). Sequential roles for Otx2 in visceral endoderm and neuroectoderm for forebrain and midbrain induction and specification. *Development.* 121: 845-856.

RIVERA-PEREZ, J. A., MALLO, M., GENDRON-MAGUIRE, M., GRIDLEY, T. AND BEHRINGER, R. R. (1995). *goosecoid* is not an essential component of the mouse gastrula organizer but is required for craniofacial and rib development. *Development.* 121: 3005-3012.

RODRIGUEZ-ESTEBAN, C., CAPDEVILA, J., ECONOMIDES, A. A., PASCULA, J., ORTIZ, A. AND IZPISUA-BELMONTE, J. C. (1999). The novel Cer-like protein Caronte mediates the establishment of embryonic left-right asymmetry. *Nature.* 401: 243-251.

ROSENQUIST, T.A.AND MARTIN, G. R. (1995). Visceral endoderm-1 (VE-1) antigen marker that distinguishes anterior from posterior embryonic visceral endoderm in the early post-implantation mouse embryo. *Mech. Dev.* 49: 117-121.

RYAN, A.K., BLUMBERG, B., RODRIGUEZ-ESTEBAN, C., YONEI-TAMURA, S., TAMURA, K., TSUKUI, T., DE LA |PENA, J., SABBAGH, W., GREENWALD, J. CHOE, S., NORRIS, D.P., ROBERTSON, E. J., EVANS, R.M., ROSENFELD, M.G., AND IZPISUA-BELMONTE, J.C. (1998). Pitx2 determines left-right asymmetry of internal organs in vertebrates. *Nature* 394: 545-551.

SAIJOH, Y., ADACHI, H., MOCHIDA, K., OHISHI, S., HIRAO, A., AND HAMADA, H. (1999). Distinct transcriptional regulatory mechanisms underlie left-right asymmetric expression of lefty-1 and lefty-2. *Genes & Dev.* 13: 259-269.

SAIJOH, Y., ADACHI, H., SAKUMA, R., YEO, C. Y., YASHIRO, K., WATNABE, M., HASHIGUSHI, H., MOCHIDA, K., OHISHI, S., KAWABATA, M., MYIAZONO, K.,

WHITMAN, M. AND HAMADA, H. (2000). Left-right asymmetric expression of lefty2 and nodal is induced by a signaling pathway that includes the transcription factor FAST2. *Mol. Cell.* 5: 35-47.

SAIJOH, Y., OKI, S., OHISHI, S. AND HAMADA, H. (2003). Left-right patterning of the mouse lateral plate requires nodal produced in the node. *Dev Biol.* **256**: 160-172.

SAKUMA, R., OHNISHI, Y.-I., MENO, C., FUJII, H., JUAN, H., TAKEUCHI, J., OGURA, T., LI, E., MIYAZONO, K. AND HAMADA, H. (2002). Inhibition of Nodal signalling by Lefty mediated through interaction with common receptors and efficient diffusion. *Genes Cells.* 7: 401-412.

SASAI, Y., LU, B., STEINBEISSER, H., GEISSERT, D., GONT, L. K. AND DE ROBERTIS, E. M. (1994). *Xenopus chordin* : a novel dorsalizing factor activated by organizer-specific homeobox genes. *Cell.* 79: 779-790.

SCHIER, A. F. (2003). Nodal signaling in vertebrate development. *Annu. Rev. Cell Dev. Biol.* 19; 589-621.

SHAWLOT, W. AND BEHRINGER, R. R. (1995). Requirement for Lim1 in head-organizer function. *Nature.* 374: 425-430.

SHAWLOT, W., DENG, J.M. AND BEHRINGER, R.R. (1998). Expression of the mouse *cerberus-related* gene, *Cerr1*, suggests a role in anterior neural induction and somitogenesis. *Proc. Natl. Acad. Sci.* 95: 6198-6203.

SHAWLOT, W., DENG, J.M., WAKAMIYA, M. AND BEHRINGER, R. (2000). The cerberus-related gene, Cerr1, is not essential for mouse head formation. *Genesis.* 26: 253-258.

SHAWLOT, W., WAKAMIYA, M., KWAN, M., KANIA, A. JESSEL, T. M. AND BEHRINGER, R. R. (1999). Lim1 is required in both the primitive streak-derived tissues and visceral endoderm for head formation in the mouse. *Development.* 126: 4925-4932.

SHIH, J. AND FRASER, S. E. (1996). Characterizing the zebrafish organizer: Microsurgical analysis at the early-shield stage. *Development.* 1313-1322.

SHIRATORI, H., SAKUMA, R., WATANABE, M., HASHIGUCHI, H., MOCHIDA, K., SAKAI, Y., NISHINO, J., SAIJOH, Y., WHITMAN, M., AND HAMADA, H. (2001). Two-step regulation of left-right asymmetric expression of pitx2: initiation by nodal signaling and maintenance by Nkx2. *Mol Cell.* 7: 137-149.

SILVA, A. C., FILIPE, M., KUERNER, K.-M., STEINBEISSER, H. AND BELO, J. A. (2003). Endogenous Cerberus activity is required for the anterior head specification in Xenopus. *Development*: 130: 4943-4953.

SOLLOWAY, M., J. AND ROBERTSON, E. J. (1999). Early embryonic lethality in Bmp5;Bmp7 double mutant suggests functional redundancy within the 60A subgroup. *Development.* 126: 1753-1768.

SOLNICA-KREZEL, L. (2003). Vertebrate development: taming the nodal waves. *Curr. Biol.* 13: R7-R9.

SONG, J., OH, S. P., SCHREWE, H., NOMURA, M., LEI, H., OKANO, M., GRIDLEY, T. AND LI, E. (1999). The type II activin receptors are essential for egg cylinder growth, gastrulation, and rostral head development in mice. *Dev. Biol.* 213: 157-169.

STANLEY, E.G., BIBEN, C., ALLISON, J., HARTLEY, L., WICKS, I.P., CAMPBELL, I. K., MCKINLEY, M., BARNETT, L., KOENTGEN, F., ROBB, L. AND HARVEY, R.P. (2000). Targeted insertion of a lacZ reporter gene into the mouse Cer1 Locus reveals complex and dynamic expression during embryogenesis. *Genesis.* 26: 259-264.

STOREY, K. G., CROSSLEY, J. M, DE ROBERTIS, E. M., NORRIS, W. E. AND STERN, C. D. (1992). Neural induction and regionalisation in the chick embryo. *Development.* 114: 729-741.

STOREY, K. G., SELLECK, M. A. AND STERN, C. D. (1995). Neural induction and regionalisation by different subpopulations of cells in Hensen's node. *Development.* 121: 417-428.

SULIK, K., DEHART, D. B., IANGAKI, T., CARSON, J. L., VRABLIC, T., GESTELAND, K. AND SCHOENWOLF, G. C. (1994). Morphogenesis of the murine node and notochordal plate. *Dev. Dyn.* 201: 260-278.

SUPP, D. M., WITTE, D., POTTER, S. S., AND BRUECKNER, M. (1997). Mutation of an axonemal dynein affects left-right asymmetry in *inversus viscerum* mice.*Nature*. 389: 963-966.

SUPP, D.M. , BRUECKNER, M., KUEHN, M.R., WITTE, D. P., LOWE, L.A., MACGRATH, J., CORRALES, J., AND POTTER, S.S. (1999). Targeted deletion of the ATP binding domain of left-right dynein confirms its role in specifying development of left-right asymmetries. *Development*. 126: 5495-5504.

TAKEDA, S., YONEKAWA, Y., TANAKA, Y., OKADA, Y., NONAKA, S. AND HIROKAWA, N. (1999). Left-right asymmetry and kinesin superfamily protein KIF3A: new insights in determination of laterality and mesoderm induction by kif3A-/- mice analysis. *J. Cell. Biol.* 145: 825-836.

TAM, P. L. AND BEHRINGER, R. R. (1997). Mouse gastrulation: the formation of a mammalian body plan. *Mech. Dev.*68: 3-25.

TAM, P. L., GAD, J. M., KINDER, S. J., TSANG, T. E. AND BEHRINGER, R. (2001). Morphogenetic tissue movement and the establishment of body plan during development from blastocyst to gastrula in the mouse. *Bioessays*. 23: 508-517.

TAM, P. P AND STEINER, K. A. (1999). Anterior patterning by synergistive activity of the early gastrula organizer and the anterior germ layer tissues of the mouse embryo. *Development*. 126: 5171-5179.

TAM, P. P., STEINER, K. A. ZHOU, S. X. AND QUINLAN, G. A. (1997). Lineage and functional analyses of the mouse organizer. *Cold Spring Harbor Symp. Quant. Biol.* 62: 135-144.

TAO, W., AND LAI, E. (1992). Telencephalon-restricted expression of BF-1, a new member of the HNF-3β/*fork head* gene family in the developing rat brain. *Neuron*. 8: 957-966.

THISSE, C. AND THISSE, B. (1999). Antivin, a novel and divergent member of the TGFβ superfamily regulares mesoderm induction. *Development*. 126: 229-240.

THOMAS, P. AND BEDDINGTON, R. P. (1996). Anterior primitive endoderm may be responsible for patterning the anterior neural plate in the mouse embryo. *Curr. Biol.* 6: 1487-1496.

THOMAS, P., BROWN, A. AND BEDDINGTON, R. P. (1998). Hex: a homeobox gene revealing peri-implantation asymmetry in the mouse embryo and an early transient marker of endothelial cell precursors. *Development.* 125: 85-94.

VARLET, I., COLLIGNON, J. AND ROBERTSON, E. J. (1997). nodal expression in the primitive endoderm is required for specification of the anterior axis during mouse gastrulation. *Development.* 124: 1033-1044.

WAIT, K. A. AND ENG, C. (2003). From developmental disorders to heritable cancer: it's all in the BMP/TGFβ family. *Nature Rev. Genet.* 4: 763-773.

WALDRIP, W., BIKOFF, E., K., HOODLESS, P. A., WRANA, J. L. AND ROBERTSON, E. J. (1998). Smad2 signalling in extraembryonic tissues determines anterior-posterior polarity of the early mouse embryo. *Cell.* 797-808.

WEINSTEIN, M., YANG, X., LI, C.L., XU, X. L., GOTAY, J. AND DENG, C. X. (1998). Failure of egg cylinder elongation and mesoderm induction in mouse embryos lacking the tumor suppressor smad2. *Proc. Nac. Acad. Sci.* 95: 9378-9383.

WINNIER, G., BLESSING, M., LABOSKY, P.A. AND HOGAN, L.M. (1995). Bone morphogenetic protein-4 is required for mesoderm formation and patterning in the mouse. *Genes Dev.* 9: 2105-2116.

WOODARZ, A. AND NUSSE, R. (1998). Mechanisms of Wnt signaling in development. *Annu. Rev. Cell Dev. Biol.* 14: 59-88.

WRIGHT, C.V. (2001). Mechanisms of left-right asymmetry: what's right and what's left. *Dev. Cell.* 1: 179-186.

XU, C., LIGUORI, G. L., PERSICO, M. G., AND ADAMSOM, E. D. (1999). Abrogation of cripto gene in mouse leads to failure of postgastrulation morphogenesis and lack of differentiation of cardiomyocytes. *Development.* 126: 483-494.

YAMADA, G., MANSOURI, A., TORRES, M., STUART, E. T., BLUM, M., SCHULTZ, M., DE ROBERTIS, E. M. AND GRUSS, P. (1995). Targeted mutation of the murine goosecoid gene results in craniofacial defects and neonathal death. *Development* . 121: 2917-2922

YAMAMOTO, M., MENO, C., SAKAI, Y., SHIRATORI, H., MOCHIDA, K., IKAWA, Y., SAIJOH, Y. AND HAMADA, H. (2001). The transcription factor FoxH1 (FAST) mediates Nodal signalling during anterior-posterior patterning and node formation in the mouse. *Genes Dev.* 15: 1242-1256.

YAMAMOTO, M., MINE, N., MOCHIDA, K., SAKAI, Y., SAIJOH, Y. MENO, C. AND HAMADA, H. (2003). Nodal signaling induces the midline barrier by activating Nodal expression in the lateral plate. *Development.* 130: 1795-1804.

YAMAMOTO, M., SAIJOH, Y., PEREA-GOMEZ, A., SHAWLOT, W., BEHRINGER, R. R., ANG, S.-L., HAMADA, H. AND MENO, C. (2004). Nodal antagonists regulate formation of the anterioposterior axis of the mouse embryo. *Nature.* 428:387-392.

YAN, Y.-T., GRITSMAN, K., DING, J., BURDINE, R. D., CORRALES, J. D., PRICE, S. M., TALBOT, W. S., SCHIER, A. F. AND SHEN, M. M. (1999). Conserved requirement for EGF-CFC genes in vertebrate left-right axis formation. *Genes & Dev.* 13: 2527-2537.

YEO, C. AND WHITMAN, M. (2001). Nodal signals to Smads through Cripto-dependent and Cripto-independent mechanisms. *Mol Cel.* 7: 949-957.

YOKOUCHI, Y., VOGAN, K. J. PEARSE II, R. V. AND TABIN, C. (1999). Antagonistic signalling by Caronte, a novel Cerberus-related genes, establishes left-right asymmetric gene expression. *Cell.* 98: 573-583.

YOKOYAMA, T., COPELAND, N. G., JENKINS, N. A., MONTGOMERY, C. A., ELDER, F. F. AND OVERBEEK, P. (1993). Reversal of left-right asymmetry : a *situs inversus* mutation. *Science.* 260 : 679-682.

YOSHIOKA, H., MENO, C., KOSHIBA, K., SUGIHARA, M., ITOH, H., ISHIMARU, Y., INOUE, T., OHUCHI, H., SEMINA, E. V., MURRAY, J. C., HAMADA, H. AND NOJI, S. (1998). Pitx2, a bicoid-type homeobox gene, is involved in a Lefty-signaling pathway in determination of left-right asymetry. *Cell.* 94: 299-305.

ZERNICKA-GOETZ, M. (2002). Patterning of the embryo: the first spatial decisions in the life of a mouse. *Development.* 129: 815-829.

ZHANG, H. AND BRADLEY, A. (1996). Mice deficient for BMP2 are nonviable and have defects in amnion/chorion and cardiac development. *Development*. 122: 2977-2986.

ZHAO, G.-Q. (2003). Consequences of knocking out BMP signaling in the mouse. *Genesis*. 35: 43-56.

ZHOU, X., SASAKI, H., LOWE, L., HOGAN, B. L. M. AND KUEHN, M. (1993). Nodal is a novel TGF-β-like gene expressed in the mouse node during gastrulation. *Nature*: 361: 543-547.

ZIMMERMAN, L.B., DE JESÚS-ESCOBAR, J.M. AND HARLAND, R.M. (1996). The Spemann organizer signal noggin binds and inactivates bone morphogenetic protein-4. *Cell*. 86: 599-606.